Analysis and Implementation of the Integrated 3x3 and 11x11 Pixel Array Infrared Detectors for the ADiR Product Line

A Major Qualifying Project

Submitted to the faculty

of the

Worcester Polytechnic Institute

Worcester, Massachusetts, USA

In partial fulfilment of the requirements for the

Degree of Bachelor of Science

on this day of

October 13, 2006

by

Lauren MacMath

Mike Raineri

Raj Vysetty

Abstract

This project investigated 3x3 and 11x11 pixel array infrared detectors prototyped by Analog Devices, Inc., Limerick for their new ADiR product line. This project verified the potential of the integrated detectors for use in non-contact thermometry applications. The main outcomes included the discovery of device and testing constraints, general detector characterisation and calibration, and the development of software capable of obtaining an absolute temperature measurement from the 3x3 array and a thermal image from the 11x11 array.

Acknowledgements

We would first like to thank Analog Devices, Limerick, for making this project possible and for providing a unique opportunity to work with next generation technology. We would like to thank John Reidy for coordinating the project and for helping us to develop contacts within the company. We would like to thank Eamon Hynes and Brendan Cawley for sharing their knowledge of the detectors and their advice for analysis and implementation. We would also like to thank Eamon and Brendan for continuously providing us with detectors to work with and the resources necessary to evaluate them. Most importantly we would like to thank them for their quick attention to project developments and for ensuring our project progress and completion. Lastly, from the Limerick office, we would also like to extend our thanks to Edward Coyne for his assistance in the lab and for his guidance in understanding the optical properties of the lens, and Claire Leahy for her continual and patient support in the software development process.

We would further like to thank Luke Pillans from the Newbury, UK office for his dedication to the project and his interest in our learning and our project outcomes. Without his knowledge in infrared, we would not have been able to develop test setups and methods to obtain reliable and repeatable data upon which to draw concrete and accurate conclusions. Furthermore, through sharing his own work, he was able to guide us toward a better understanding of the detector characteristics so that we could work together for a thorough and multi-faceted analysis.

We would next like to thank our advisors Professor Rick Vaz and Professor Rick Brown for their advice and assistance throughout the project. They provided valuable assistance in development of project scope and goals and in determining the best ways to organise and present the abundance of data obtained and knowledge gained throughout the project.

Finally, we would like to thank Charlotte Tuohy, the local coordinator for the WPI Limerick Project Centre. Her dedication to the students and attention to detail ensured a positive experience and the continuance of the project centre.

Table of Contents

Table of Figures

Executive Summary

Infrared radiation is an invisible, yet tangible phenomenon that is emitted and absorbed by all physical objects. Infrared radiation is the reason a fire keeps you warm in the winter and why the inside temperature of a car rises on a sunny day. Even without physical contact, heat emission, absorption, and transfer occur continuously between all objects. Similarly to how infrared from the sun is able to heat the inside of a car without physical contact, it is able to heat temperature-sensing elements without contact. The sensors are capable of translating the absorbed heat into a temperature measurement.

Analog Devices, Inc. (ADI) developed the next generation of technology for non-contact thermometry utilising a microelectromechanical system. This technology integrates a lens, sensors, multiplexer, ADT7301 ambient temperature monitor, and AD7794 analogue-to-digital converter onto a single integrated circuit. This technology is the foundation for their new ADiR product line of three-by-three and eleven-by-eleven pixel array infrared detectors. These detectors will be geared towards absolute temperature measurement and thermal imaging applications.

In preliminary stages of product development, the ADI engineers were focused on IC development and quality improvement. With less then four months to go at the start of this project, until the initial product release to potential customers, ADI required system level implementation and analysis of their ADiR product line prototypes.

This project entailed execution and analysis of Analog Devices, Inc.'s next generation infrared sensing technology. This project had five main goals: (1)explanation of full detector system behaviour, (2)development of accurate and repeatable test setups, (3)generation of an absolute temperature measurement using the detector and USB evaluation board, (4)enhancement of the LabVIEW ADiR Evaluation Software (AES) for full communication with the detectors, data collection, and display capabilities, and (5)development of a proof of concept for a customer demonstration and thermal image display.

The first goal was to generate a general explanation of the detector system behaviour while verifying individual sensor functionality. Before any testing was done on the prototype integrated circuits, they had to be checked for functionality using a pre-fabricated applications board and the AES. The integrated circuits snapped into and out of a socket on the application board before the AES was started with each of the detectors. Since the detectors were the first generation prototypes, yield was low and led to multiple sessions of functionality testing as the wafers were fabricated. For the working detectors, their general behaviour was observed to draw conclusions about the way the portions of the detector interfaced with one another and the surrounding environment. The AD7301, ambient temperature sensor, and the AD7794, analogue-to-digital converted were uncorrected devices that required calibration to produce desired

results in both the three-by-three and eleven-by-eleven pixel arrays. To understand the calibrations necessary, further investigation was done to understand the lens and field of view.

The second goal was to develop accurate and repeatable test setups and methodologies. While endeavouring to characterize the behaviour of the detectors, multiple test setups and methodologies were utilised and analysed to determine the variables present when working with infrared radiation detection. Test equipment was already available to test and calibrate the ADT7301, while test setups for the angular response of the pixels, calibration of the AD7794 output, and error identification were carefully designed. The angular response testing was done in conjunction with an ADI employee from the Newbury, UK office. The ultimate purpose of these tests was to obtain the data necessary for achieving the final demonstration goals.

The third goal was to produce an absolute temperature using the detectors. The test setups provided the data necessary to produce calibration equations for the entire system. The calibrations produced a temperature reading from pixel five, the centre pixel in the three-by-three array with reasonable accuracy. Once the calibrations were complete, a smaller scale test was designed utilising similar setups to prove or disprove hypotheses about data integrity and irregularities.

The fourth goal, which spanned the entire course of the project, was enhancement of the AES for full communication with the detectors and extensive capabilities for data collection and display. The AES was reconfigured to communicate with all pixels in each of the arrays. Further adjustments were made to the increase the speed and change the order in which data was collected from the detector via the evaluation board. The final changes simplified the user interface for temperature display with the three-by-three pixel array and thermal imaging using the eleven-by eleven pixel array. The original options for data collection and analysis remained if the user desired the raw data for their own characterisation.

The final goal of the project was the creation of a proof of concept for a customer demonstration with the three-by-three and eleven-by-eleven pixel arrays utilising the USB evaluation board and AES. For the three-by-three array, constraints due to the lens design and inability to easily limit the field of view of the prototypes required the demonstration to continue focusing just on pixel five and use the test setup designed in this project. The test setup, however, can be easily mimicked using a canister package bonded to the detector to place it in thermal equilibrium with the system. The size of the aperture in the canister and the distance between the sensors and the aperture will simulate the test setup proving comparable results. For the eleven-by-eleven array, despite the smaller pixel size and hence greater directivity, the lens prevented the outer pixels in the array from receiving the full intensity. Because of the smaller pixel size, the induced voltage will be smaller, significantly decreasing the strength of the signal for all

pixels. Though the signal was significantly decreased, varying the angle of incidence of the incoming IR varied the positioning of the hot spot on the screen confirming the imaging potential of the eleven-by-eleven array.

The detectors developed by Analog Devices Inc. utilise next generation technology that will introduce new fabrication techniques for mass production of IR detectors. As with any new innovation, the implications, capabilities, and limitations of the new fabrication process and detector implementation have yet to be fully realised. The recommendations offer improvements to be made to the test methodologies to better simulate the results, propose changes in the demonstration for improved operation with the current detectors, and suggest areas of IC design that require further attention for future prototypes.

1 Introduction

Non-contact temperature sensing can be useful in a variety of commercial applications from industrial assembly line monitors to handheld ear thermometers. In recent years, there has been a continuous development of technology for these devices. Multiple companies have sought and realised cost-effective methods and designs for silicon sensors and lenses. Analog Devices Inc. (ADI), as an integrated circuit (IC) designer and manufacturer that specialises in signal processing, has been enhancing their existing expertise in other portions of the temperature measurement processes such as on-chip temperature sensing and data conversion, while developing next generation technology for sensor and lens fabrication. As technology in general moves forward so does the demand for smaller, faster, less expensive, more accurate, and more reliable devices. A high performance, low cost IC would effectively penetrate the market and drive technology for remote temperature sensing.

Previous research on products from other manufacturers provided ADI with a general understanding of IR temperature sensing devices. They further researched the implications of entering the IR sensing market and decided to focus their attention on industrial spot pyrometers, handheld thermometers, ear thermometers, and automotive applications. With specific applications in mind, ADI developed a microelectromechanical system (mems) to integrate the entire temperature measurement process from sensing to signal processing onto a single integrated circuit. They produced several IC's with single pixel, three-by-three pixel array, and eleven-by-eleven pixel array sensors to utilise in non-contact thermometry applications, but without any previous implementation they were limited to theoretical knowledge of the infrared detectors. ADI developed a program using LabVIEW which communicated with the detectors using a USB evaluation board. The software was able to determine if the parts were working and exhibiting the anticipated behaviour. Further development and testing was needed to understand, improve, and market the IR sensing integrated circuits.

ADI's next steps required enhanced software functionality and physical testing to ensure a marketable detector. ADI's requests were two-fold from the fabrication engineering and marketing department. Neither department had anything more than theoretical knowledge of the detector's actual capabilities. The single pixel, three-by-three pixel array, and eleven-by-eleven pixel array detectors had yet to be calibrated or tested for functionality by ADI engineers. The fabrication engineering department requested test data and thorough analysis of the detectors' accuracy and reliability. The marketing department required this information as well but simply to offer a characterisation of the detector to potential customers. Time and fabrication constraints led to a primary focus on developing a full understanding of the three-by-three array which would provide methodologies applicable to the single pixel and eleven-by-eleven

pixel arrays. The scope for this project was to develop a demonstration setup for the three-by-three array and a small-scale thermal imaging demonstration utilising the eleven-by-eleven array along with LabVIEW software to give to customers with an evaluation board which provides a preview of the detectors' capabilities.

This project took a first look at the actual behaviour of the next generation integrated IR sensing systems developed by ADI. It required attention to the needs of the fabrication engineering and marketing departments working toward a successful emergence in the IR temperature sensing market. This project provides an in depth guide to understanding the detectors and details methodologies capable of obtaining data to develop expectations of performance in a given application. It also offers an assortment of software evaluation methods for data viewing and analysis. The final portion of the report supplies ADI with next steps to both improve upon the current technology and to enhance the marketing demonstration.

2 Background

The following chapter contains information essential to understanding the properties of infrared radiation and the technology behind IR thermometry. It presents a basic explanation of what causes IR and the laws that govern it. It further provides an understanding of the spatial characteristics of IR sensing in order to explain its thermal imaging capabilities. It then details parameters used to characterise non-contact thermometry IR devices and gives background information on the integrated circuit solutions that are currently being tested at ADI.

2.1 Infrared Radiation Thermometry

Infrared radiation is an invisible, yet tangible phenomenon that is emitted and absorbed by all physical objects. IR is the reason a fire keeps you warm in the winter and why the inside temperature of a car rises on a hot day. Without physical contact, heat emission, absorption, and transfer occur between all objects. The understanding of IR begins on an atomic level with the notion that every atom is in a continuous state of motion. These atoms in motion are constantly losing and gaining electrons as they collide with one another. All atoms hence have variable electric fields, which lead to alternating magnetic fields. The electric and magnetic components together create what is known as electromagnetic radiation. The electromagnetic radiation from an object that falls within the IR spectrum is a quantity the can be measured through non-contact methods to determine the temperature of a given object. The infrared region of the spectrum includes the wavelengths that are longer than visible light, but shorter than radio waves. The literal translation or infrared is “below red” because it has shorter wavelengths than red light which has the longest wavelengths in the visible spectrum.

2.1.1 Electromagnetic Spectrum

Electromagnetic waves can be characterised by their wavelengths and intensities. The wavelength of the IR has an inverse relation to the heat of the object. As the object gets hotter, the wavelength becomes shorter and vice versa. Extremely hot objects with wavelengths between 0.4μm and 0.7μm fall in the visible portion of the electromagnetic spectrum and can be viewed by the human eye. Cooler objects radiate light in the infrared region, which is not visible. For example, human skin radiates electromagnetic waves with wavelengths between 5μm and 15μm, which falls in the IR range, and hence is not visible (Sandberg 88). The infrared portion of the spectrum is roughly between 1mm and 0.75μm as shown in Figure 1.

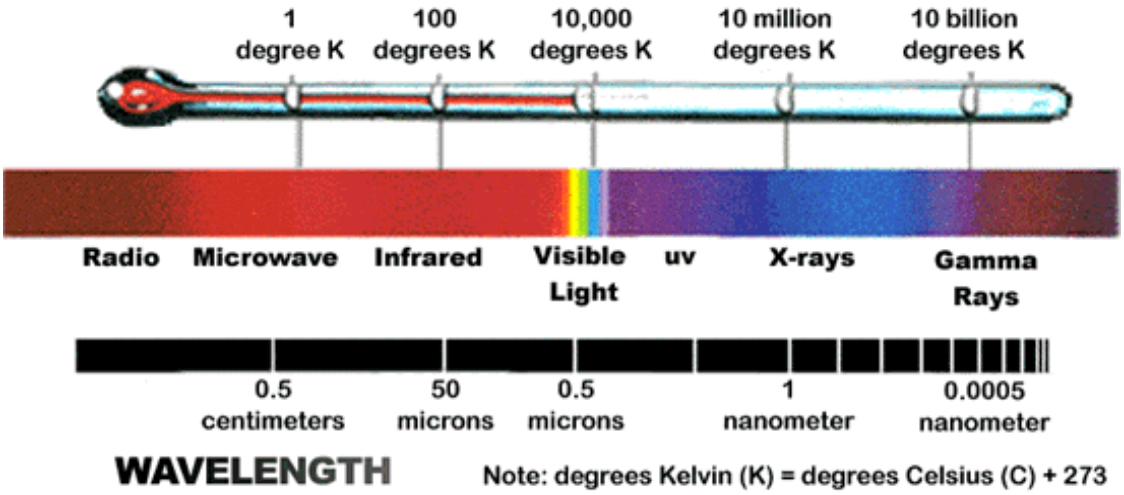

Figure 1: The electromagnetic spectrum (Porro, Irene and Kathryn Flanagan)

2.1.2 Fundamental Laws of Infrared Radiation

There are two fundamental laws that explain the quantification of IR and the relationship between temperature and wavelength. The first law, represented by Equation 1, is Planck's law. Planck's law quantifies the relationship between wavelength (λ) and absolute temperature (T) according to the emissivity of an object and the power or intensity emitted per unit of wavelength.

Equation 1: Planck's Law

$$W_\lambda = \frac{\varepsilon(\lambda).C_1}{\pi.\lambda^5(e^{C_2/\lambda T} - 1)}$$

where,
W_λ = power per unit wavelength
$\varepsilon(\lambda)$= Emissivity of an object
$C_1 = 3.74*10^{-12}$ Wcm^2
$C_2 = 1.44cmK$

While Planck's Law provides the most accurate interpretation of the relationship between temperature and wavelength, the equation is complex and does not lend itself well to quick numerical calculations. A simpler approximation of this equation is Wien's Law which is given in Equation 2.

Equation 2: Wien's Law

$$W_\lambda = \frac{C_1}{\pi}\varepsilon(\lambda)\lambda^{-5}e^{C_2/\lambda T}$$

A more intuitive approximation of Wien's Law is given in Equation 3. This equation is valid because temperature is a measure of the kinetic energy in an object. The kinetic energy relates to a frequency and therefore wavelength of a given wave. To find the wavelength, the first derivative of Equation 2 is equated to zero giving Equation 3.

Equation 3: Wien's Law

$$\lambda = \frac{2898}{T}$$

From this equation, we can easily see that Wien's Law confirms the inverse relationship between the temperature (T) of an object in Kelvin and the wavelength (λ) of the IR in microns. It indicates the expected wavelength for a given temperature. With this known wavelength, information can further be obtained about the spectral radiance of the emitter which is discussed further in the next section.

2.1.3 Spectral Radiance and the Blackbody Source

The spectral radiance of an object is the amount of IR emitted per unit wavelength of a given source. The wavelengths of interest for infrared sensing fall between 3μm to 10μm, covering the temperature range between 200K and 800K. This area in the infrared spectrum is the foundation for non-contact thermometry. The relationship between the spectral radiance, wavelength, and associated temperature are shown in Figure 2. This figure shows the spectral radiances under ideal conditions.

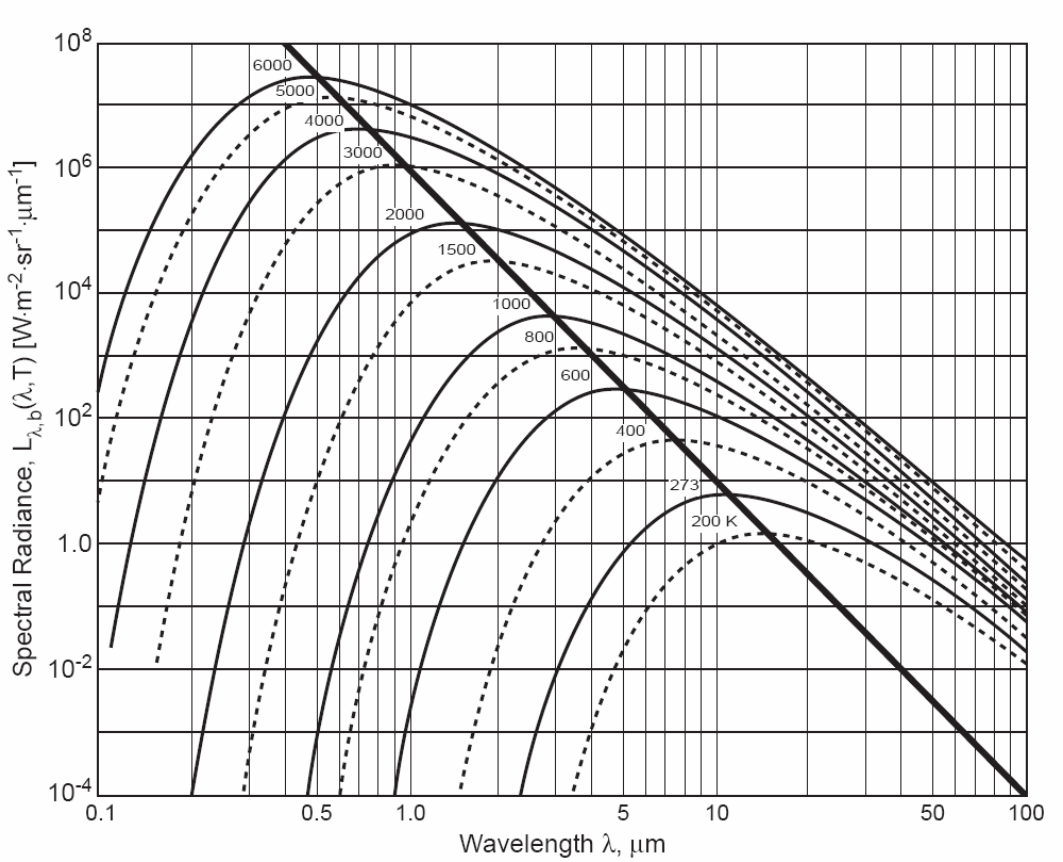

Figure 2: Spectral radiance of a blackbody at different temperatures (Sandberg 89).

The spectral radiances in Figure 2 are considered ideal values because they are those calculated for the blackbody source. A blackbody source is an ideal emitter and absorber of electromagnetic radiation. Ideal means having an emissivity of one. Emissivity is a ratio between zero and one of the amount of radiation emitted from a surface to the amount that would be emitted from a blackbody source at the same temperature. Ideal blackbody sources with emissivities of one do not exist in reality, but there are practical blackbodies made that have an emissivity close to one. The blackbody is the most accurate device for the calibration of non-contact infrared thermometers.

2.1.4 Non-contact Sensing Methods

Non-contact heat detectors utilise the temperature difference between a reference point and a variable IR absorber. Thermopiles and bolometers are two types of non-contact sensors which measure temperature using an induced or referenced voltage. Both thermopiles and bolometers are currently used in industry. ADI developed prototype devices with both types of sensors to explore the implications of each for future product releases.

2.1.4.1 Thermopiles

A thermopile is multiple thermocouples connected in series to amplify an induced voltage created by each thermocouple. A thermocouple consists of two different conducting materials that are connected at one end (hot junction), while the other two ends are attached to a voltage meter (cold junction). A temperature gradient exists across each material as a result of the two junctions as shown in Figure 3.

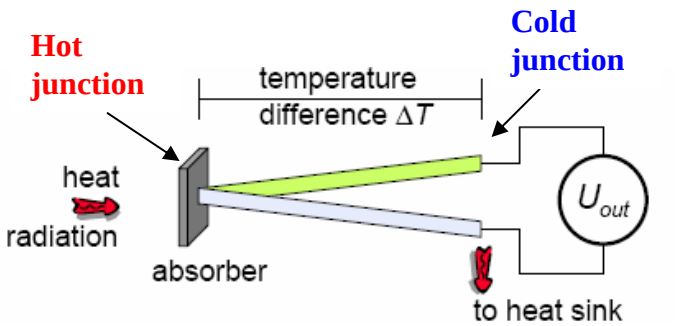

Figure 3: Thermocouple (Schilz, pg.3)

A thermometric property known as the Seebeck effect explains that where there is a temperature gradient, there is also an electric field. A voltage is induced by the electric field as a result of the temperature difference between the hot and the cold junctions. This voltage can then be measured and the temperature determined using the voltage and known Seebeck coefficients of the two conductors. The current semiconductor technology allows the production of thermopiles with hundreds of thermocouples in a small area. They are preferred over bolometers in applications that require a quick response (Schilz, pg.3).

2.1.4.2 Bolometers

Bolometers are small resistive temperature devices (RTDs) integrated with infrared absorption material that can absorb anything from infrared to microwave radiation. When used in infrared applications, bolometers are structures with extremely thin frames and a relatively large cross-sectional area as shown in Figure 4.

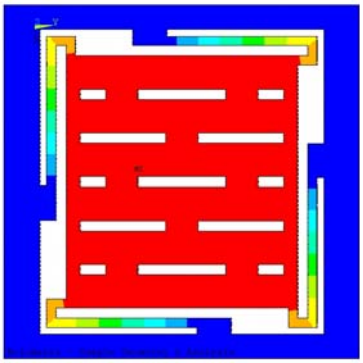

Figure 4: Bolometer

The un-shaded areas in Figure 4 represent air gaps to allow air circulation beneath the sensing element for thermal isolation from the rest of the device. The gradient shows the heat distribution across the IR absorbing element. The thin frame minimises heat loss due to diffusion across the contact points with the rest of the device. Bolometers make use of a bias voltage which is external to the device to convert the resistance change of the sensing element to a change in temperature. They are commonly used in two-dimensional arrays with as many as 80,000 sensors for thermal imaging (Sandberg 99).

2.2 Thermal Imaging and Spatial Characteristics of IR

In addition to making single spot measurements, non-contact thermometry sensors can be used in arrays to create thermal images for a spatial understanding of the IR emitted from an object or objects. Arrays of sensors can be used to make two-dimensional images while multiple arrays at different viewing angles can be used to make three-dimensional images. For the purposes of this project, the focus remains on two-dimensional imaging. ADI is planning to emerge in the IR sensing market with sensor arrays capable of small-scale thermal imaging. The arrays are able to create an image because with a lens, each pixel in the array views a slightly shifted area from the one adjacent to it. The thermal imaging capabilities of a sensor are determined by its lens, spatial characteristics regarding the distance-to-spot ratio, and the size of the array.

2.2.1 Thermal Imaging

In traditional photography, the sensing devices record the light characteristics of an object or objects to form an image. Thermal imaging, however, utilises infrared emissions rather than light to generate a picture of the heat characteristics. An infrared thermal imager measures the IR emission and translates it using a temperature-colour scale as shown in Figure 5. The thermal image makes it relatively simple to identify the hot and cold spots of the object or objects in the viewing area of the sensor.

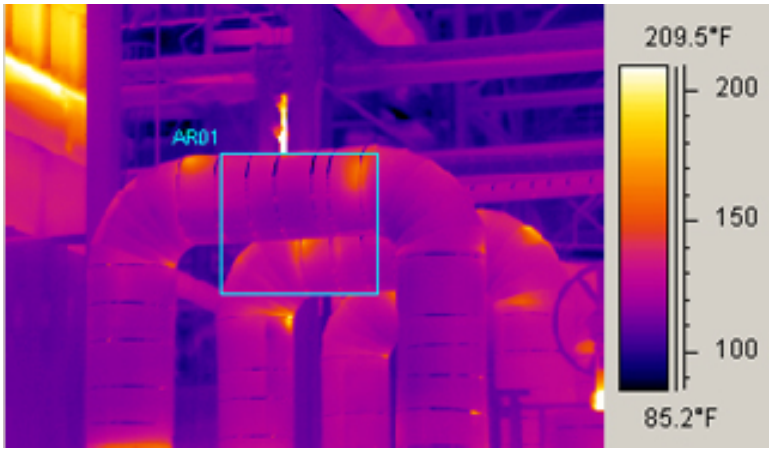

Figure 5: Thermal image of pipes in a factory (infrared1.com)

Thermal imaging is an applicable monitoring technique for many industries. The ability to continuously monitor the temperature of an object or objects protects both the people and the equipment involved in a process. It is also valuable because it obtains information about an object or objects that cannot be seen with the naked eye. As thermal imaging devices become less expensive and easier to implement, they are being used more in everyday consumer applications broadening the market for IR sensing devices.

2.2.2 Distance-to-Spot Ratio

The quality of an infrared image is determined by the distance-to-spot ratio of the sensing device. The distance-to-spot ratio is a comparison of the distance between the object and the sensor to the diameter of the spot being measured. As shown in Figure 6, the absorption area resembles a cone. A sensor with a 6:1 distance-to-spot ratio absorbs IR from a one-inch diameter spot when it is six inches from the object. The ratio grows proportionally, so when the distance doubles, the spot size does as well.

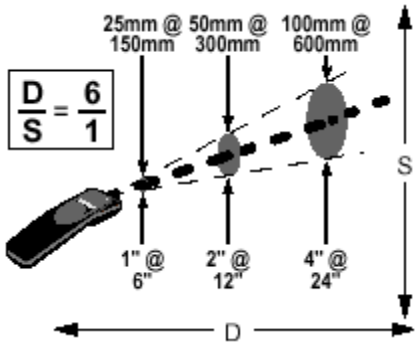

Figure 6: Distance to spot ratio of an IR thermometer

The distance to spot ratio is determined by the focal point of the lens and the packaging which is limiting the viewing area of the sensor. It is an extremely important parameter because in order to gain accurate measurements of an area or areas, the spot

which represents the field of view must be smaller than the object of interest. The most precise results are obtained when the size of the spot being measured is smaller than the object emitting the IR (Gruner, 2003).

2.2.3 Array Size and Implications

Another important parameter in thermal imaging is the size of the sensor array in the device. With a sensor array, multiple temperature readings can be taken at a given time. Each pixel in the array has a similar but slightly varied view of the object. The distance to spot ratio can be applied not only to the overall field of view of the device, but to the field of view of the individual pixels as well. Figure 7 displays a possible pixel and array field of view. The dotted circles represent the field of view of each of the sensors in the array, but the square corresponds to where that circle would be represented on a thermal image. Different types of lenses change the specific shape of the area and how the field of view circles overlap, but it is impossible to define clear borders for the pixels that would cause no overlap and leave no gaps.

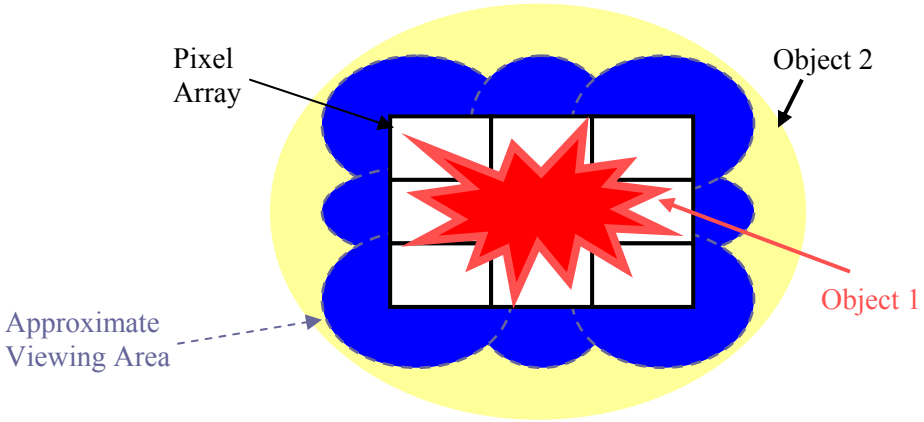

Figure 7: Pixel and array viewing area

Figure 7 also emphasises the importance of understanding the field of view of a sensing device. Suppose the red and yellow shapes are objects. Object 1 is in front of and hotter than the object 2. If a user wanted to measure just the temperature of object 1 using all nine pixels, the measurement would not be accurate from this distance. IR would also be absorbed from the object 2 lowering the reading at each of the pixels except for the centre one. For an accurate absolute temperature reading, the object of interest must fill the entire field of view. Accurate temperature measurements however could be obtained of the object 2 because the field of view is contained inside the object.

If absolute temperature measurements are not required for an application, a useful thermal image can be produced of the object or objects in the field of view. Because of the small number of pixels in this example, the thermal image would be a useful but would have low resolution. The image could still identify a single hot spot, cold spot, or

a significant thermal transition in the field of view. Larger pixel arrays increase resolution and produce higher quality images, more accurate temperature representations, and greater differentiation between hot and cold spots. Without any previous experience working with IR thermometry, ADI recognises the key to successfully producing pixel arrays of various sizes with multiple applications is to understand their small-scale fundamental behaviour.

3 Product Description

As an industrial leader in innovative and high performance signal processing solutions, ADI is planning their emergence with unique IR sensing technology. After studying the current technology and range of devices available, ADI developed a series of integrated devices that join their expertise in semiconductors with newly developed IR sensors. They combine all portions of the IR sensing system using a microelectromechanical system (mems). ADI's devices place the lens, sensors, ambient temperature monitoring, signal conditioning, and analogue-to-digital conversion on a single integrated circuit (IC). They have developed the products in Figure 8 to facilitate testing, analysis and their technology demonstrations. The Round evaluation board utilises J-Leaded Chip Carrier (JLCC) packaging, and the square board uses a Dual-inline Package (DIP).

The product provided by ADI for the purposes of this project is represented by the block diagram in Figure 9. The product can be broken down into three main system blocks, the IC packaged prototypes with thermopile or bolometer sensors, the USB evaluation boards that provide an interface between the ICs and a computer, and the LabVIEW ADiR Evaluation Software (AES). Each of these system blocks is discussed in the subsequent sections. The product is then further detailed in relation to the implications that arise during testing procedures.

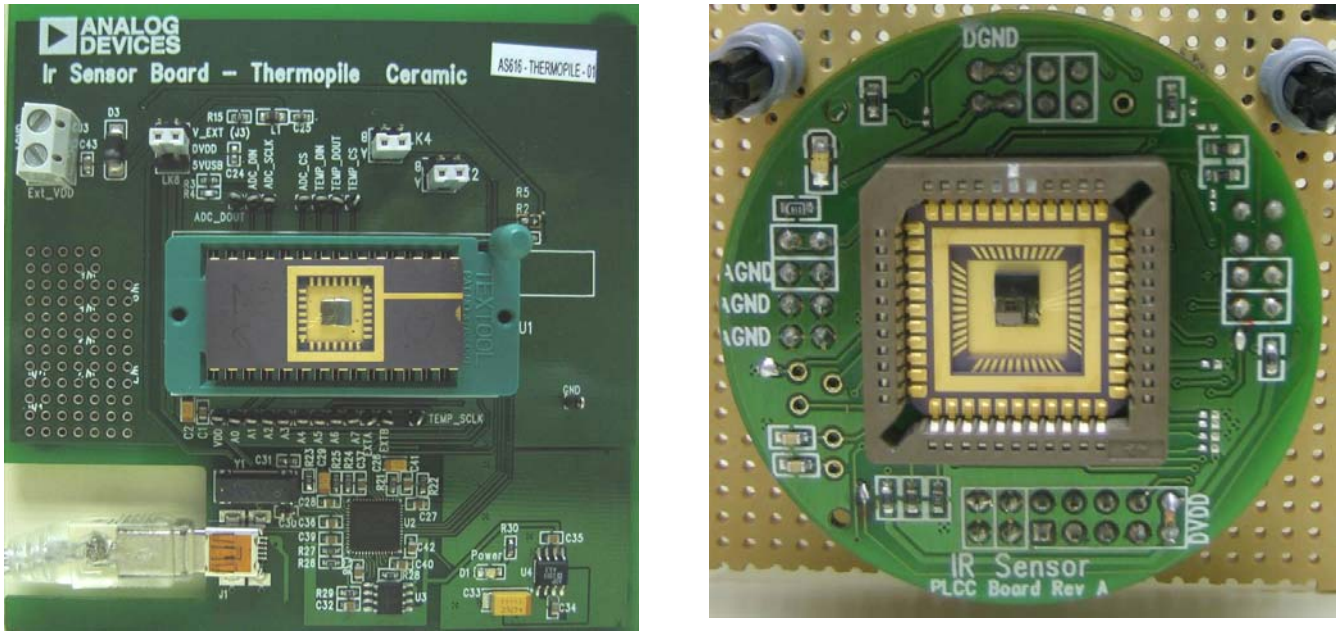

Figure 8: JLCC (left) and DIP (right) packages and evaluation boards

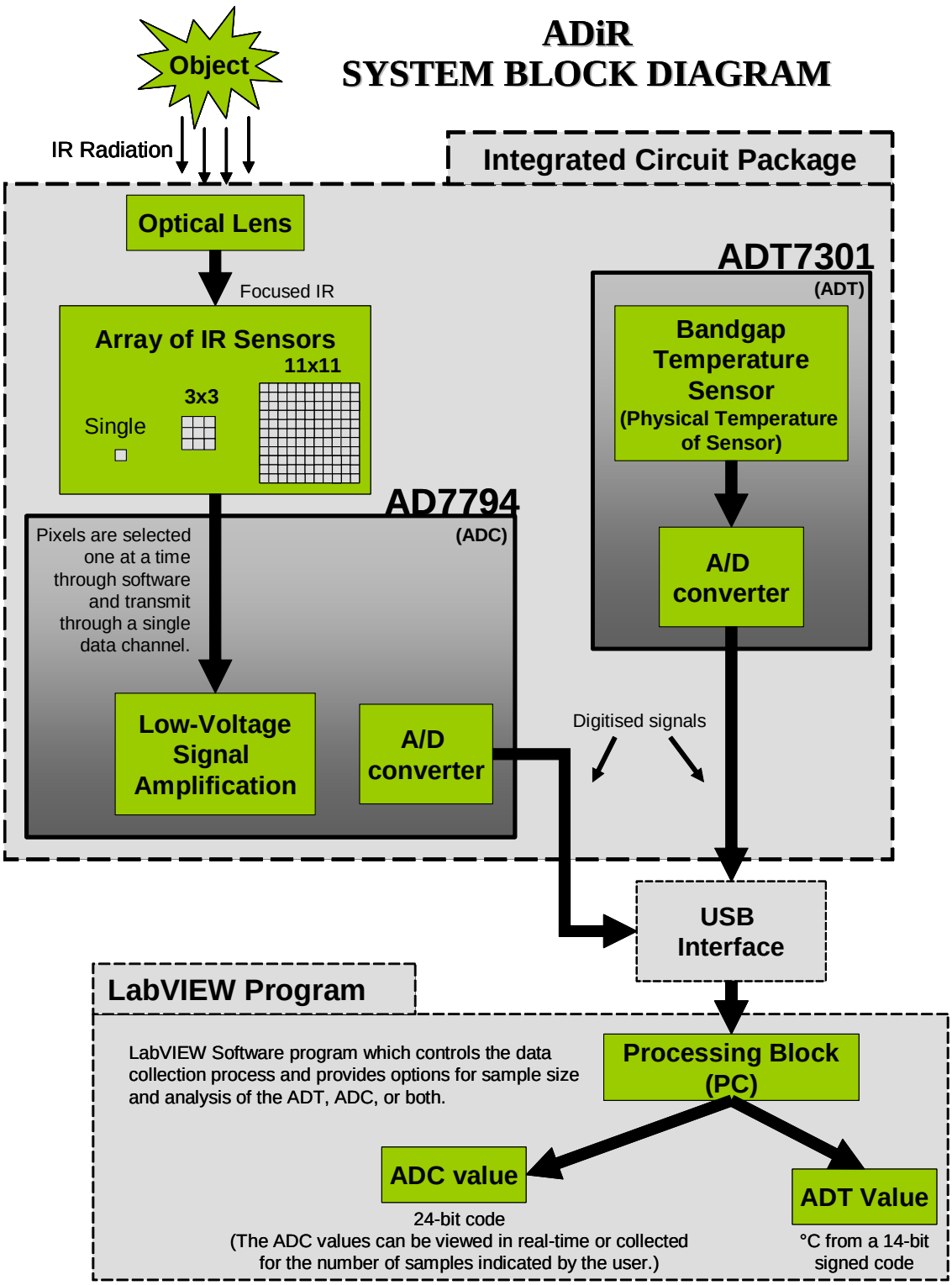

Figure 9: System block diagram for ADI's IR sensing system.

3.1 ADI's JLCC and DIP IR Detectors

The first system block is the one for the integrated circuit packages. ADI fabricated three different integrated circuits to test and characterise their new technology. The three ICs include a single pixel sensor, a three-by-three sensor array, and an eleven-by-eleven sensor array. The labels for each sensor were assigned according to their location on the wafer and are written on the back of the detectors. The current ICs are for testing purposes only and do not resemble the future packaged product. Each integrated circuit contains a diffractive single step phase lens, a thermopile sensor or sensors depending on whether it is a single pixel or array, analogue-to-digital converter, and a bandgap temperature sensor. Each device utilises the same design pattern shown in the Integrated Circuit Package block in Figure 9.

The system starts with the absorption of IR by the sensor through a single step phase lens with diffractive grating. The lens significantly affects the directivity of the pixels in the sensor arrays. As it was the first lens designed for the product, it is not ideal or the lens that will be used on the final product, but it is essential to understand the lens properties in light of the implications it had for this project. The lens, placed over the pixels as shown in Figure 10, creates signal gain and focuses the IR on the centre pixel causing that pixel to see a larger percentage of the incoming IR and more accurately measure the temperature. This characteristic is referred to as directivity. High directivity allows objects with lower intensities to be accurately measured at greater distances giving the sensor a high the distance to spot ratio (Travers, Jahanzeb, Butler, and Çelik-Butler, 1997). Because the lens is so close to the sensors however, it had a considerable effect on the image quality at the outside pixels in the array. For the real image to reach the outside thermopiles, it would have to propagate at a sixty degree angle of incidence. As a result the sensors receive a less intense signal and cannot see the real image, what they do see is a virtual image from IR that has been diffracted. A virtual image is a representation of an object in a position where it does not exist. The virtual image is seen because the lens is too close to the sensor causing the sensor to see an image that is not actually in the field of view. As a result, this particular detector needed to be appropriately manipulated to have imaging capabilities.

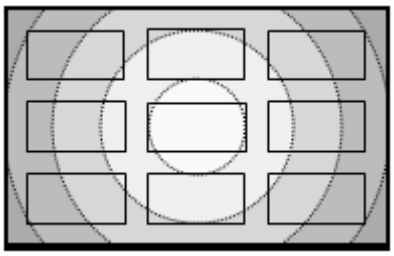

Figure 10: Diffractive lens for the ADI prototypes

To measure temperature, the sensor absorbs the IR and outputs a voltage proportional to the radiation absorbed, which means the greater the temperature, the higher the voltage. The voltage is a result of the difference between the ambient temperature of the device and the incoming IR. For accurate measurements, the IR temperature sensing materials must be thermally isolated from the silicon substrate by an air cavity. Figure 11 gives a side view of the sensor with the air cavity beneath it.

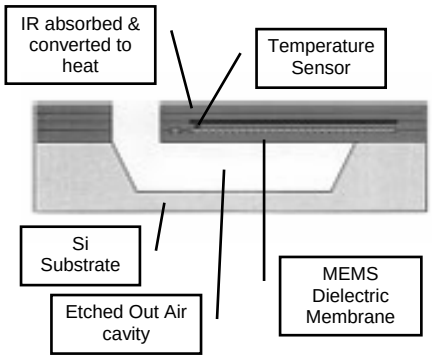

Figure 11: Cross section view of MEMS thermally isolated sensor technology (IR to Digital: FAE Training).

The next part in the IC Package block is an ADT7301 bandgap temperature sensor. The ADT7301 outputs a 14-bit digital signal which represents the ambient temperature of the sensors, while the AD7794 relays the signal received from the thermopile sensor. The ADT7301 is a 14-bit temperature sensor that is accurate within 1°C. The sensor itself consists of two PNP diodes with programmable current sources. Two different currents are forced through the diodes, which correspond to the temperature of the sensor. The current is based on the physical properties of the diodes, so the actual current varies between sensors. However, since there are two diodes that are supplied two different currents, the ADT7301 is able to calibrate itself and to measure its temperature consistently. The ADT7301 then converts the analogue signal representing the temperature to a 14-bit digital signal which is retrieved by the AES. Typically, the output of the ADT7301 would be translated directly as the ambient temperature. In this application, however, the ADT7301's sensor is separated from the rest of its circuitry. A figure showing the sensor placement is provided in Figure 12. The sensor is placed adjacent to the thermopile sensors and connected by wire leads. In this case the temperature measured is the temperature of the thermopile sensor bodies plus an offset and gain factor introduced by the wire leads. This device will hence require calibration to be accurate.

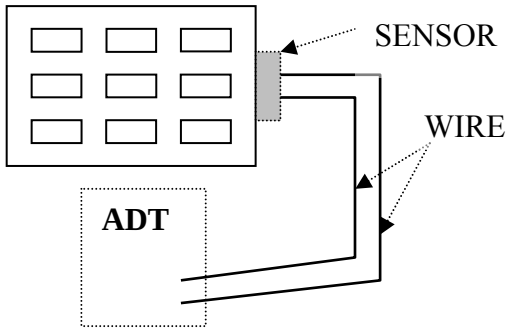

Figure 12: Diagram showing the sensor placement of the ADT7301.

The final part of the IC Package block is an AD7794 analogue-to-digital converter. The purpose of the AD7794 is to digitise the signal received from the thermopile or the Bolometer. The AD7794 consists of a 24 bit Σ-Δ analogue-to-digital converter. The device also has a low-noise amplifier that allows signals of small amplitude to interface directly with it. The AD7794 can convert an analogue signal into a digital signal effective up to 23 bits. The AD7794 signal is then also transmitted to the AES, combined with the ADT7301 signal and translated to a temperature.

3.2 Evaluation Boards

The second system block is the USB interfacing. ADI produced two USB evaluation boards that connect to a computer through a standard USB cable. Each board requires a different type of physical packaging. The Round USB board shown in Figure 8 uses a JLCC package. This board is smaller and the USB connection is on the back of the board. The prototype packages, however, are difficult to insert into and remove from the board because insertion force is required, and are very delicate with exposed contacts and no cover. If not done properly, the contacts can break or short rendering the package unusable for further testing. The other board is a DIP USB board, which uses a Dual In-line Package (DIP) chip. This chip is much easier to handle because it requires no force to install. The board, however, is bigger, and the USB connection is on the front of the board which is less convenient for test setups that require the evaluation board to be mounted.

3.3 ADiR Evaluation Software Capabilities

In order to evaluate the prototype devices using the USB evaluation boards, ADI wrote a program in LabVIEW to collect and present the data output by the devices. LabVIEW is a tool that allows users to create Virtual Instruments on a PC. It is a programming language like C++ or Java, but with two main differences. First, LabVIEW is almost entirely graphical; instead of writing lines of code for a program, you create a user interface first, and then make a multi-layer block diagram, which acts as the code.

The interface can display numerical fields, switches, graphs, dials, and other common measuring tools. Second, LabVIEW programs execute by data flow, not sequentially like in C++ or Java. If there are two sets of block diagrams on a page that do not interact, they appear to occur simultaneously. The high data processing speed of the software makes it impossible to tell which one executes first. The AES created by ADI used LabVIEW to communicate with the IR sensing devices through a USB port on the evaluation boards.

3.3.1 User Interface

The AES offers two different modes of collecting data. Each mode is accessed by selecting the corresponding tab. The first mode is Real Time. This mode collects the sensor's AD7794 and ADT7301 data then displays them on two separate graphs. Data is collected and compiled until the user presses the stop button. The graph of compiled data remains until the start button is pressed again clearing the data cache.

The other mode, titled Analysis, collects a user-specified number of samples for the AD7794 and ADT7301 before displaying a graph for each. Analysis mode also provides the minimums, maximums, and means for the collected data, and provides an option for saving the data to a file in either decimal or hexadecimal format. A codes/volts button changes the display to show either the output code from the AD7794 or the output voltage from the sensor.

There are further a few buttons and options that are available for both modes of operation. First, is a reset button that resets the settings to the default detector settings. Next are a setup button that opens a menu with configuration parameters for the device and options to turn on or off the AD7794 or ADT7301 data collection and an exit button that closes the program.

3.3.2 Main Process Loop

In the main loop of the program, the AES monitors the activity of select buttons and responds accordingly. It first checks if the Quit button is pressed, and quits the program if it was pressed. It then checks if the Reset button is pressed, and resets the settings to the default setup if it was pressed. Then it checks if the Codes/Volts button on the Analysis tab is pressed, and updates the graphs on the Analysis tab if it was pressed. Then, if the Setup button is pressed, the setup menu is displayed. Finally, if either of the Start buttons is pressed under each tab, then the program begins to display or collect data.

3.3.3 Data Collection

Figure 13 is a pictorial representation of the data collection process executed in the software. The process begins at the red box, which is the USB evaluation board. Once the device is plugged into the computer, the LabVIEW program is able to run and

collect data. An option is then available to view the data in real-time or to log a specified number of samples before displaying the data as shown in the two graphs. The real-time mode continues running until the stop button is pressed whereas the analysis mode stops once the data collection is complete. The analysis mode also displays the min, max, mean, spread, and RMS noise of the sample. If the user pushes the save to file button before collecting the samples, the data is logged and available for later use.

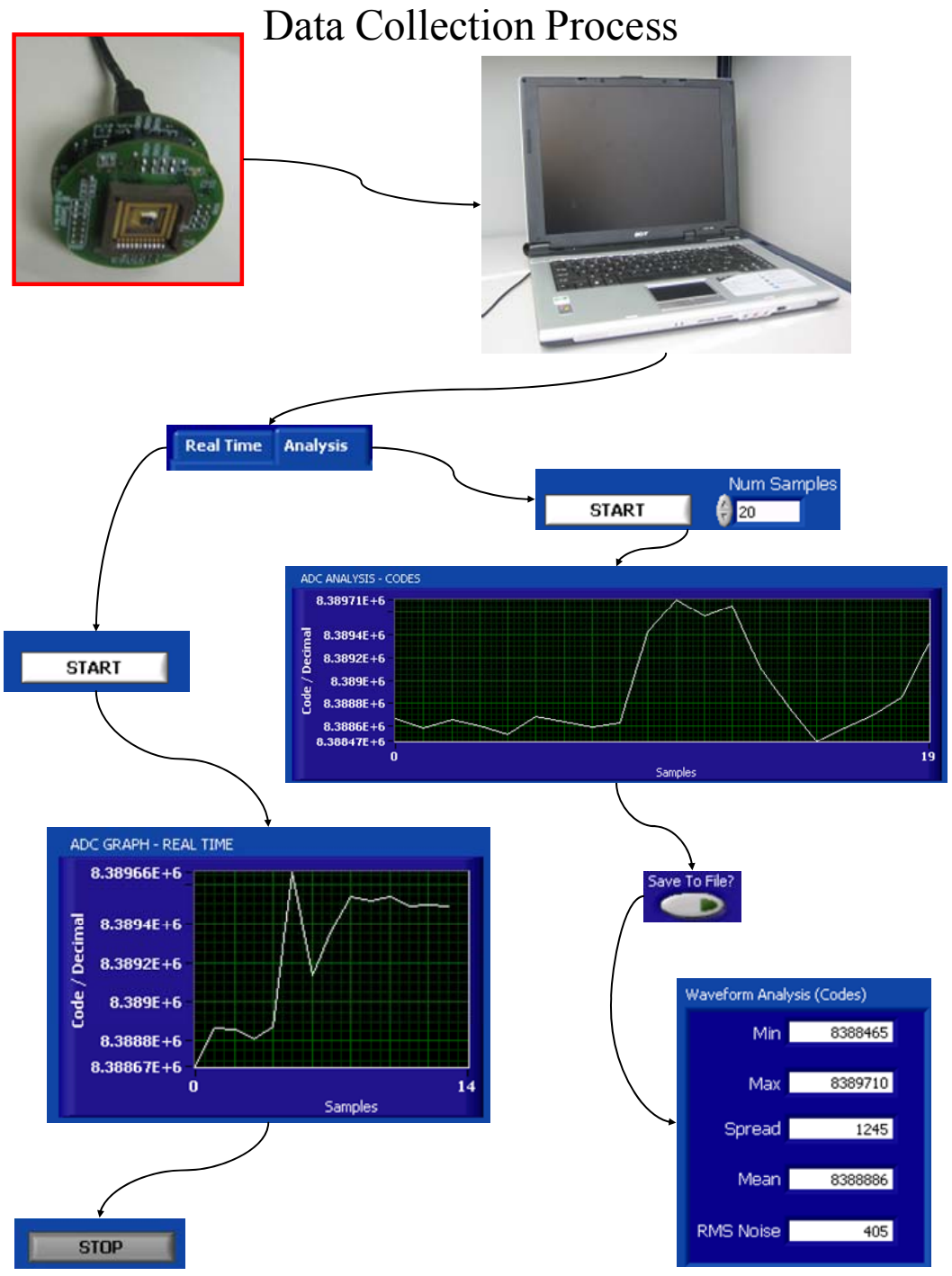

Figure 13: System diagram for the data collection process

3.4 ADiR Detector System

Prior to this project, the single pixel and three-by-three prototype devices had verified functionality using the prototype sensors, evaluation boards, and AES provided by ADI. The eleven-by-eleven prototypes, however, had not yet been physically implemented. The full system, utilising the detectors, evaluation boards, and AES to obtain a temperature reading or thermal image was not implemented by the ADI engineers prior to this project.

4 Goals and Objectives

The goals and objectives established addressed engineering and marketing needs for the project. With only three months until the initial prototype release to customers, ADI needed to fully implement the detectors and develop a thorough understanding of their operation. The following goals and objectives were worked toward simultaneously until we reached the three major milestones: verification of test setups and procedures, production of an absolute temperature measurement with the three-by-three pixel array, and creation of a thermal image with the eleven-by-eleven pixel array.

- The first goal for the project was to fully implement the detectors and verify their functionality utilising a USB evaluation board and the AES provided by ADI. To achieve this goal, we:
  - Tested each of the detectors using the evaluation board to identify the working prototypes.
  - Tested each of the working detectors using the blackbody source.
  - Developed a general understanding of the different functional blocks of the ADiR detectors and how they interface.
- The second goal was to develop test setups and procedures that are accurate and repeatable. This goal required that we:
  - Learned how to use the temperature forcer to obtain data to characterise the behaviour of the ADT7301.
  - Created an experiment to understand the intensity of IR seen by each pixel for varying angles of incidence.
  - Designed an experiment using the blackbody source to characterise the behaviour of the thermopiles when exposed to a temperature range.
  - Controlled the environment surrounding the test setups to minimise unforeseen variables.
  - Rationalised any irregularities in the data through theoretical explanations or further physical testing.
- The third goal was to convert the data output from the detectors into an absolute temperature reading. To produce this we:
  - Calibrated the ADT7301 using data obtained from the temperature forcer testing to create an equation to adjust its output for offset and gain.
  - Set the AD7794 to self calibrate its offset and gain.
  - Calibrated the AD7794 output using the data collected from the blackbody testing to develop an equation to turn the output code into the temperature difference between the physical temperature sensor and the object of interest.

- Combined the ADT7301 and AD7794 calibrated outputs to produce the absolute temperature of the object.

❖ The fourth goal of the project was to redesign the AES to increase and improve the functionality it provides. In order to reach this goal we:
- Changed the software to communicate and retrieve samples from all of the pixels.
- Devised a method and procedure to obtain and save the data in useable formats.
- Removed redundant features in the software.
- Created two additional user interfaces to show the absolute temperature readings and thermal image display.

❖ The final goal was to develop a demonstration or proof of concept design to verify the functionality of the three-by-three and eleven-by-eleven pixel array detectors. For this final task we:
- Made a demonstration to show the ability of the three-by-three array to measure temperature with reasonable accuracy.
- Designed a setup which displays the imaging capabilities of the eleven-by-eleven pixel arrays.

The following chapters document the completion of the objectives and achievement of the goals. Chapter 5 details the methodology for designed the experiments and testing the detectors. Chapter 6 presents the data gathered which verified the methodologies used and enabled us to draw valid conclusions with quantifiable proof. Chapter 7 explains the changes made to the AES. Finally, Chapter 8 illustrates the setups used for proof of concept demonstrations that substantiates the claims for functionality asserted by ADI at the start of the project.

5 Methodology

After the goals and objectives for the project were delineated, the next step was to develop a methodology to reach those goals. The actual test development process spanned most of the length of the project. As our knowledge of the detectors increased through hands-on experimentation, so did our knowledge of infrared radiation and optics. The test setups and methodologies presented here represent the final versions which provided us with the data to make analyses and conclusions. Though the tests are applicable to both the three-by-three and eleven-by-eleven pixel arrays, they were conducted most with the three-by-three arrays. The immediate demand to create a thermal image did not require calibration of the detectors. Eleven-by-eleven detectors were tested using these methods for comparison purposes.

5.1 ADT7301 Calibration

As mentioned earlier, the purpose of the ADT7301 in the overall system is to monitor the temperature of the physical sensors. In the device that ADI developed, the sensors are not capable of determining an absolute temperature. The sensors are thermopiles that can only measure the temperature difference between its own body temperature and the incoming IR. The ADT7301 provides the detector system with the body temperature. The absolute temperature of the object can be determined by adding temperature difference extracted from the code output of the AD7794 to the calibrated temperature output of the ADT7301.

5.1.1 Purpose for ADT7301 Calibration

Calibration of the ADT7301 is necessary in order to eliminate the offset and gain introduced by the wire lead connection between the ADT7301 and its sensor as explained in section 3.1. The sensor is placed next to the thermopile array for the most accurate physical temperature readings of the sensors. It is thought that the thermopile sensor bodies themselves would be hotter than the rest of the chip. This is critical because the final temperature reading of an object is the temperature output of the ADT7301 added to the difference of temperature of the object and the physical temperature of the thermopile sensors themselves. If the ADT7301 measurement is off by a few degrees, then so will the measured temperature of the object.

5.1.2 Procedure for ADT7301 Calibration

To calibrate the ADT7301, a constant known temperature source was needed to eliminate temperature as a variable in order to develop an equation for the sensor output. A temperature forcer, which blows air through a tube at a specified temperature onto an object, was used for this calibration. The air path is sealed around the sensor so that the

air cannot escape from the tube or enter it at a different temperature. A thermocouple is used at the base of the tube to monitor the air temperature near the sensor and ensure that air is not escaping from somewhere in the system. If the forced air temperature is the same as the temperature reading from the thermocouple, then the system is well insulated and accurate. Figure 14 shows a diagram of the test setup.

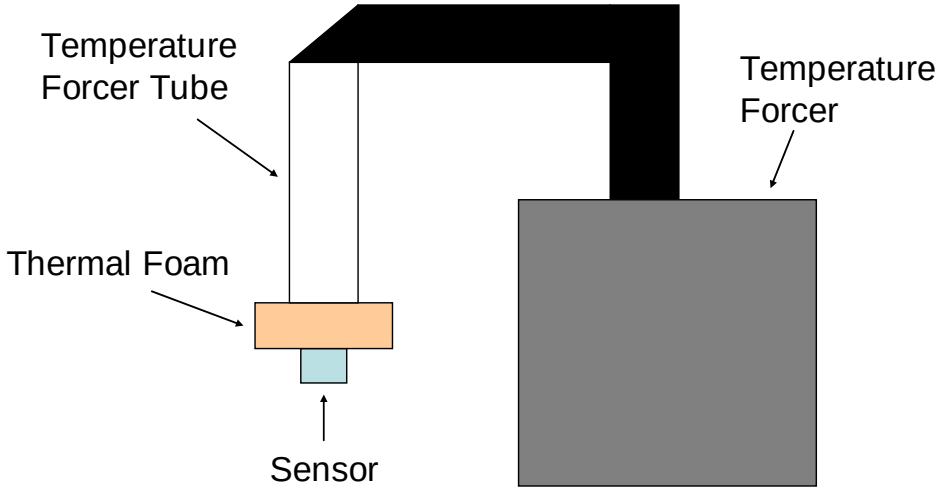

Figure 14: ADT7301 calibration setup

The temperature forcer was used over a temperature range from -25°C to 100°C in 5°C increments. Fifty samples were collected at each temperature from the ADT7301. This process was repeated for five three-by-three and one eleven-by-eleven sensors.

5.2 Angular Response Test

The initial ADiR prototypes are raw detectors packaged for testing purposes. As a result, they have no external packaging on the detectors to limit the field of view and they have a lens which utilises new technology. Before marketable packages can be made, the properties of the individual pixels and the lens must be determined. The packaging will be designed according the needs of the device. For these detectors, a diffractive single step phase lens was used and designed to focus IR onto the pixels. Each pixel has a slightly different field of view. Figure 15 shows the ideal response for a row of three pixels.

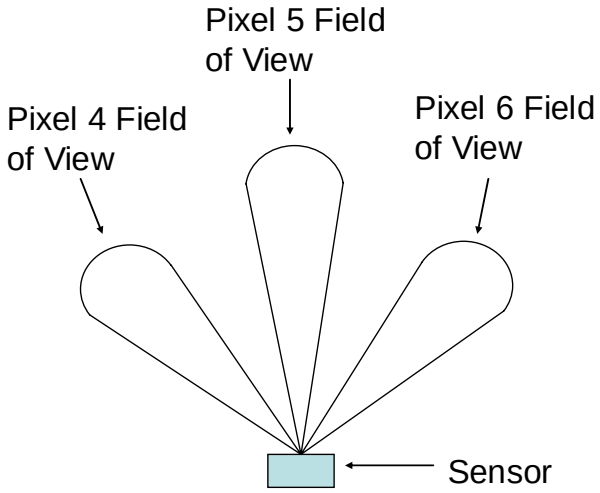

Figure 15: Field of view for pixels 4, 5, and 6

5.2.1 Purpose for Angular Response Testing

For thermal imaging purposes, it is important to know how each pixel receives infrared radiation incident at different angles. An understanding of this angular response is essential for determining the directivity of the pixels when IR is incident at a given angle as well as the calculating the signal-to-noise ratio. The lens utilised for the prototypes was designed to refocus the IR to enable it to be used for thermal imaging. Without a lens, all of the pixels would all nearly see the same image. Analysis of the lens design on the pixel directivity is essential to see the effectiveness of the lens design and implications for pixel responsivity.

5.2.2 Procedure for Angular Response Testing

In order to test the field of view of the pixels, the sensor was mounted on an apparatus designed using Lego pieces that rotates the sensor 180° horizontally and vertically. A diagram of the apparatus is shown in Figure 16. A point source was situated a few centimetres away from the sensor. The point source was used because it creates a small, concentrated beam of IR so that the lens can focus it on one pixel at a time, depending on the angle at which the sensor is placed with respect to the source. The entire setup is enclosed in a large cardboard box. The cardboard has a high emissivity value, so the IR from all parts of the box should be equal and can be easily distinguished as a uniform background to the sensor. The box also protects the experiment from stray IR coming from outside the setup. The output AD7794 codes were collected over the entire 180° range for each pixel, and the data were plotted on polar graphs to give us a representation of the response of each pixel at different angles.

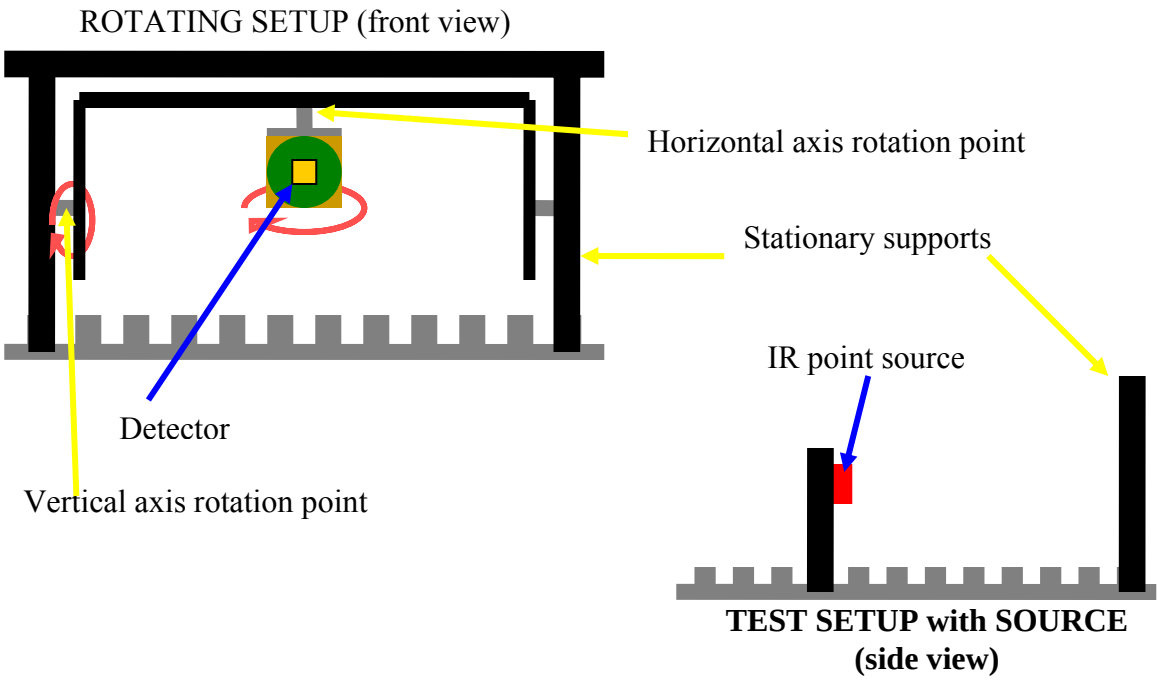

Figure 16: Sensor rotating apparatus without the surrounding cardboard box.

5.3 Pixel Response Test

Once a general understanding of the lens' effect on the directivity was determined, the pixel response was tested over a range of temperatures. This test provided the data necessary to develop equations to convert the AD7794 output code representing the thermopile temperature difference to degrees centigrade.

5.3.1 Purpose of the Pixel Response Test

To develop calibration equations for the detectors, they need to be tested multiple times to verify consistency in their results. The detectors also had to be tested for their response when used at different distance-to-spot ratios. Similarly to the ADT7301, a generic equation was preferred, but not likely to be possible for the prototypes currently available.

5.3.2 Procedure of the Pixel Response Test

For this test, the detector was placed in front of the blackbody source, and a metal plate with a round aperture was placed between the sensor and the blackbody. The plate filled the field of view of the sensor so that each pixel would detect a uniform background. The sizes of the apertures were chosen to control the spot size seen by the sensor. The metal plate was black on the side that faced the sensor so it would high emissivity, and shiny on the side that faced the blackbody so that stray IR coming from

the blackbody would be reflected away from the sensor. The entire setup was enclosed in a large cardboard box to eliminate extraneous IR in the environment. With a fixed spot size created by the aperture and a fixed temperature of the blackbody to emit a certain amount of IR, the response of each pixel was measured over a range of temperatures. A diagram of the setup is shown in Figure 17 without the cardboard box.

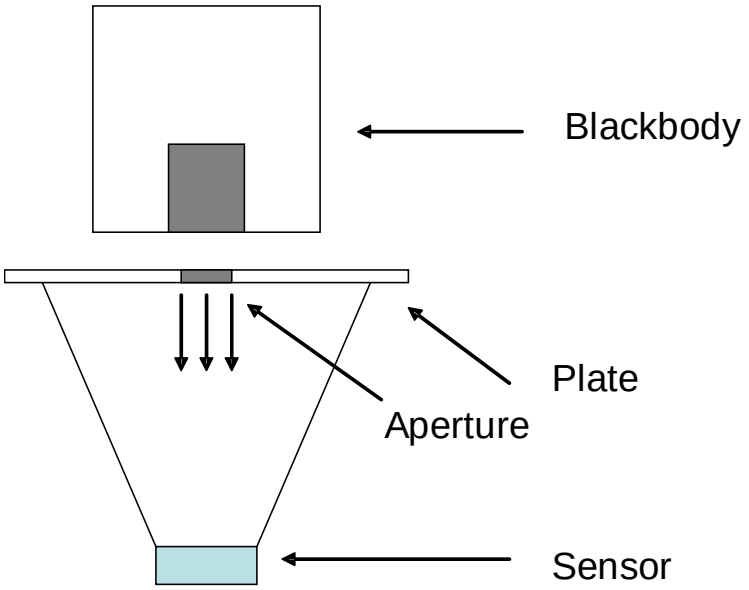

Figure 17: Pixel response test setup

The blackbody was 2cm from the reflective side of the aperture plate and sensor was 4 cm from the black side. The sensor was carefully aligned with the aperture in the plate. The apertures were 2cm, 1cm, and 5mm in diameter. Since the sensor had a large field of view, the distance between the sensor and aperture, the distance between the aperture and blackbody, and the aperture size had a great effect on the output code as they control the distance-to-spot ratio. The outputs of the detectors were expected to vary between apertures because they were being exposed to differing amounts of IR.

Once the setup was assembled, the AD7794 output codes for pixel five on the three-by-three pixel array and were collected over a blackbody range of 25°C to 300°C. A dataset containing 100 samples from the AD7794 and the ADT7301 was collected at each temperature across a temperature range. After a dataset was collected, the temperature of the cardboard box was measured in three places where it might be in view of the sensor. The temperature of the aperture was also then measured in five different places on the black side of the metal plate which faces the sensor. This was to ensure that the temperature of the box and aperture remained constant throughout the experiment.

Two different methods were utilised for varying the apertures in this experiment. Other variables were introduced with the metal aperture plates. The primary concerns

were heating of the aperture plate and correct alignment of the detector, aperture, and blackbody. To reduce the effects of the heating aperture plate the experimental method proposed was to sample all three apertures at a given temperature before incrementing. It was thought that switching the plates constantly would keep them from heating up and affecting the output. The other method suggested was to test only one aperture plate at a time leaving it stationary during the entire range of samples. Both test methods were utilised for a single detector in order to decide which method was preferred for future testing. Testing on further detectors was done utilising the method preferred after analysing the results of two test methods.

5.4 Heated Aperture Plate Test

Without the ability to create ideal conditions in a test setup, error sources are expected to exist. In order to maintain confidence in collected data, single-occurrence irregularities and unexpected results must be explained.

5.4.1 Purpose of the Heated Aperture Plate Test

After collecting and graphing data from the previous tests, there appeared to be a few sources of error. Multiple pixel response tests on a single sensor did not produce identical results. The characteristics were similar but slightly offset from one another. It was hypothesized that the temperature of the metal plate with the aperture was contributing significantly to the results. The main source of IR in the experiment was the IR that was allowed to pass thorough the aperture. The sensor however was seeing a much larger area than the aperture; it was seeing a large area of the metal plate. A small temperature difference in the plate temperature would be magnified in the sensor measurement. The purpose of this test was to verify the hypothesis and explain the error source in the collected data.

5.4.2 Procedure of the Heated Aperture Plate Test

The setup for the heated aperture plate test was physically identical to the test for pixel responsivity in Figure 17. For this test however, the box was not used, and the medium-sized aperture was first removed from the setup and heated above room temperature to about 30°C using the temperature forcer while the blackbody was heated to 150°C. Once heated to a given temperature, the aperture plate was retuned to the setup. Continuous data collection from the ADT7301 and AD7794 then began. In addition to the values from the ADT7301 and AD7794, the temperature of the aperture plate was recorded at four points surrounding the aperture. Samples were collected every thirty seconds for fifteen samples. Between samples, the detector was shielded from the blackbody using a piece of cardboard to prevent significant rise in the physical temperature of the sensor.

6 Data and Results

Once reliable test methods were developed, the next task was to collect and analyze the data produced by the experiments. This chapter documents the data and results collected from the tests in the previous methodology chapter.

6.1 ADT7301 Calibration

For use of the three-by-three pixel array as a non-contact thermometer, the outputs of the device had to be calibrated for an accurate output. As was mentioned earlier, though normally a self-calibrating device, the ADT7301 was altered for this design creating an offset and gain that needed to be eliminated from output temperature before it could be used in the final characteristic equation for the detector. The eleven-by-eleven detectors will eventually be calibrated for absolute temperature measurement as well, but for the purpose of this project the calibration was not necessary. The thermal image is produced by measuring the temperature difference indicated by the AD7794 output code without taking the ADT7301 into account. A single eleven-by-eleven detector has been temperature forced, however, but for observational purposes and for general comparison with the three-by-three array only. Figure 18 shows a photograph of the physical setup test setup. The methodology for this test is detailed in section 5.1.2.

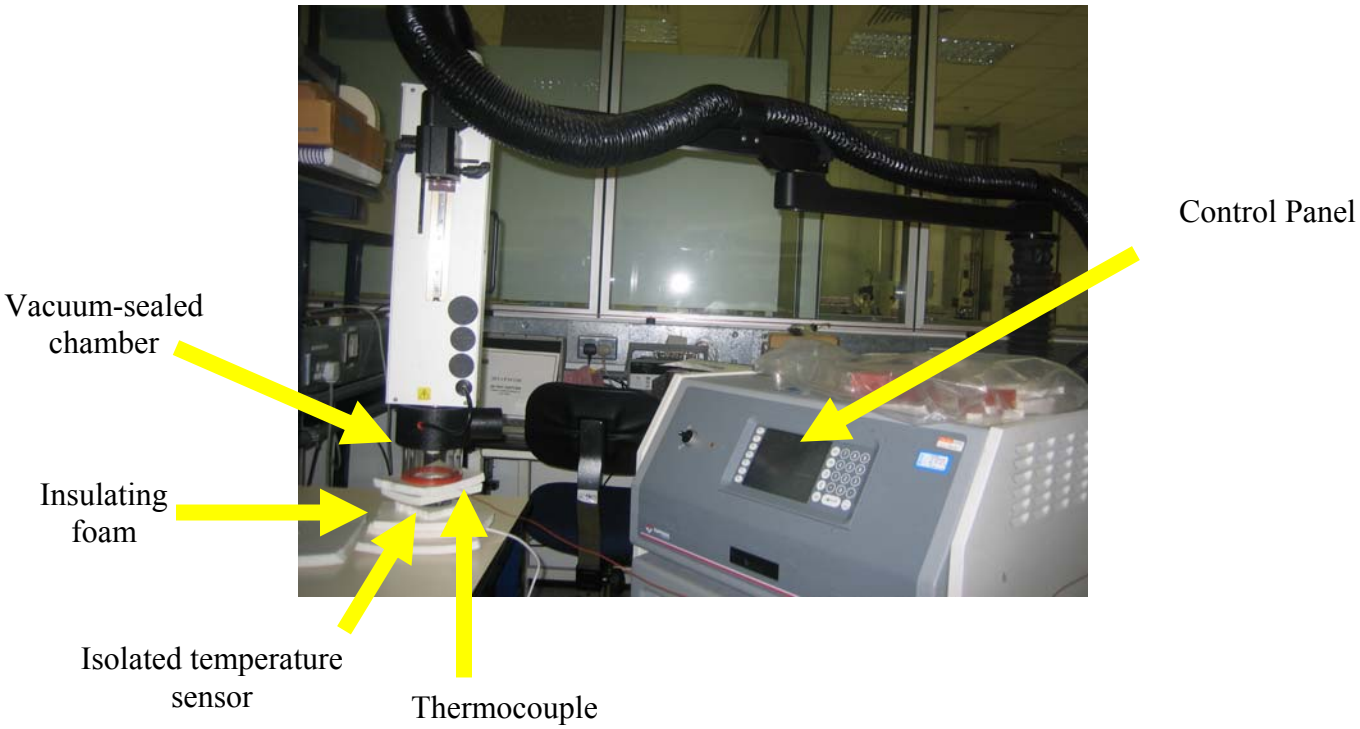

Figure 18: ADT7301 calibration setup

6.1.1 ADT7301 Calibration Data

To determine a characteristic equation for each device, the collected data was manipulated using averaging. After testing was completed on a unit, the 50 samples from the ADT7301 at each temperature were averaged. The resulting mean values were then plotted against the forced temperature as shown in Figure 19. The mean values and a calibration graph for each of the detectors are in Appendix A. The plot had the forced temperature on the x-axis and the averaged output from the ADT7301 on the y-axis. Next, a trend line was created for the sensor and its equation and r-squared value displayed on the graph using Excel. This was repeated for six sensors. A table of all the trend line equations with their corresponding sensor is shown in Figure 20 where y is the ADT7301 output and x is the actual forced temperature.

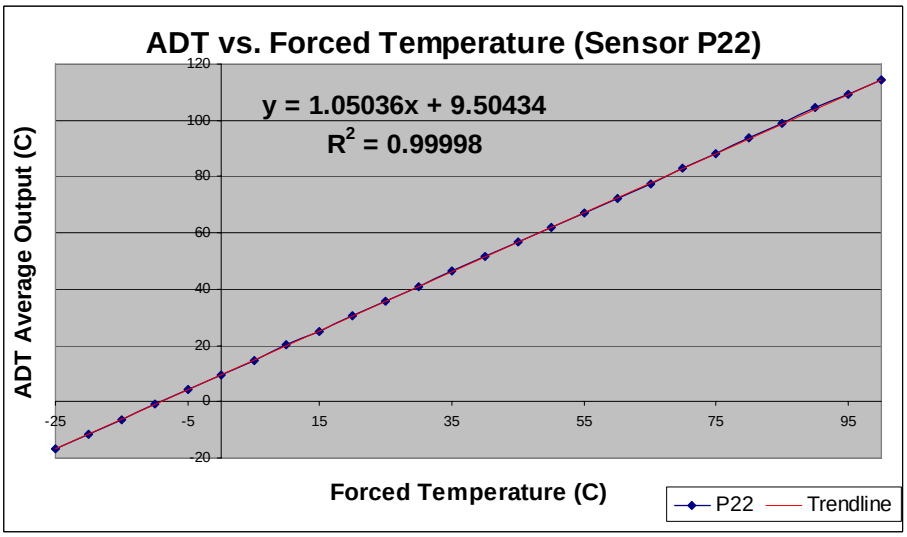

Figure 19: Forced temperature vs. ADT7301 output for detector P22

	Sensor	ADT7301 Linear Trend Line	r-squared value	Calibration Equation
3x3	26a	y = 1.02756x + 10.80394	0.99990	$x = \left(\frac{y - 10.80394}{1.02756}\right)$
	P22	y = 1.05036x + 9.50434	0.99998	$x = \left(\frac{y - 9.50434}{1.05036}\right)$
	J10	y = 1.04069x + 6.91801	0.99992	$x = \left(\frac{y - 6.91801}{1.04069}\right)$
	D30	y = 0.98402x + 13.73529	0.99924	$x = \left(\frac{y - 13.73529}{0.98402}\right)$
	F6	y = 1.03109x + 9.34601	0.99992	$x = \left(\frac{y - 9.34601}{1.03109}\right)$
11x11	L12	y = 1.08621x + 20.21429	0.99992	$x = \left(\frac{y - 20.21429}{1.08621}\right)$
y = ADT Output & x = Temperature				

Figure 20: Table of equations and r-squared values for the given detectors

6.1.2 ADT7301 Calibration Results

Once the data from each of the units were graphed and fit with a trend line, the r-squared values were analysed. An r-squared value is the ratio of two sources of variation which are the two sets of data. The ratio which is between 0 and 1 indicates how well the trend line fits the data. The closer the ratio is to 1, the more linear the model. The r-squared values for all of the units were almost equal to one. Once linearity of the characteristic was confirmed, the data from all of the units were combined. The data series for each detector was compiled in one graph that is shown in Figure 21. The offset data series is that of the eleven-by-eleven pixel array. With further testing of the eleven-by-eleven arrays, the offset could be attributed to a difference in the detector designs for the three-by-three and eleven-by-eleven pixel arrays.

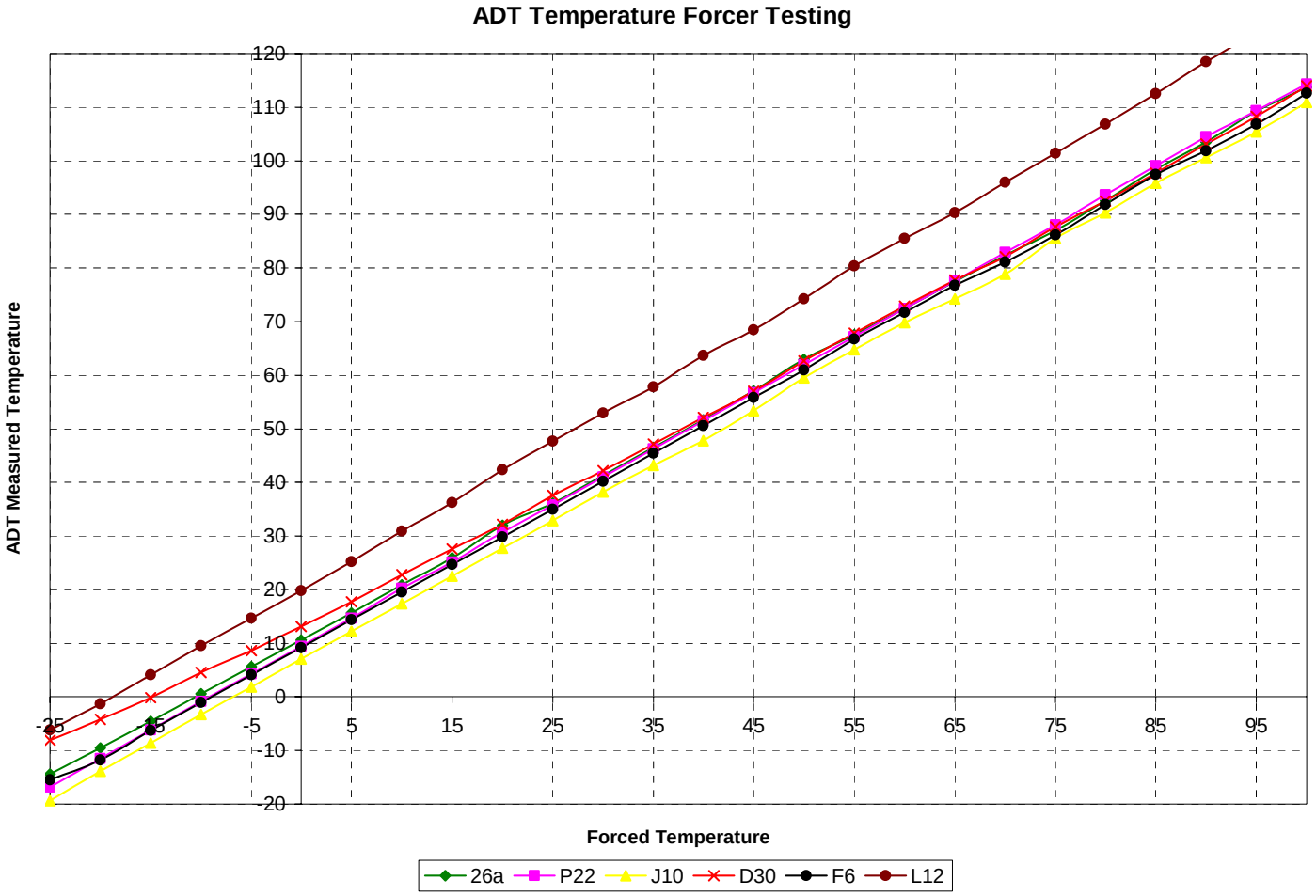

Figure 21: Forced temperature vs. the ADT7301 measured temperature for all sensors

The initial intentions were to average the linear fit lines of all of the sensors to determine a general calibration equation. From looking at the graph, however, it is evident that the trend lines have a large spread, which is attributed to their own gain and

offset. This means that with a single calibration equation, the result could have an error of up to six degrees Celsius. To reduce this error, the sensors will use their specific calibration equation rather than the general equation. Once the calibrations were complete for the ADT7301 devices in each of the detectors, the focus was shifted to the output of the AD7794 which represented the output of the thermopile sensors.

6.2 Angular Response Test

The first test of the AD7794 output was an angular response test which had multiple purposes in the experimentation process. The first was to gain perspective on what the full effect of the lens was on pixel directivity. Without the lens, the pixels would be expected to have nearly uniform directivity, but with it, the effect has yet to be fully determined. The lens is a diffractive single step phase lens that focuses onto the centre or central pixels. It was designed to create signal gain for greater pixel directivity. This setup and testing was done with Luke Pillans, an ADI employee at the Newbury, UK office who has a PhD in Infrared Optics. Preliminary testing was done with the setup while he was in Limerick, but further testing along with the data calculations and graphing of this test was done by Luke in Newbury where the setup remains. He then shared the results with us to discuss the implications of this and further testing.

A full description of the test setup utilised for this experiment is available in section 5.2.2, and a photograph of the setup is provided in Figure 22. Figure 23 shows screen captures of the pixel's responses after a single horizontal sweep. The legends on the right show which pixels are on each graph and which colour is which pixel. Before the numerical data was collected, observation was necessary to determine what data would be the most useful in drawing conclusions about the angular response.

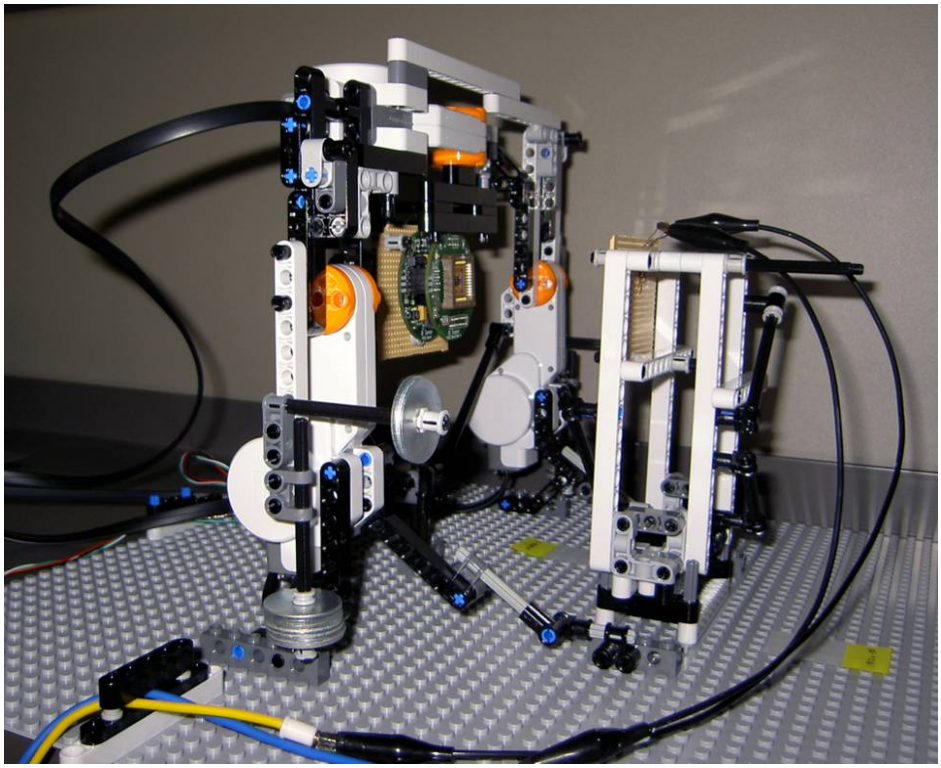

Figure 22: Angular response test setup

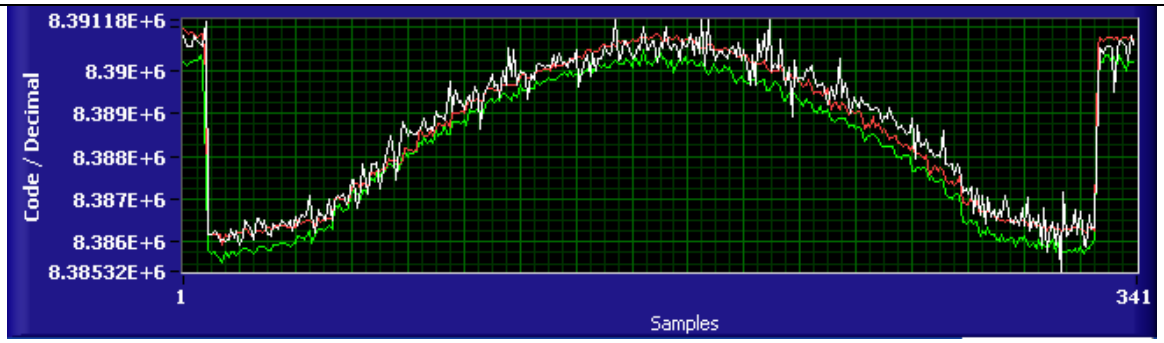

Pixel 1 = White
Pixel 2 = Red
Pixel 3 = Green

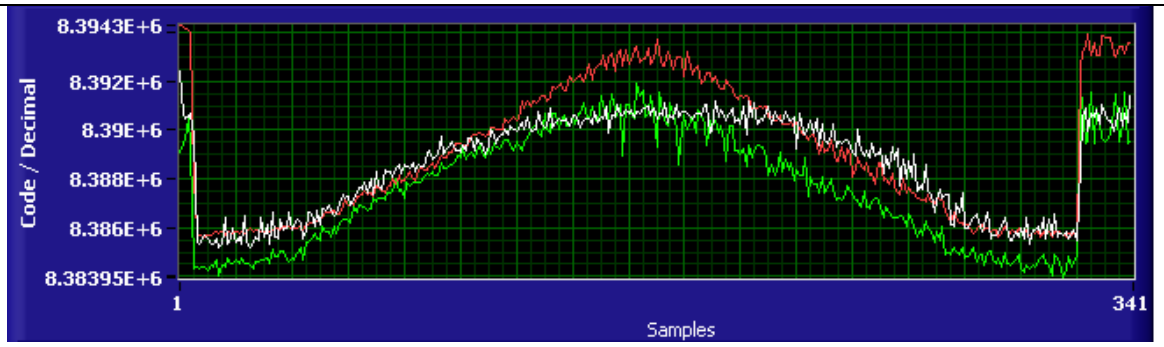

Pixel 4 = White
Pixel 5 = Red
Pixel 6 = Green

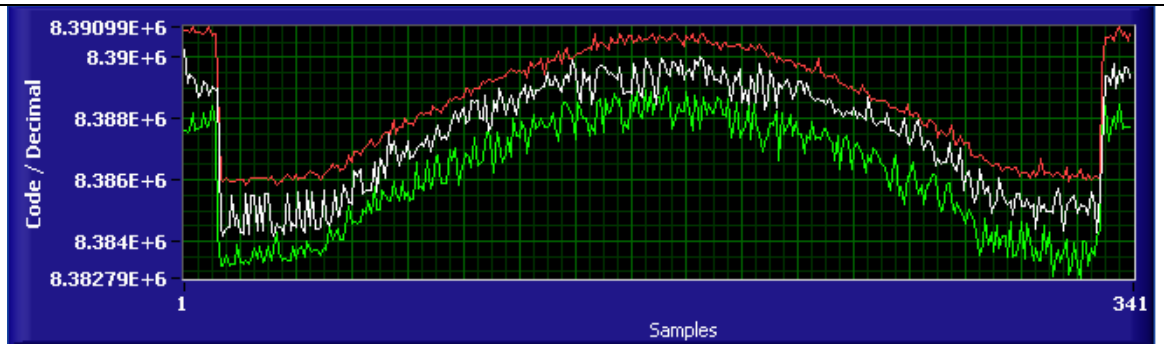

Pixel 7 = White
Pixel 8 = Red
Pixel 9 = Green

Figure 23: AD7794 output codes for a horizontal sweep across the IR point source for all nine pixels.

From the real time outputs in Figure 23, it was evident that even with a strong point source, the intensity of the signal was significantly lower at the outside pixels. For pixels 1 through 3 and 7 through 9, the signal was not strong enough to show the response shift that would have taken place as the sensor rotated on the horizontal axis. On the centre graph, this behaviour is just barely visible as the different peaking locations of pixels 4 and 6. Consequently, further testing was only done on pixels 4, 5, and 6, with the majority of testing focusing on pixel 5. The full test procedure was then carried out for these three pixels at three different distances. A horizontal sweep at the three distances produced a graph with the same shape, but lower responses further away. This is shown in Figure 24. Data was collected from 4cm because of the higher and less noisy response.

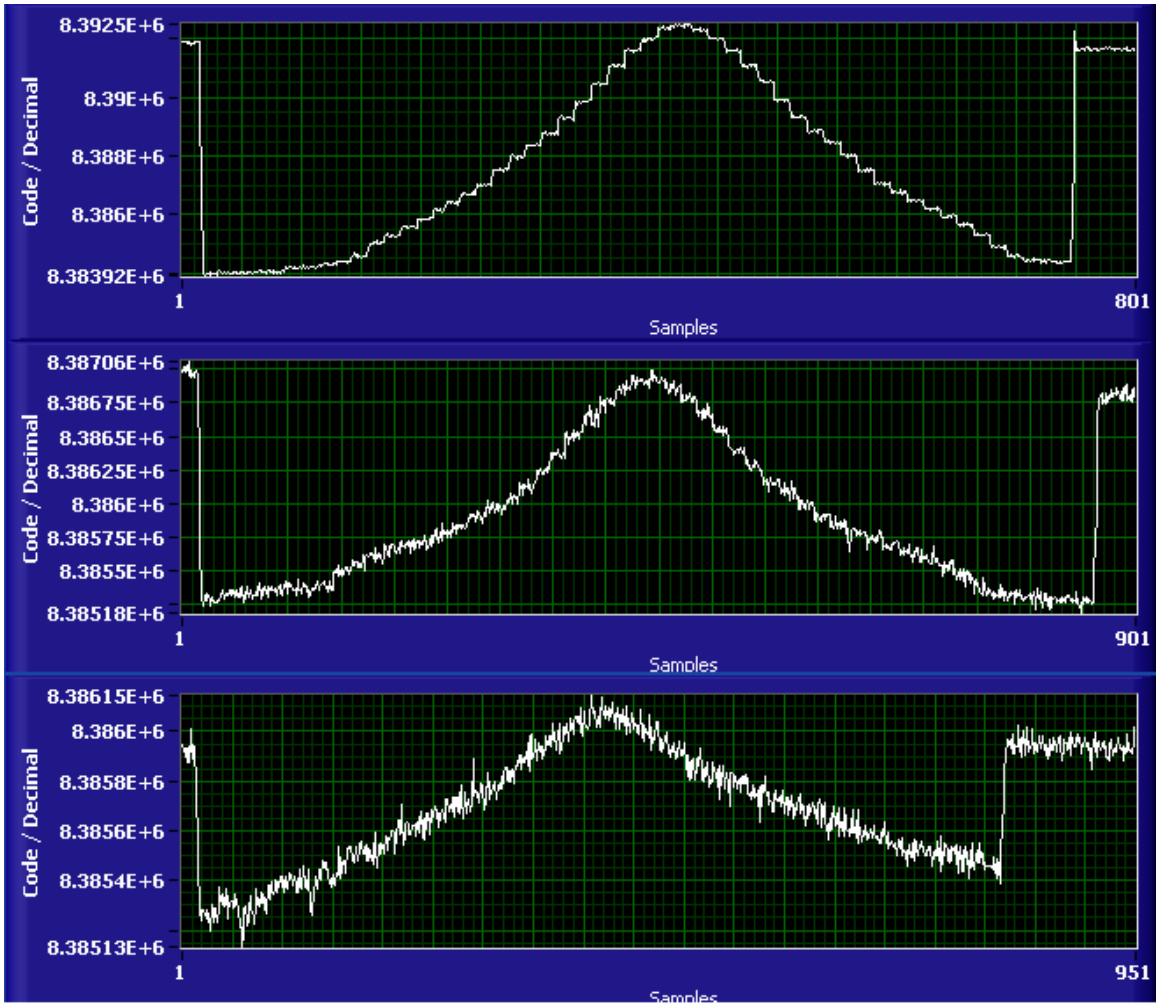

Figure 24: Pixel 5 response at 4cm (top), 10cm (middle), and 20cm (bottom).

6.2.1 Angular Response Data

Once the data was collected, the polar graph shown in Figure 25 was generated showing the response of the pixels four, five, and six. The data was first normalised which means the on the magnitude scale, the zero value was the response code when the sensor was facing at 0°.

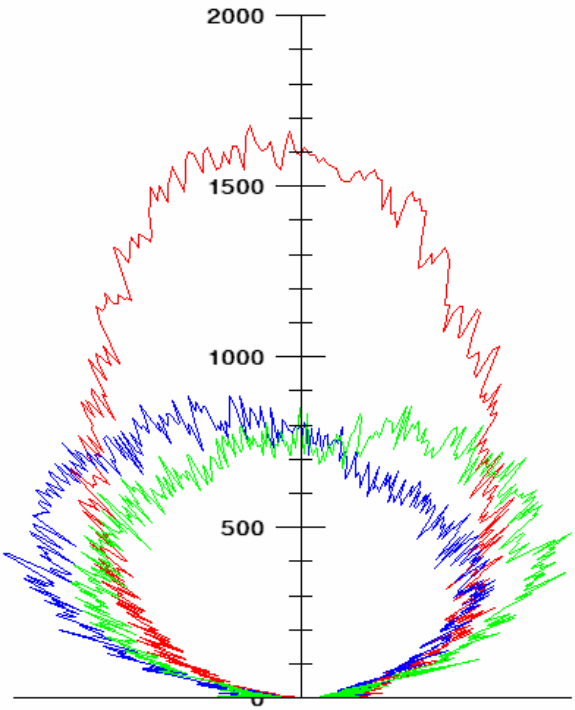

Figure 25: Polar graph of the responsivity of pixels 4(blue), 5(red), and 6(green)

6.2.2 Angular Response Results

From the polar graph we can see that the response of the side pixels is significantly low in comparison with the centre pixel, even when the sensor is rotated. With such a small response to a high temperature, intense signal, it is unlikely that testing on the outer pixels will be very effective for understanding the individual pixels. In addition, a different lens needs to be used for more favourable directivity from the outer pixels, so further analysis would need to be done with that lens. For the current prototypes, the focus must be on pixel five since it is the only way to display the capabilities of the detector. Further testing will therefore be done solely on pixel five.

Before any further testing was done however, apertures were designed to limit the field of view. Through previous trial and error testing not wholly relevant on a quantitative basis for this project, it was determined that the large field of view of the detectors had to be controlled if useable data was to be obtained. Using the polar responses of the detector at two different distances and the size of the blackbody plate inside the cavity, apertures were designed by Luke for our use in further testing. An aperture is a hole created in a uniform surface with a specific size used to control what passes between objects on either side of it. The three aperture plates made for this project were painted black on one side for high emissivity and left shiny on the other to reflect IR

away from the plate and detector. The plates were designed with 2cm, 1cm, and 0.5cm giving distance to spot ratios of 2, 4, and 8 respectively.

6.3 Pixel Response Test

As mentioned in the previous section, preliminary testing helped identify unexpected variables that would need to be controlled during the testing process. Once the metal aperture plates were designed, the next variable of concern was the influence of extraneous IR.

The test setup as described in section 5.3.2 was created to test the response of pixel five. A picture of the test setup for both methods is shown in Figure 26.

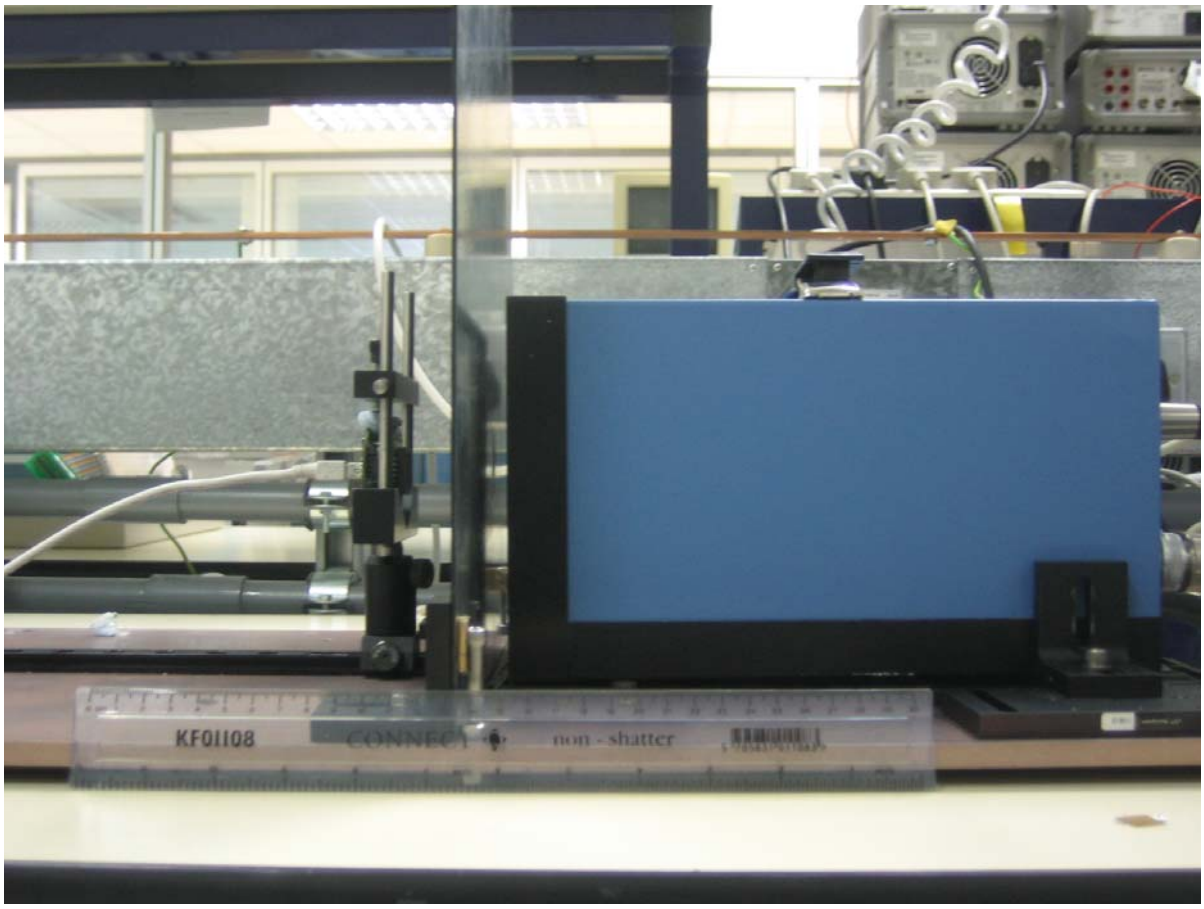

Figure 26: Pixel response test setup

6.3.1 Pixel Response Data

As mentioned in the earlier section, two slightly different methods were used for varying the apertures in this test. The average AD7794 code values for each aperture were plotted with the blackbody temperature. Figure 27 shows the data collected for sensor 26a. The data shown in Figure 27 was collected by switching the apertures from large, to medium, and to small after a set of one hundred samples was collected for each.

The ADT7301 samples were adjusted according to the sensor's specific ADT7301 offset and gain. Then, the temperature of the blackbody was increased after a set of data from all of the apertures was collected. Each set of data for each aperture is set to a best fit polynomial, which is also shown in the figure with its r-squared value. The collected temperature readings for the box and apertures when testing sensor 26a along with the averaged ADT7301 readings are shown in Figure 28. The three points collected on the box were averaged and the five points on the aperture were also averaged for each aperture and blackbody temperature.

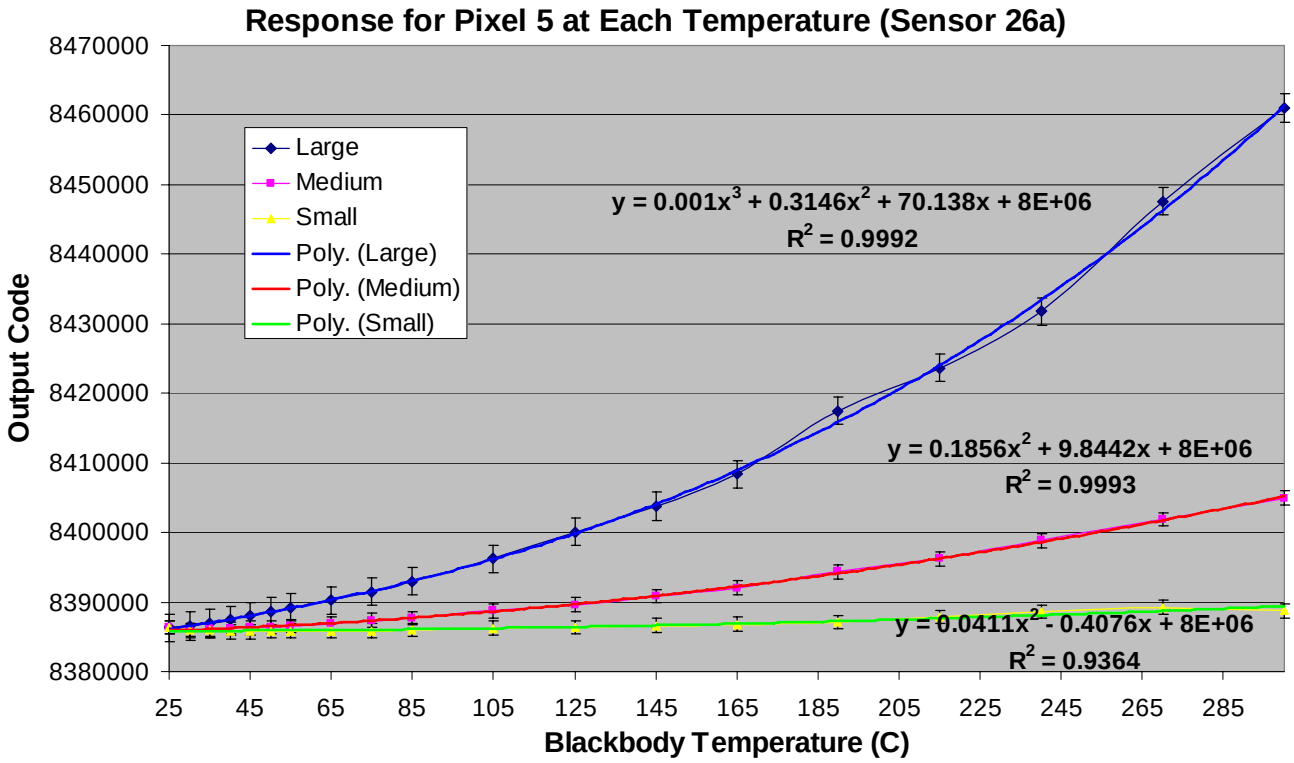

Figure 27: Response from pixel 5 for sensor 26a

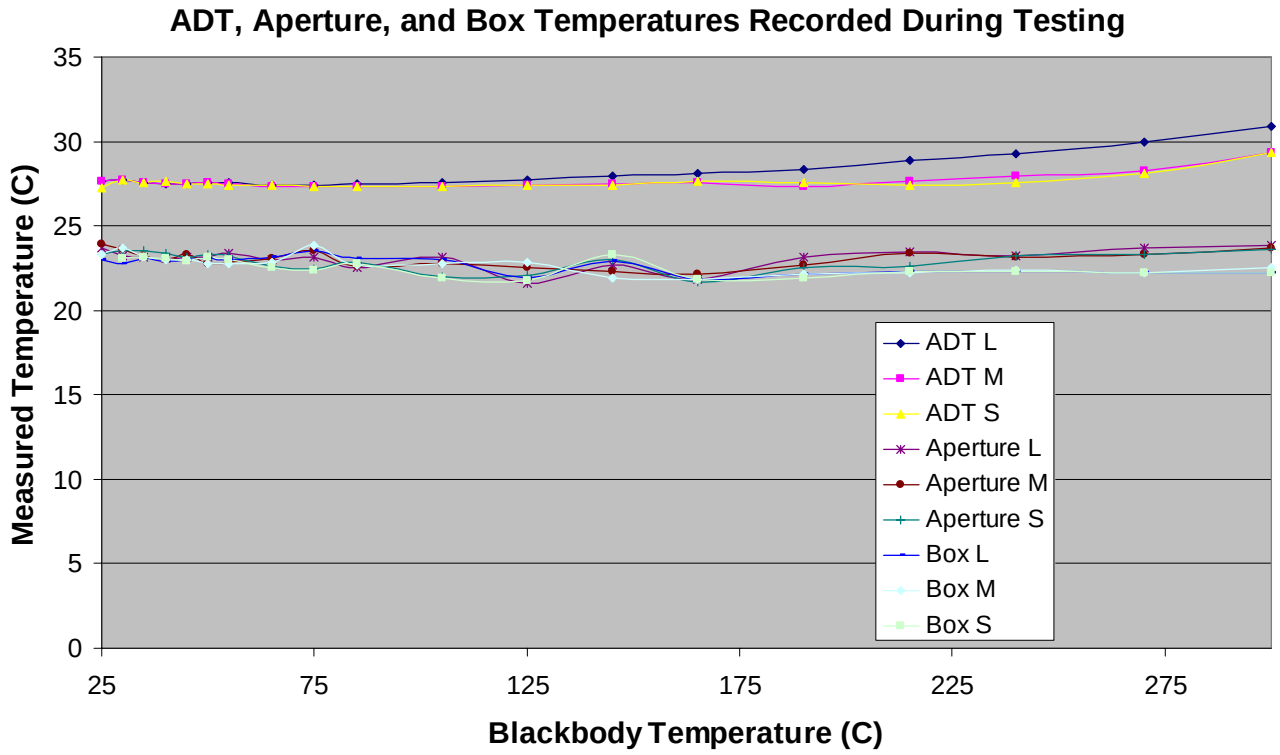

Figure 28: ADT7301, aperture, and box temperatures for sensor 26a

When looking at Figure 28, the box and aperture temperature measurements stay consistent within 2°C throughout the test. It was decided that collecting this data was not necessary for testing other sensors. Figure 28 verifies that the box and aperture are behaving as expected in terms of emitting IR, which is that the amount of IR they emit is constant and uniform.

The graphs in Figure 27 show that the response curves do not fit the best fit polynomial. It was decided that the rest of the pixel response tests would be done by using one aperture for one temperature sweep which would smooth out the response curve. Sensor 26a was tested again in this manner four more times. The data for the large aperture is plotted in Figure 29. It was evident that keeping the apertures stationary and doing individual apertures provided smoother curves than the consecutive aperture testing. The data collected for sensor 26a on September 25th and September 26th is noticeably lower than the other two sets of data collected. It is believed that since we did not have the apertures marked off on the setup board at that time, there may have been some misalignment with the aperture and the sensor. It was also decided that because of the small response measured when using the small aperture, testing would not be done with the small aperture.

Figure 30 is the data collected using the larger aperture for sensor J10. The testing done on October 2nd and October 3rd do not match the two sets of data collected

on October 4th. A test was developed to explain this variation, which is discussed in section 6.4.

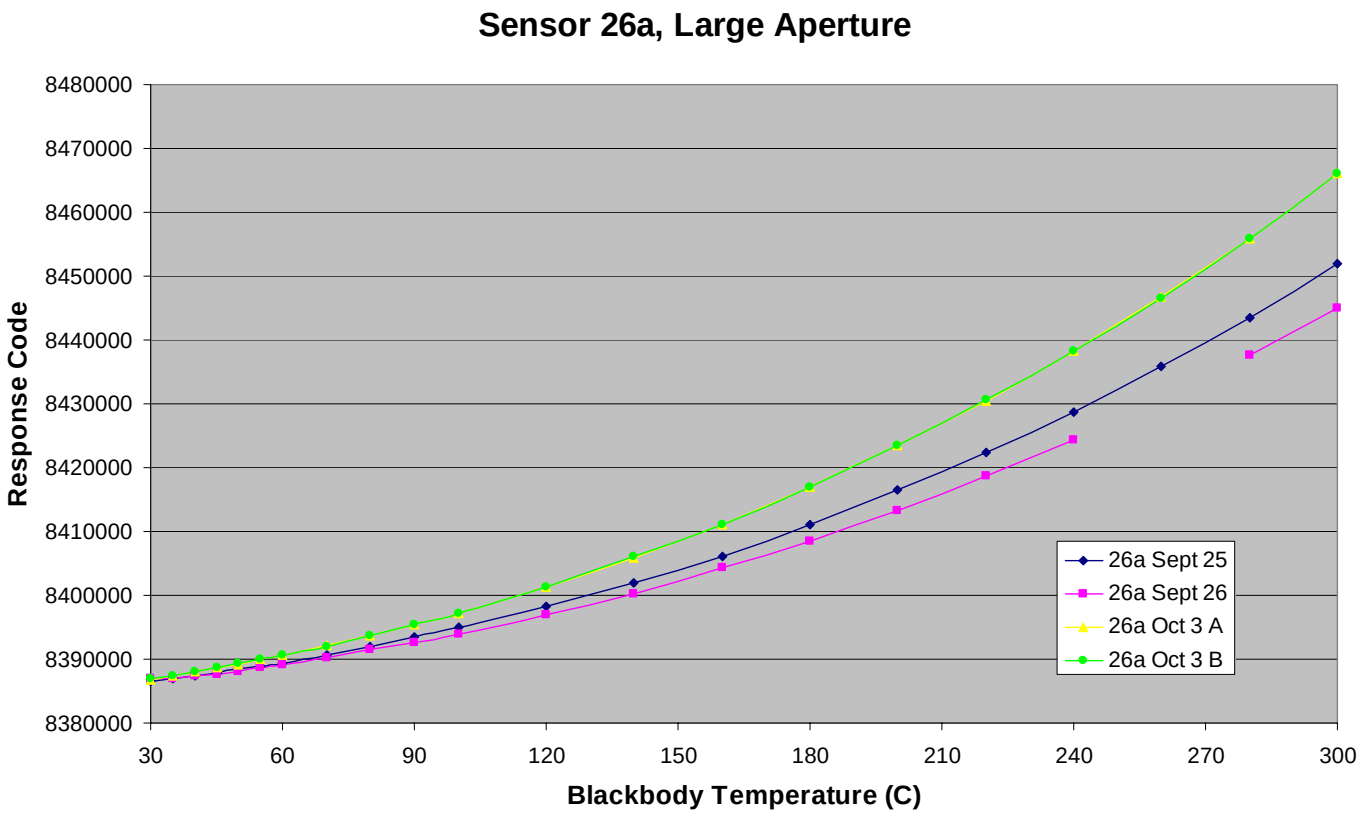

Figure 29: Pixel 5 means with large aperture for sensor 26a

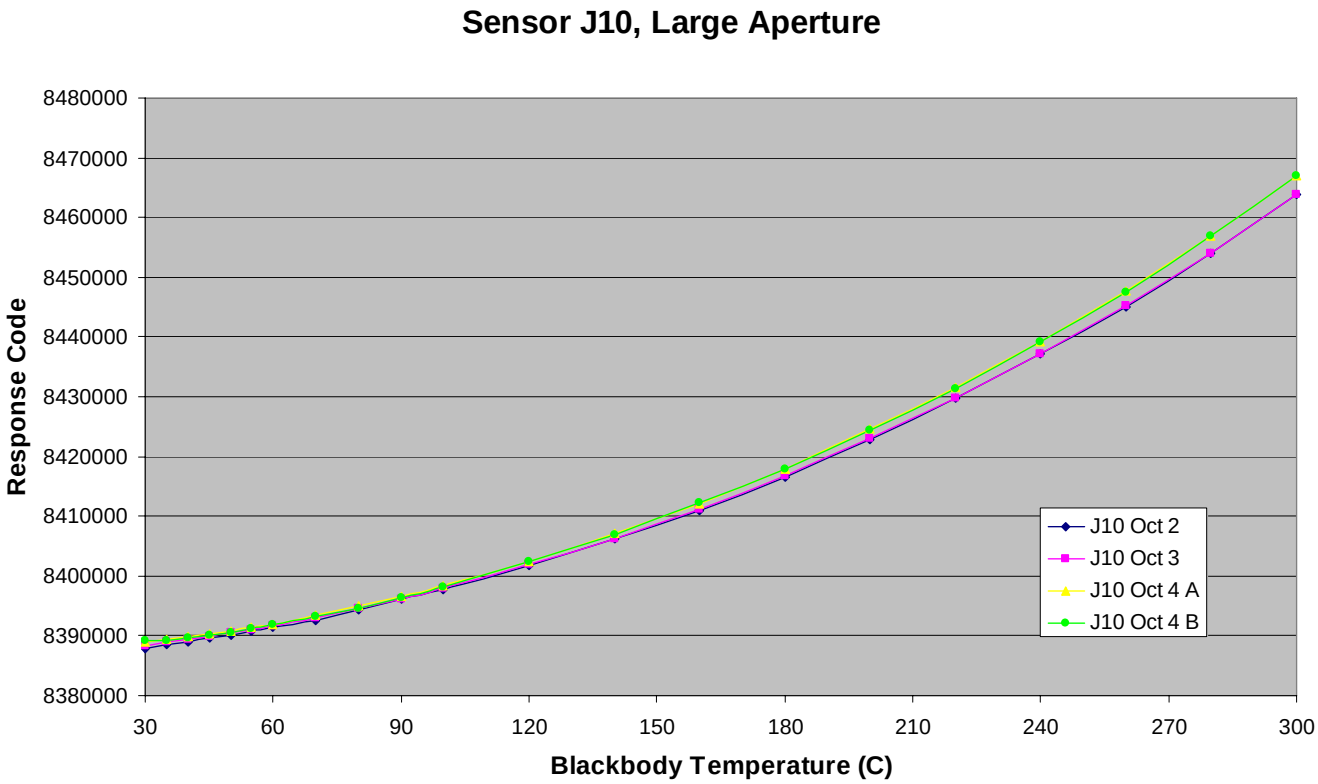

Figure 30: Pixel 5 means with large aperture for sensor J10

6.3.2 Pixel Response Results

With the collected AD7794 data, it is possible to show how a code can represent a temperature difference between the IR source and the sensor. This was done by taking the blackbody temperature for a set of data and subtracting the average ADT7301 value from it. The resulting average graphs for each of the sensors 26a, P22 and J10 using the large aperture are shown in Figure 31 and Figure 32. A best fit equation was applied to each curve, which gives us the output code as a function of the temperature difference between the blackbody and the sensor. A table of all of the conversion equations is shown in Figure 33 where *Temp* is the calculated temperature difference and *Code* is the AD7794 code output.

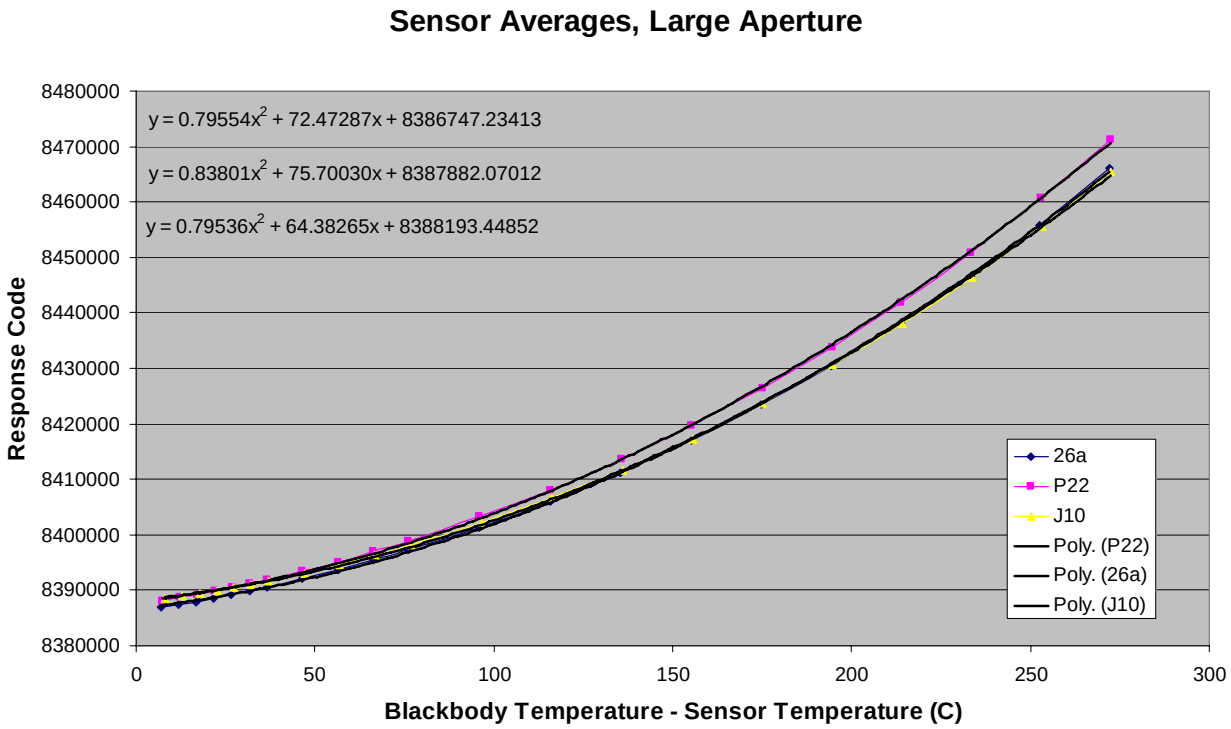

Figure 31: Output code vs. temperature difference of the blackbody and ADT7301 for the large aperture

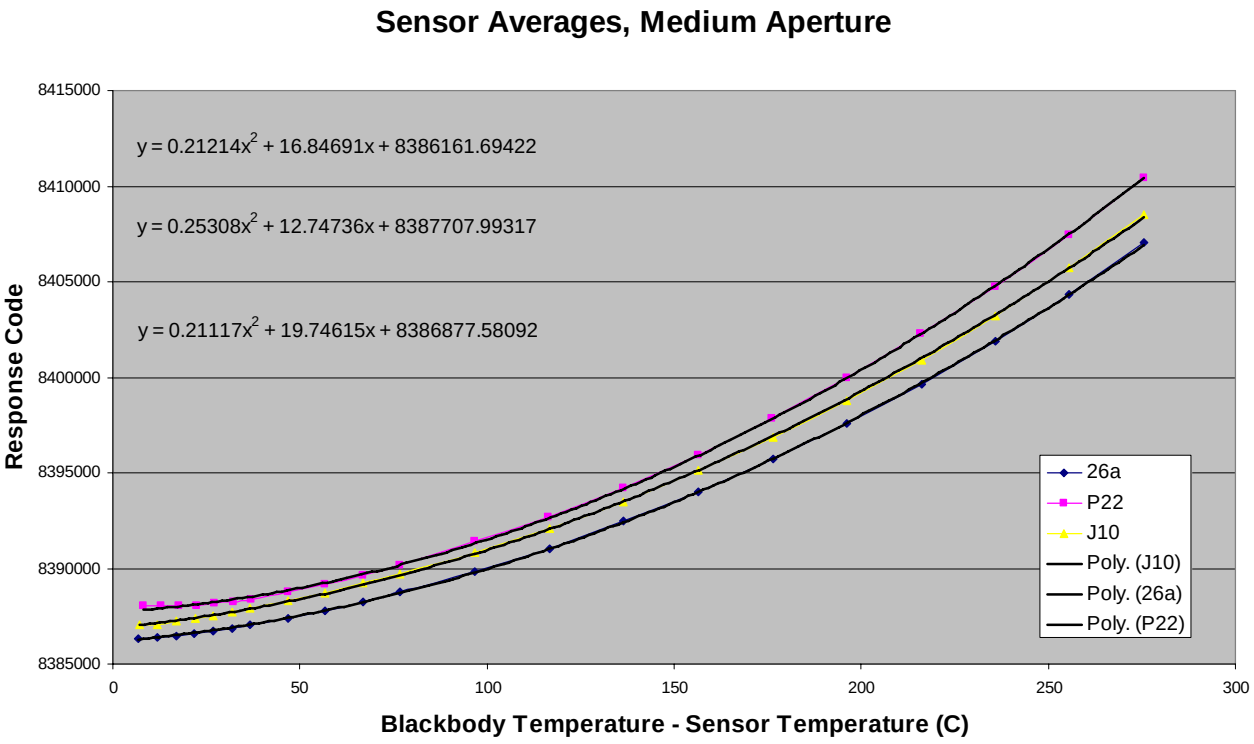

Figure 32 : Output code vs. temperature difference of the blackbody and ADT7301 for the medium aperture

Sensor	Aperture	Conversion Equation
26a	Large	$Temp = 1.12015\left(\sqrt{Code - 8385101} - 40.49586\right)$
	Medium	$Temp = 2.13760\left(\sqrt{Code - 8385714} - 21.19027\right)$
P22	Large	$Temp = 1.09238\left(\sqrt{Code - 8386172} - 41.34690\right)$
	Medium	$Temp = 1.98779\left(\sqrt{Code - 8387546} - 12.66955\right)$
J10	Large	$Temp = 1.12129\left(\sqrt{Code - 8386890} - 36.09583\right)$
	Medium	$Temp = 2.17613\left(\sqrt{Code - 8386416} - 21.48505\right)$

Figure 33: Code to temperature equation for each sensor and aperture

The conversion equations shown in the table in Figure 33 show that it is possible to convert the output code from the AD7794 into a temperature difference between an IR source and the sensor itself. This temperature difference can be added to the ADT7301 value to get the temperature of the source. However, there are limitations to the sensor. Since the field of view is so wide, pixel five sees the spot on the blackbody from the hole in the aperture and a large portion of the aperture itself. So, the conversion equations created are specific for each test setup.

6.4 Heated Aperture Plate Testing

The purpose of the heated aperture test was to verify the data used to calibrate the detectors. Though the previous tests had expected and repeatable results, there were discrepancies that had to be explained before we could be confident in our conclusions.

6.4.1 Heated Aperture Plate Data

The blackbody source was set to 150°C and the medium aperture was heated to 30°C. The temperature of the plate and the output codes from the AD7794 were recorded every 30 seconds. At each time the temperature of the plate was recorded, the output code was also recorded. The output codes were then put into the conversion equation for the corresponding sensor and aperture to get what the temperature difference between the blackbody and sensor should be with that code. The plate temperature was plotted against the output code, and the temperature difference was plotted against the output code as well. The temperature difference plot was moved down 160°C, since what matters is the change in temperature. The graph is shown in Figure 34. For a small change in plate temperature, there is a large change in the temperature difference. This is a large source of error, since the room temperature affects the temperature of the plate.

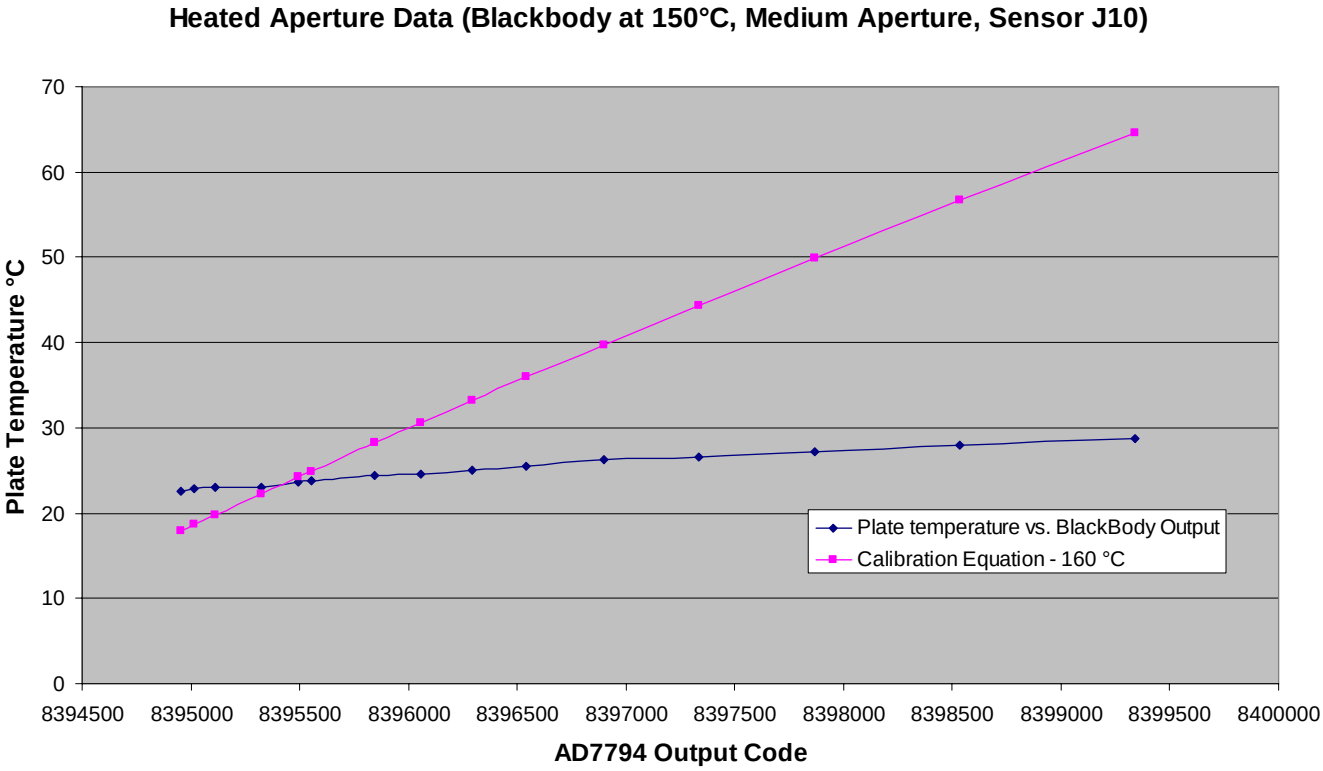

Figure 34: Temperature difference and plate temperature vs. output code

6.4.2 Heated Aperture Plate Results

From the plots, it was obvious that the temperature of the aperture plate had a slight affect on the ADC output code. As the temperature of the aperture plate gradually cooled, the ADC output codes decreased until the plate reached room temperature and the ADC output codes levelled off. Hence, it was a safe assumption that the slight changes in aperture plate temperature (a direct outcome of room temperature) might have caused the small discrepancies in the repeated pixel response tests. However, in the eventual packaging the aperture plate would be mimicked by a small metal can which would be in thermal equilibrium with the sensor.

7 ADiR Product Line Evaluation Software (AES)

The original program provided by ADI had very limited options for collecting and presenting the data for the user. There were several features added to the program that are useful for gathering and displaying data. The key idea was to give the user more options for collecting and showing data. These options provide the greatest flexibility in the program in order to meet the user's needs.

7.1 User Interface

The AES layout consists of three main areas. The first is along the top, which has basic buttons such as the Setup, Reset, and Quit buttons. Below that is the main area where data is collected and displayed. This area has three tabs for different modes of data collection. The three-by-three sensor has a Temperature tab for displaying an absolute temperature, and the eleven-by-eleven sensor AES has an Imager tab for displaying thermal images. Both versions also have an Analysis and Real Time tab for collecting raw data. To the right is a pixel selection area. The three-by-three sensor AES has a keypad to select pixels, and the eleven-by-eleven sensor AES has a button that opens a window for selecting pixels in a similar manner as with the three-by-three sensor AES.

7.1.1 Temperature Mode – Three-by-three Only

A new mode for data collection was added to the three-by-three sensor AES. There are two graphs; one displays the sensor's temperature and the other displays the temperature of the object. The top portion of the Temperature tab consists of a Start/Stop button, a number field for the number of samples to be taken, the current sample the sensor is recording, and the current pixel number. On the right is a calibration box for the sensor's ADT7301 and AD7794. The ADT7301 on each sensor has a different offset and gain, and the output from the ADT7301 must be adjusted. Since the sensor has a wide field of view, an aperture was used to limit the field of view. The AD7794 calibration coefficients depend on the size of the aperture used, and the sensor itself. The coefficients only apply to pixel five, since the other pixels respond poorly with the current lens. Below the calibration box is a box for saving data. When the Save Data button is pressed after samples were collected, the program will save the data in the format corresponding with the File Type menu below, which is either in Excel, MatLab, or a comma separated value format. To the right of the screen, there is a keypad that enables or disables pixels the user would like to collect data from. This keypad is used with the other modes in the three-by-three sensor AES. Figure 35 is a screenshot of the Temperature tab.

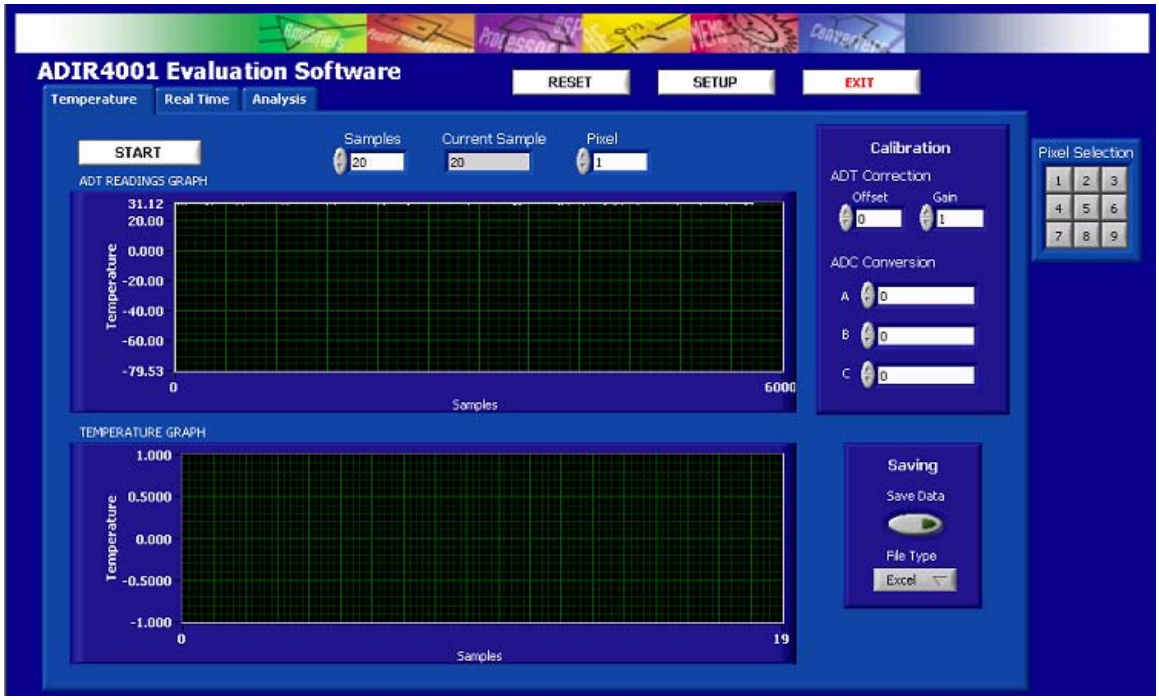

Figure 35: Temperature mode (3 by 3 software)

7.1.2 Imager Mode – Eleven-by-eleven Only

For the eleven-by-eleven sensor AES, an Imager tab was added to create thermal images from data collected by the eleven-by-eleven pixel array. A large box is in the middle of the tab, which displays the thermal image of the scene. To the right is a save box. The save box allows the user to save data in two ways. The first way is to save all of the collected raw data in an Excel, MatLab, or comma separated value format. The other save button allows the user to save the current image displayed to a JPEG file. Along the top of the window, there is a Start/Stop button for collecting data, and a numerical field that tells the user which pixel data is currently being collected. To the right of the screen is a button for opening a window to enable or disable pixels on the eleven-by-eleven array. Figure 36 is a screenshot of the Imager tab.

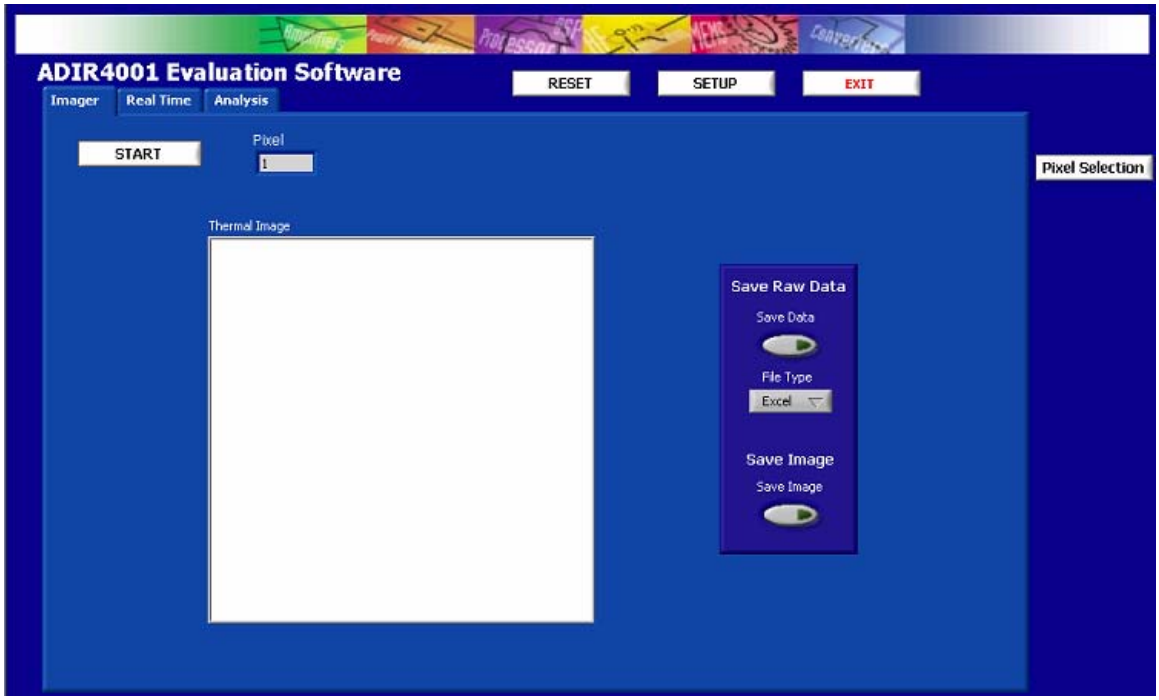

Figure 36: Imager mode (11-by-11 software)

7.1.3 Real Time Mode

The Real Time tab was kept the same. It consists of the two graphs; one graph displays the collected AD7794 data, and the other displays the ADT7301 data. The AD7794 data for all of the enabled pixels is displayed at once so that it is easy to compare the differences in the data between the enabled pixels. The top of the tab has a Start/Stop button for collecting data. Figure 37 is a screenshot of the Real Time tab.

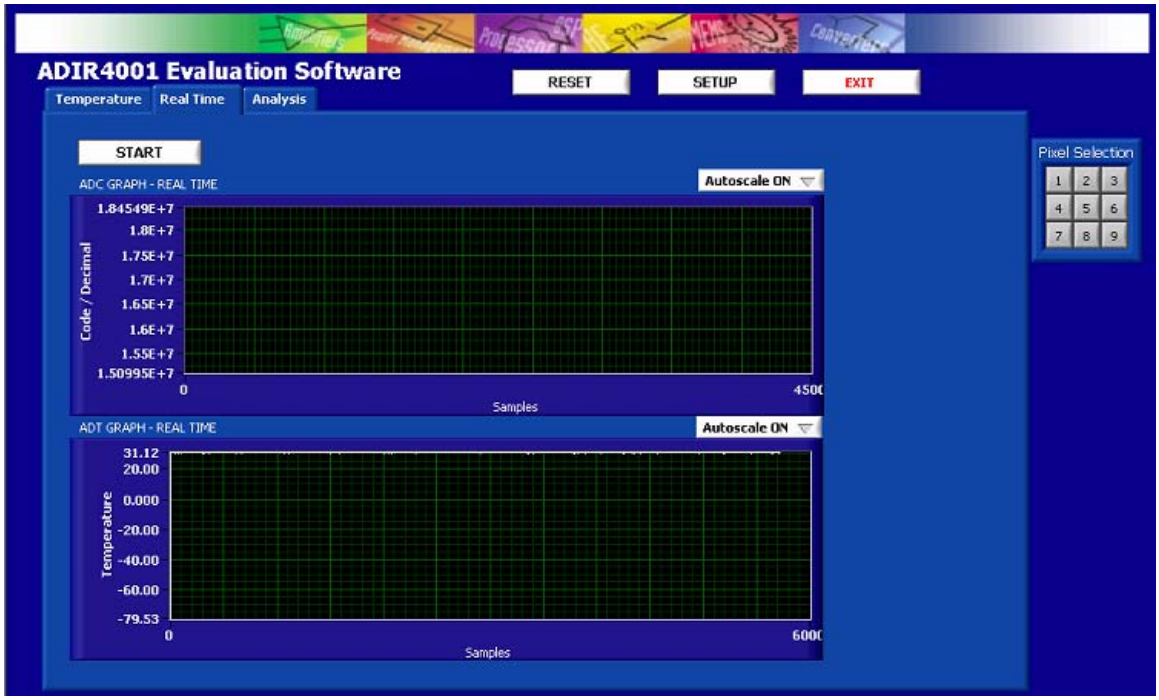

Figure 37: Real time mode (3-by-3 software)

7.1.4 Analysis Mode

Analysis mode contains two graphs; one plots the collected AD7794 data, and the other plots the collected ADT7301 data. On the right, there is a box that contains a brief analysis of the AD7794 data collected, such as the minimum value, maximum value, and mean. There is also a button below the box that allows the user to convert the AD7794 codes into the input voltage to the AD7794. Below that there is a numerical field to change the current pixel data being viewed, and a switch to display all of the AD7794 data at once. At the bottom is a saving box, which allows the user to save the data in an Excel, MatLab, or a comma separated value format. The AD7794 data can also be saved as hexadecimal values when saving in the Excel format. At the top is the Start button to begin the data collection process, and a numerical field to determine the number of samples to collect from each pixel. Figure 38 is a screenshot of the software in analysis mode.

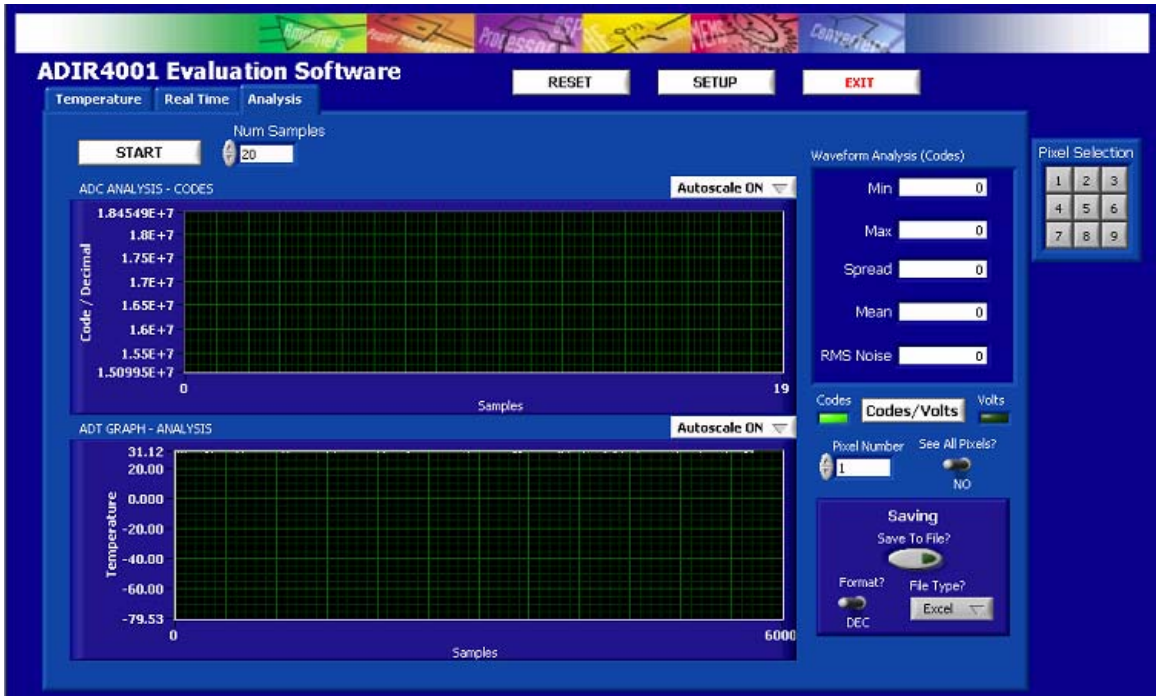

Figure 38: Analysis mode (3-by-3 software)

7.2 Main Process Loop

In the main loop, the program makes checks for different user inputs, such as checking the state of different buttons. If the Quit button is pressed, the program closes. If the Reset button is pressed, the program resets the sensor to the default settings. If the Setup button is pressed, the software opens the setup menu. If the Codes/Volts button is pressed or the Pixel Number fields are changed, then the program updates the graphs for the new changes. If the save button is pressed, the program will save the data in the selected format. Figure 39 is a block diagram of how the Main Process loop operates.

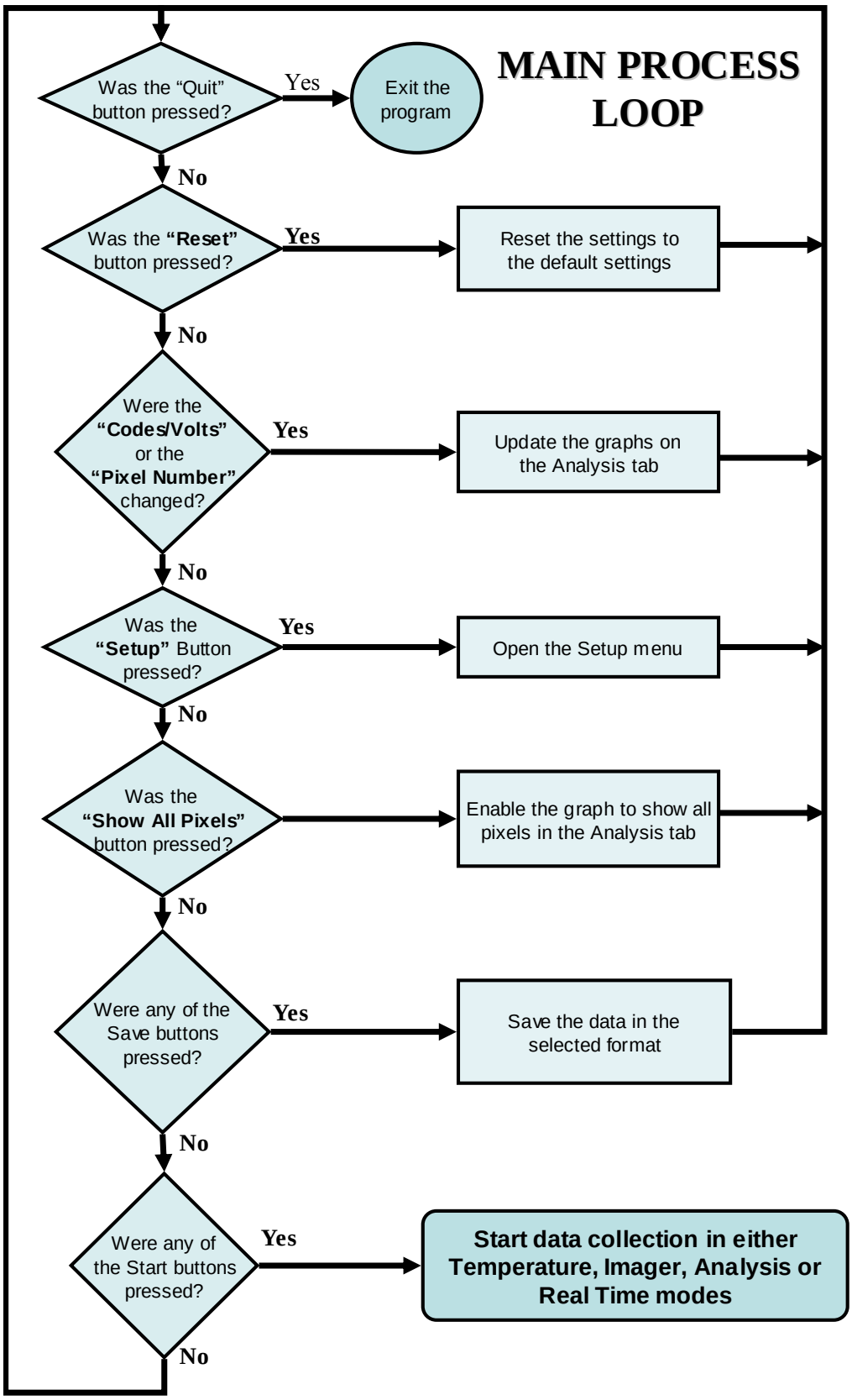

Figure 39: Main process loop block diagram

7.3 Data Collection

There are four modes for data collection. Each mode corresponds with one of the tabs in the sensor AES. Both the three-by-three and the eleven-by-eleven sensor AES use Real Time and Analysis modes. The three-by-three sensor AES has a Temperature mode, and the eleven-by-eleven sensor AES has an Imager mode.

7.3.1 Real Time Mode

If the Start button under the Real Time tab is pressed, then the program collects data in Real Time mode. The program continues to do so until the Stop button is pressed. It then checks if the temperature sensor enable setting is turned on. If it is on, it gets the current reading from the ADT7301 and puts it on the ADT7301 graph. If not, it skips to the next step. The program enters a loop that goes for 9 iterations in the three-by-three software and 121 iterations in the eleven-by-eleven software, one iteration for each pixel. The current loop count plus one is assigned to the MUX Value. If the corresponding pixel is not enabled, then it goes to the top of the loop for the next pixel. If the pixel is enabled, then the state of the AD7794 sample enable is checked. If it is turned on, then it gets the current output from the AD7794 and displays it on the AD7794 graph. If not, then it goes to the next step, which is looping back to the top of the loop for the next pixel. Once all nine iterations have been completed, the program then loops back to checking if the temperature sensor enable setting is on. The AD7794 and ADT7301 graphs continue to build until the user presses the Stop button, which returns the program to the main loop. Figure 37 shows the screen when using real time in raw data mode. Figure 40 shows a block diagram of the Real Time mode.

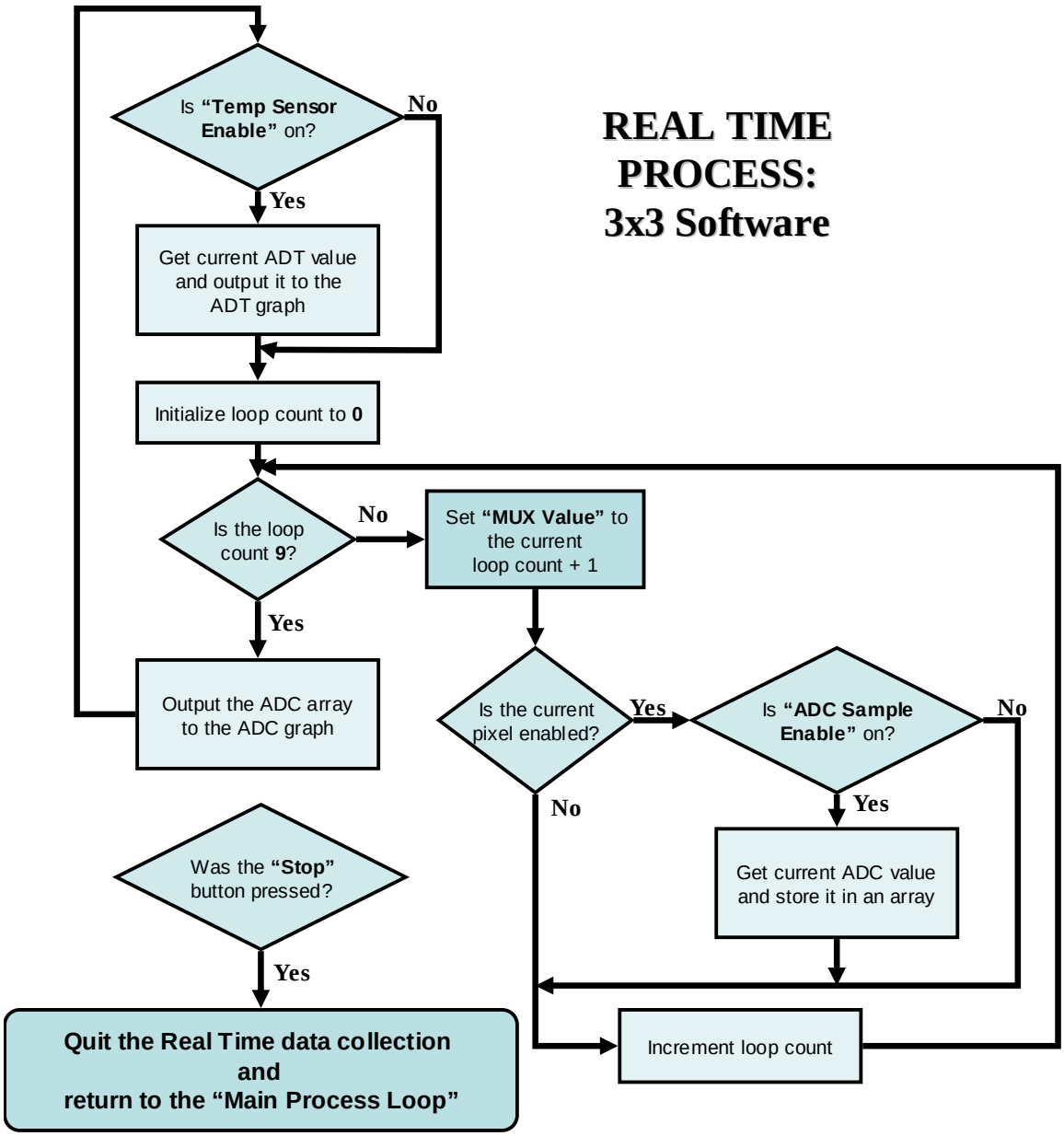

Figure 40: Real time data collection (3-by-3 software)

7.3.2 Analysis Mode

If the Start button under the Analysis tab is pressed, then the program collects data in Analysis mode. The program collects as many samples specified by the Num Samples field. The program first records the current pixel selection settings. Then a loop is started that goes for the number of requested samples. Another loop is started that goes for 9 iterations in the three-by-three software and 121 iterations in the eleven-by-eleven software, one for each pixel. The program checks if the current pixel is enabled. If not, it starts the next iteration. If the current pixel is enabled, the MUX Value is set to the current iteration plus one. The program then checks if the AD7794 sample enable is on.

If it is turned on, then it gets the current output from the AD7794 and displays it on the AD7794 graph. If not, then it goes to the next step. It then checks if the temperature sensor enable setting is turned on. If it is on, it gets the current reading from the ADT7301 and puts it on the ADT7301 graph. If not, it skips to the next step. The program records the AD7794 and ADT7301 values, along with a timestamp of when the samples were taken to three different arrays. Once the program has gone through all the pixels, it repeats the same loop until all the samples are collected. The program then displays other information about the collected samples, such as the minimum, maximum, and mean of the AD7794 codes. The program now returns to the main loop. Figure 41 shows the block diagram of the Analysis mode.

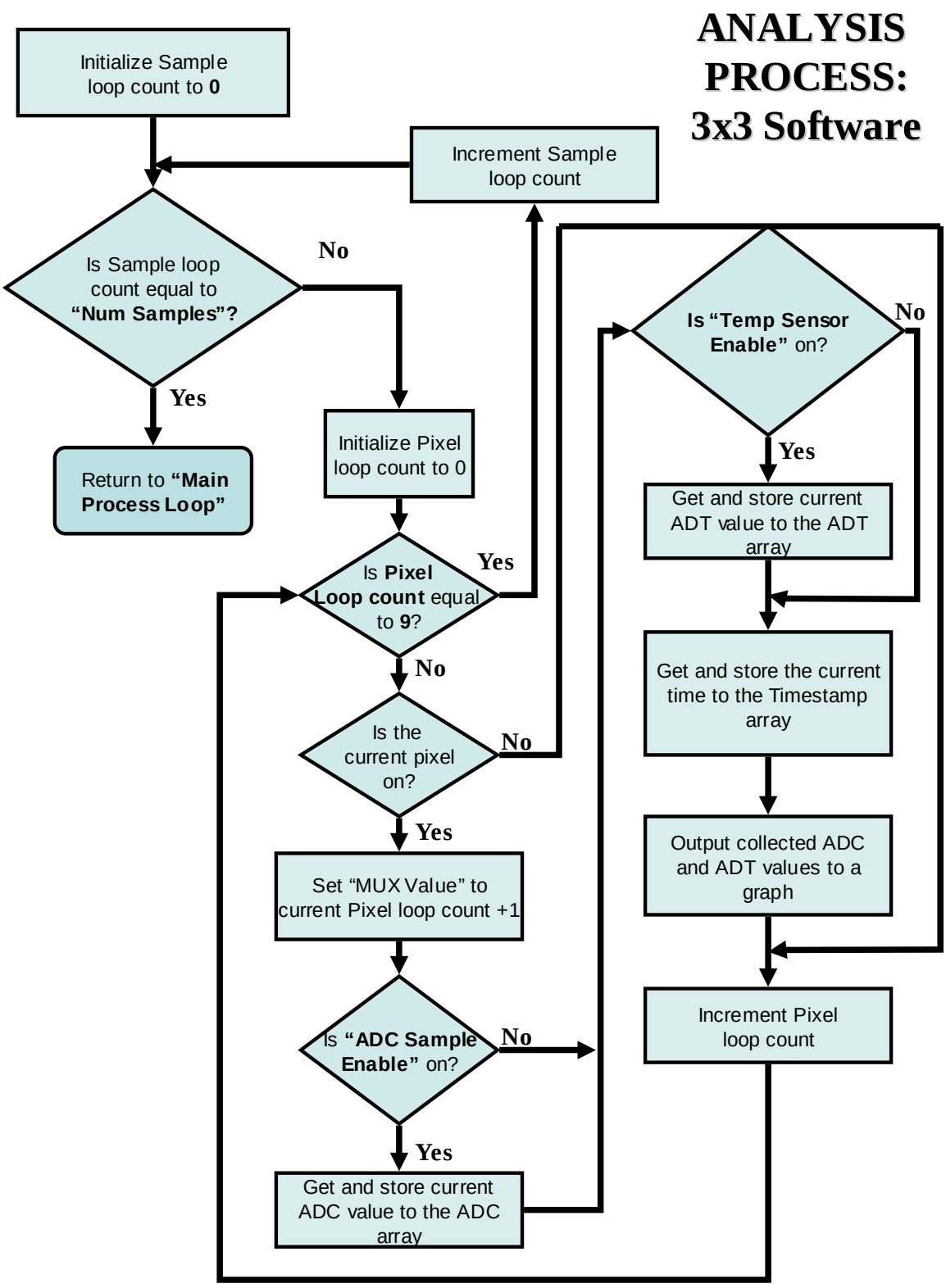

Figure 41: Analysis data collection (3-by-3 software)

7.3.3 Temperature Mode – Three-by-three Only

If the Start button under the Temperature tab is pressed, then the program collects data in Temperature mode. The program collects as many samples specified by the Samples field, or until the Stop button is pressed. The program first records the current pixel selection settings. Then a loop is started that goes for the number of requested samples. Another loop is started that goes for nine iterations, one for each pixel. The program checks if the current pixel is enabled. If not, it starts the next iteration. If the current pixel is enabled, the MUX Value is set to the current iteration plus one. The program receives a sample from the ADT7301, then applies the offset and gain correction to it to convert it to the actual temperature of the sensor. The program then receives a sample from the AD7794, and applies the conversion coefficients to it to calculate a temperature difference between the sensor and the source. This value is added to the corrected ADT7301 value to get a temperature. The program records the source temperature and corrected ADT7301 values, along with a timestamp of when the samples were taken to three different arrays. Once the program has gone through all the pixels, it repeats the same loop until all the samples are collected or the Stop button is pressed. Figure 42 is a block diagram of the Temperature mode process.

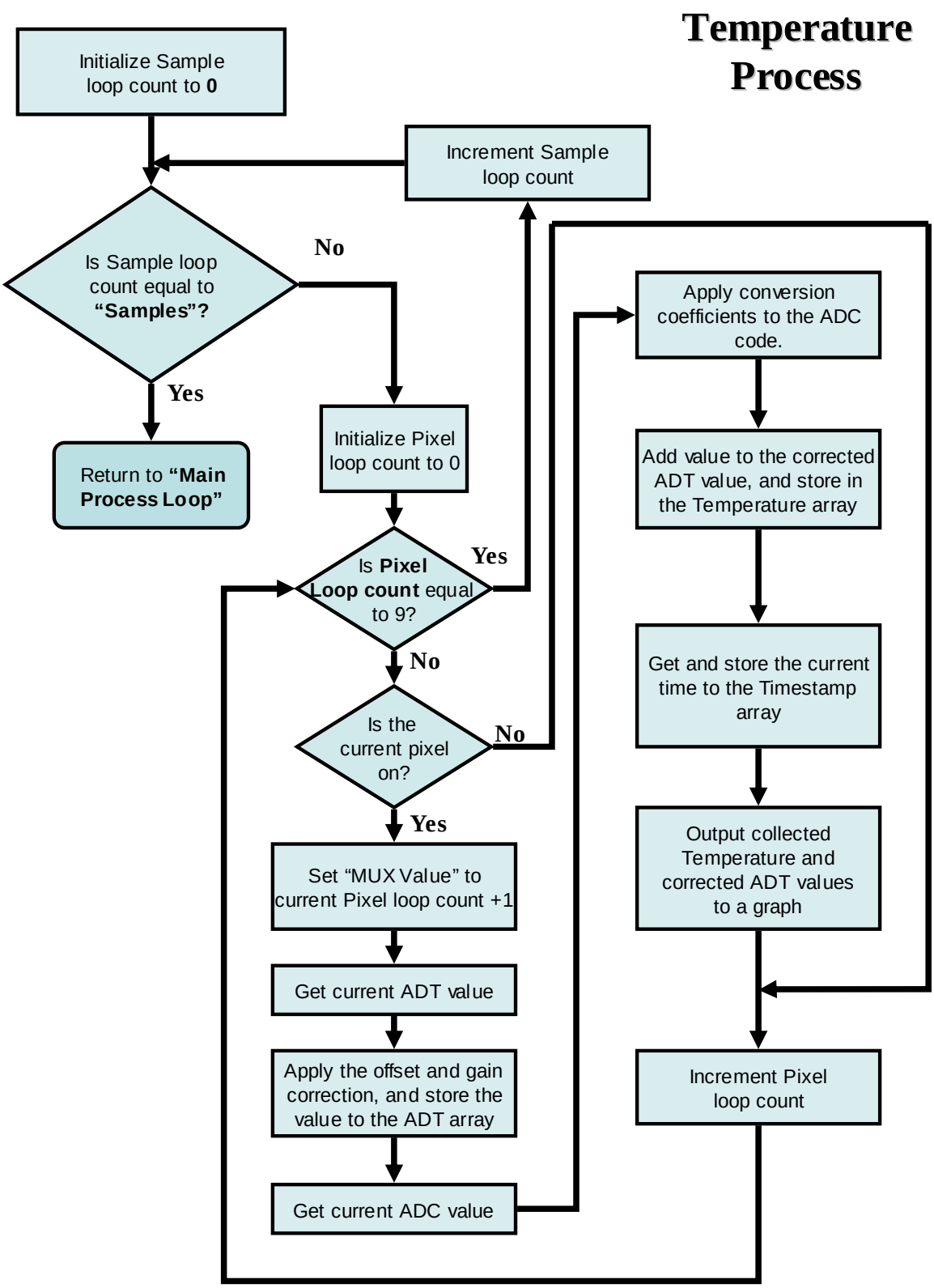

Figure 42: Temperature data collection

7.3.4 Imager Mode – Eleven-by-eleven Only

If the Start button under the Imager tab is pressed, then the program collects data in Imager mode. The program continues to do so until the Stop button is pressed. A loop is started that goes for 121 iterations, one for each pixel. The program checks if the current pixel is enabled. If not it puts the value -500 into an array that will go into the thermal imaging process, then it starts the next iteration. If the current pixel is enabled, the MUX Value is set to the current iteration plus one. The program gets the current output from the AD7794 and stores it in an array going to the thermal imager. The program then gets the current reading from the ADT7301. The program records the AD7794 and ADT7301 values, along with a timestamp of when the samples were taken to three different arrays. This is so that someone is able to save the raw data collected during the imagine process. Once a sample has been collected from each pixel, an array is sent to the thermal imaging process, and it converts the codes into an image of the scene, which is output to the Thermal Image box. Whenever the Save Image button is pressed during the process, the image will be saved to a JPEG file. Figure 43 is a block diagram of the Imager mode.

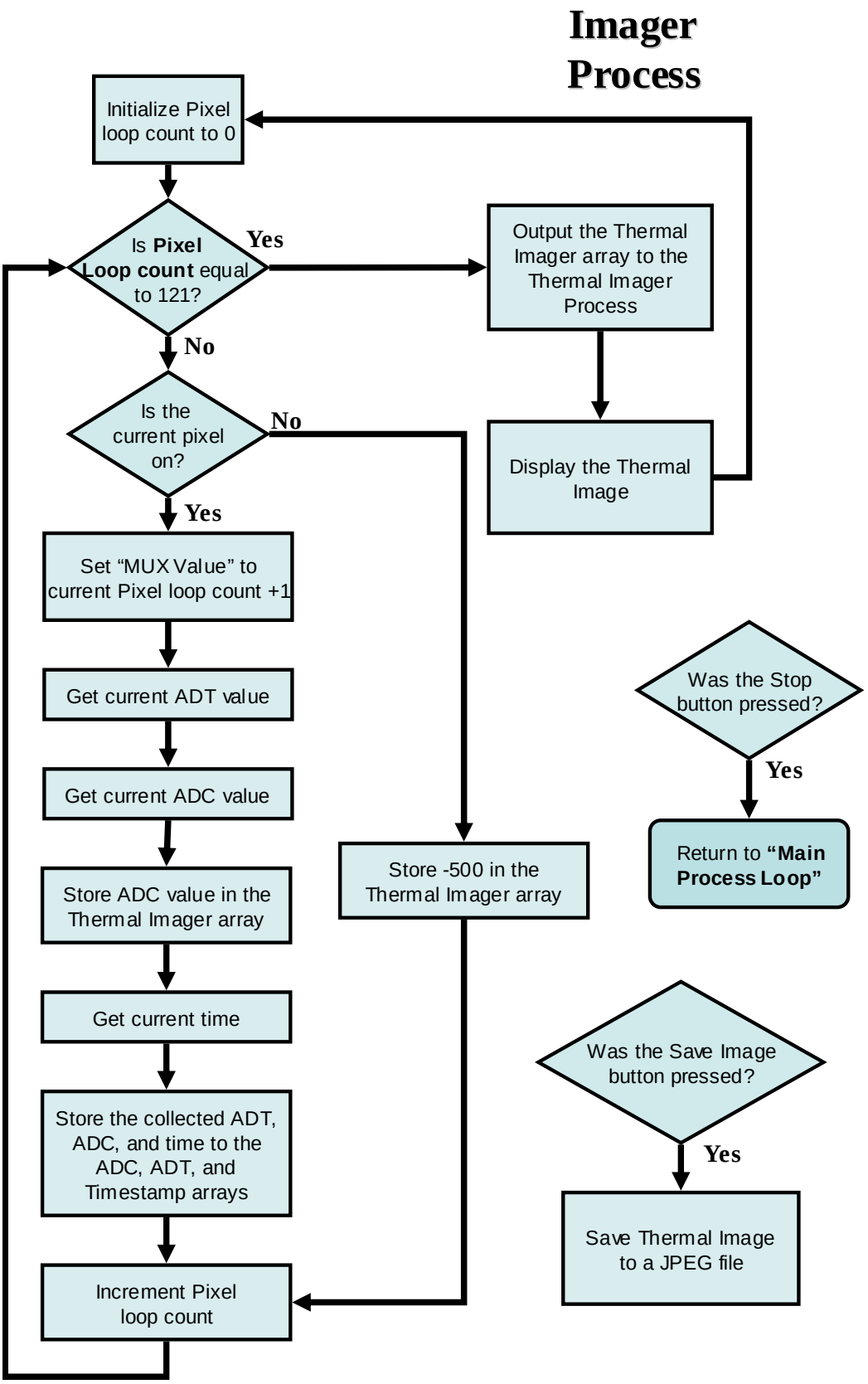

Figure 43: Imager data collection

7.4 Other Software Changes

There were two other changes made to the AES to better control the detector. The first change was to automatically calibrate the AD7794 when the program loads. The second change was a new option in the Setup window to help reduce noise in the ADC during conversion cycles.

7.4.1 Automatic AD7794 Calibration

Every AD7794 has a slightly different offset and gain correction for producing accurate outputs. However, when the AD7794 is turned on, it uses the default offset and gain correction values in its offset and full-scale registers. The AD7794 has two modes for internally calibrating these registers. The first mode is the internal zero scale calibration mode, which automatically sets the offset register. The second mode is the internal full-scale calibration mode, which sets the full-scale register to correct the gain.

The software has a start-up routine which sets the default values for the sensor. A step was added in this routine to set the AD7794 into internal zero scale calibration mode, then into internal full-scale calibration mode. Once this is completed, the AD7794 is returned to its default mode, which is continuous conversion mode.

7.4.2 AD7794 Filter Flushing

When multiple pixels are enabled during data collection, the pixels are sampled one at a time and cycled. Old data in the filters in the AD7794 are not flushed with just one conversion. It takes two conversion cycles for the filter to be flushed, which means if you take a set of ten samples from a single pixel, the first two samples will contain parts of old data and the last eight will be valid.

An option in the Setup window was added to take three samples from the ADC for each sample of each pixel. When enabled, the first two samples are ignored and the third one is stored. This makes the data collection process three times longer, but it should provide for more accurate data.

8 Demonstration Design

Implementation of the three-by-three and eleven-by-eleven pixel arrays in a temperature measurement and a thermal imaging application respectively was the ultimate goal of the project. The methodologies, test designs, data collection and analysis, and software development all built up to reach this final goal. The three-by-three and eleven-by eleven are theoretically both able to measure absolute temperature and create a thermal image. The demonstration designs chosen utilise the currently available prototypes verify full functionality from a design perspective, and address the imminent marketing needs for an initial product release.

8.1 Three-by-three Pixel Array

The demonstration for the three-by-three pixel array focused on absolute temperature measurement from the centre pixel only. The weakened signal, resulting from the lens design previously explained, received by the outer pixels was too significant to merit their use in this application. Next generation prototypes will be re-evaluated for multi-pixel applications. With a customer release planned before the next generation parts would be available, a useful demonstration was needed showing the potential of the detectors using those currently available.

8.1.1 Demonstration Setup

After eliminating the other eight pixels from the demonstration, the sole focus was manipulating the output of the centre pixel, pixel five. Despite the signal loss at the other pixels, pixel five was receiving an amplified signal as a result of the lens. Taking into account the previously learned implications of the detectors, it was established that in order to show the customer a temperature, the detectors would have to be individually calibrated and utilised in the test setup used to calibrate them. The variances between detector responses due to environmental change and individual physical properties made it unreasonable to apply a general equation. Despite creating a unique calibration for each of the detectors, they were still not capable of stand-alone use. Outside of the test setup, the detectors had approximately a 110 degree field of view. Until a cap could be fabricated to mimic the limited the field of view, accurate demonstration would only be shown using the test setup.

8.1.2 Demonstration Procedure

With the setup determined, the next step was to convey to an onlooker the capabilities and potential of the detectors. To determine expectations for accuracy of the full detector system, multiple items were placed in front of the detector on the other side

of the aperture plate. The temperature recordings of these items were compared to the readings obtained with a handheld device to assess its accuracy shown in Figure 44.

Object	Device temperature(°C)	IR thermometer temperature(°C)
Laptop Charger	46.68	42.4
Cardboard	21.91	22.2
Hand	37.3	32

Figure 44: Device readings compared to the handheld device.

A temperature sweep was run for a range of temperatures from 50°C to 300°C using the blackbody to measure the accuracy. The graph in Figure 45 shows that the large aperture shows a more consistent reading than the medium aperture over a range of temperatures. The maximum error noticed was 4.7% on the large aperture. The data for both the large and the medium apertures in provided in Appendix F

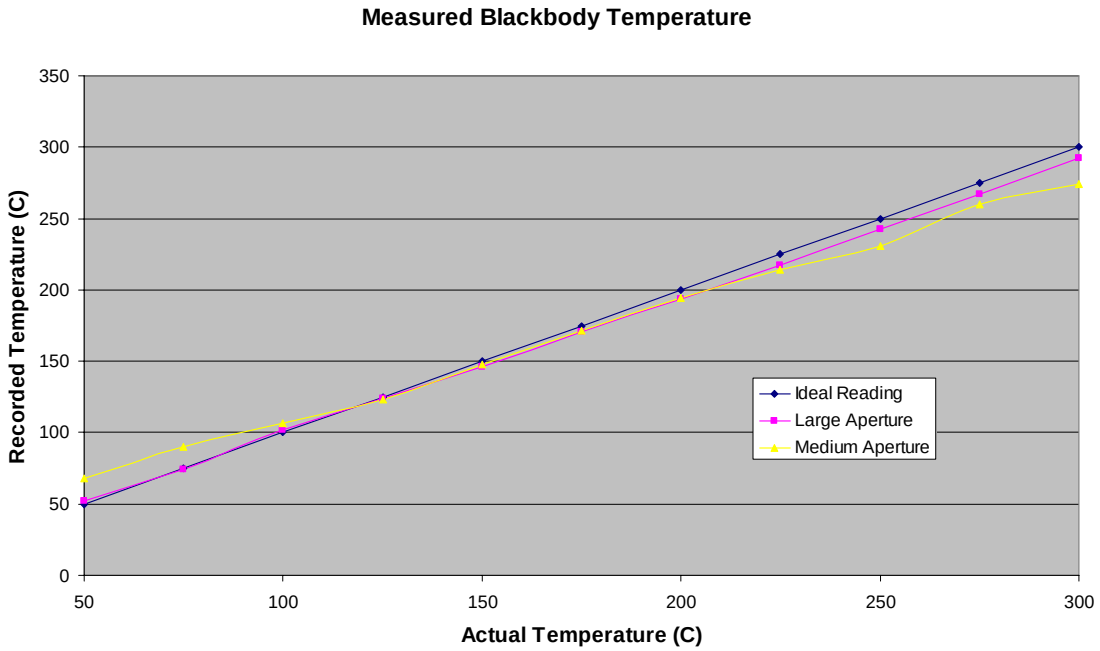

Figure 45: Measured blackbody temperature vs. actual blackbody temperature

8.2 Eleven-by-eleven

The demonstration for the eleven-by-eleven pixel array focused on its thermal imaging capabilities as an array. Previous implementation of a pixel in the three-by-three pixel array as a non-contact thermometer indicated that the centre eleven-by-eleven pixel could do the same using the same calibration method and test setup. For this proof of concept, however, the main focus was to verify that an image showing thermal gradients

could be produced by using and translating measurements taken from the device. This detector was not scheduled for release and will undergo a great deal more of analysis before its release. Effective implementation of the device in a thermal imaging application, however, was necessary to warrant further design and analysis.

8.2.1 Demonstration Setup

The testing up to this point confirmed that the lens significantly reduced the amount of IR that could be seen by outer pixels on the array. The lens, however, effectively passed through and amplified any signal that passed directly through the focal point of the lens for a wide range of incident angles. Despite the effects of the lens, the smaller pixel size was expected to increase the directivity enough to produce an image.

For this demonstration, the detectors were implemented without testing the pixel response. Because of the way the thermopile sensors operate, displaying the differences in temperature across a scene requires no knowledge of the absolute temperatures. The primary portion of this demonstration setup was the display of the thermal image in LabVIEW. Section 7.3.4 details the software translation of 121 pixel output codes into a picture. Once the software adjustments were complete, the detector was able to identify hot and cold spots in the field of view.

8.2.2 Demonstration Procedure

To fully demonstrate how the detector was producing an image, the blackbody and a heat gun were introduced into the field of view of the sensors and placed in various positions. Similar to the three-by-three pixel array, the outside pixels were less responsive overall. Their response did change however in accordance with the placement of the heated objects in the field of view. This experimentation both verified the capabilities of the device, as well as, depicted the effects of the lens when implemented in an application.

8.2.2.1 Scanning a Scene with a Single Heat Source

In order to test the functionality of the eleven-by-eleven sensor in an imaging application, the blackbody source was positioned facing the sensor, by at a distance so the entire field of view of the sensor is larger than the blackbody. The blackbody was set to 350°C. This setup is shown in Figure 46. The image in Figure 47 was produced on the screen in LabVIEW.

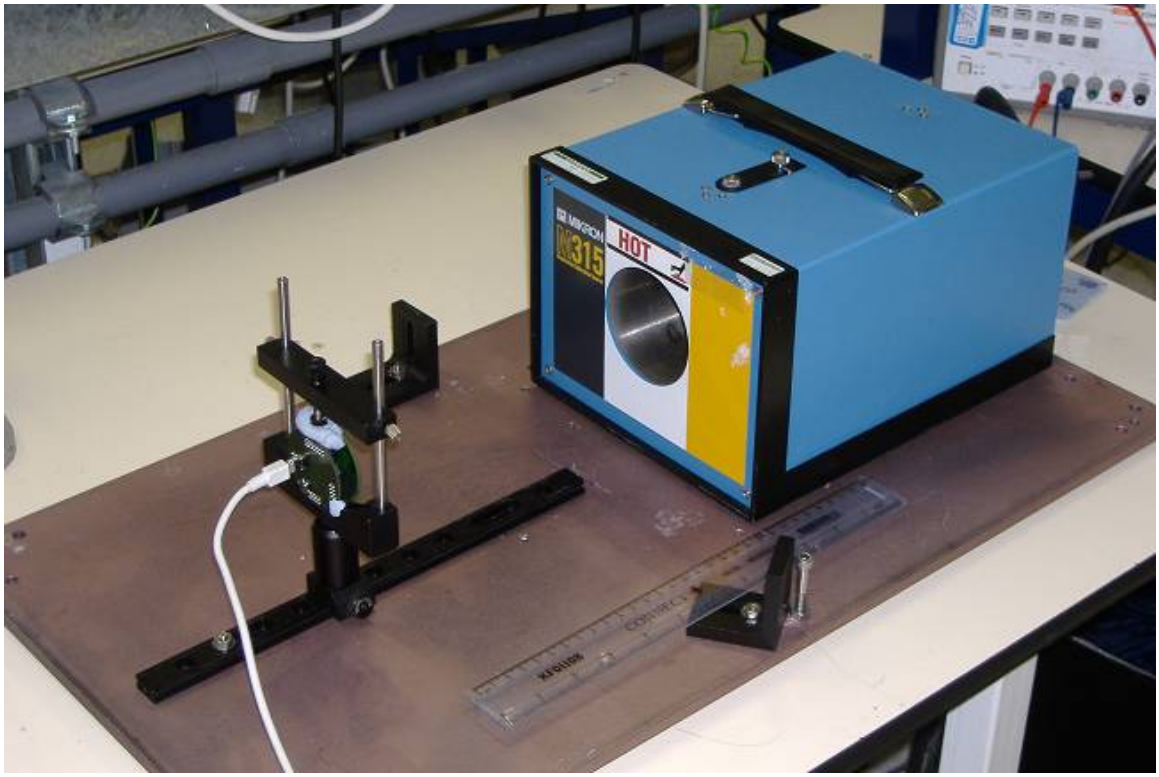

Figure 46: Imaging test with the sensor directly facing the blackbody.

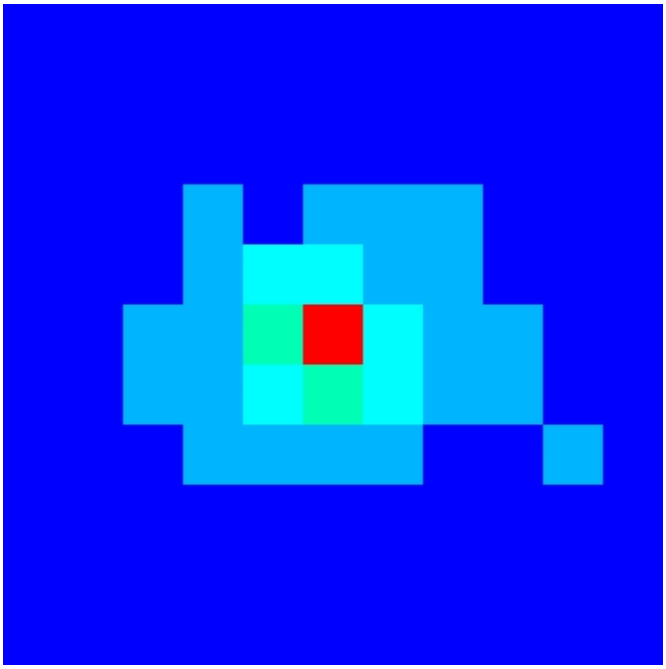

Figure 47: Image produced with a sensor directly facing the blackbody.

The dark blue areas are pixels with the lowest code readings and the red box in the centre is the pixel with the highest code reading. With the type of lens on the sensor,

this image is to be expected. The IR radiation is more focused on the centre pixel, and the pixels further from the centre receive a blurred image. The next step was to rotate the sensor to see if the image moves. Figure 48 shows the sensor rotated to its right and Figure 49 shows the sensor rotated to its left. Figure 50 is the image produced when the blackbody source is to the left of the sensor, and Figure 51 is the image produced when the blackbody is to the right of the sensor.

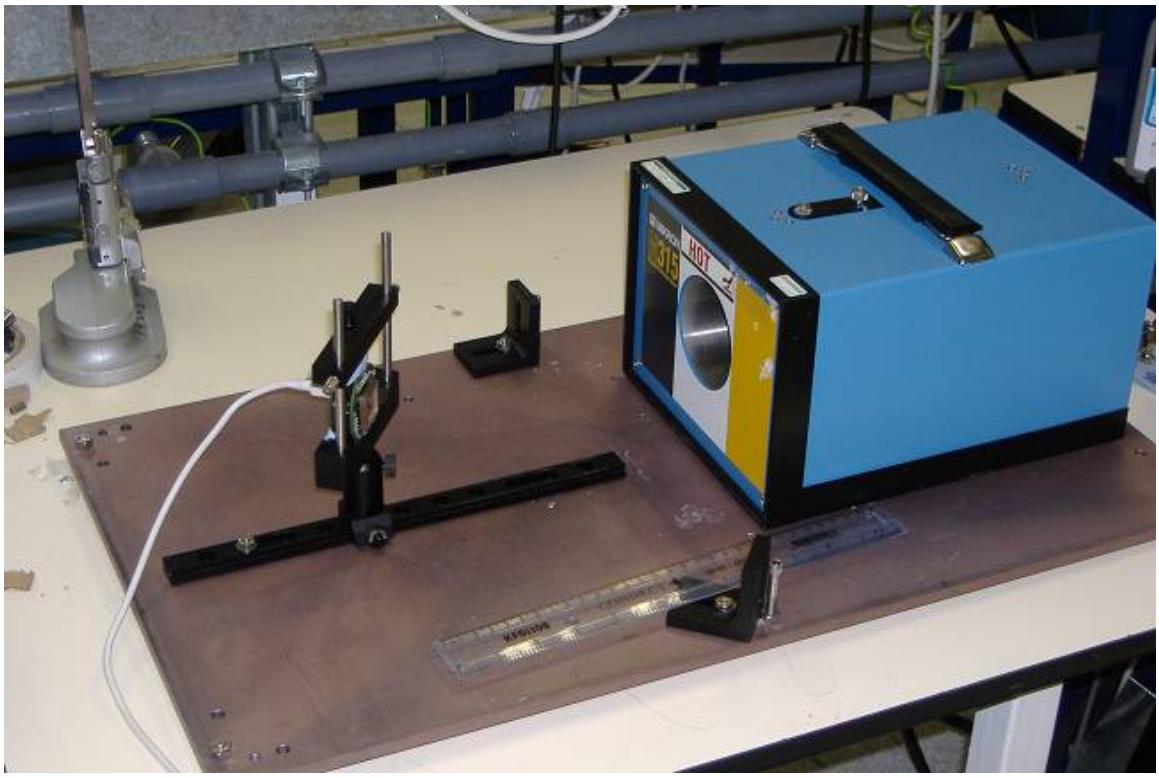

Figure 48: Imaging with the blackbody to the left of the detector.

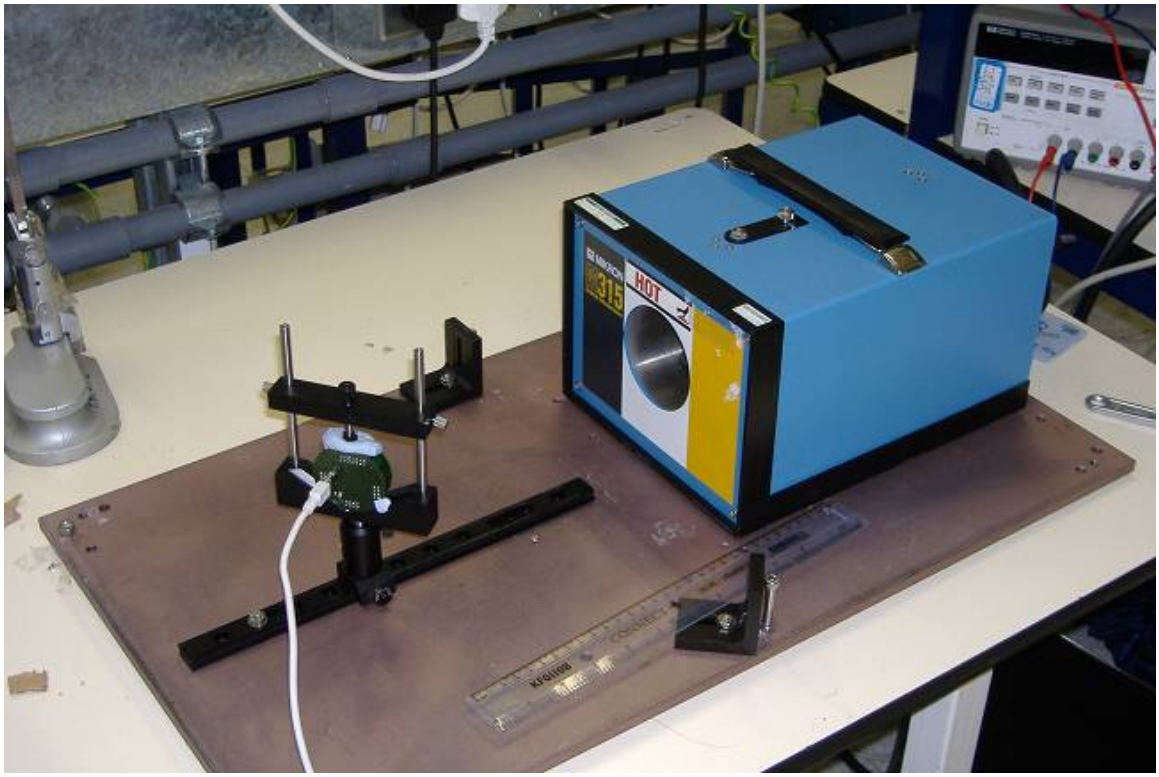

Figure 49: Imaging with the Blackbody to the right of the sensor.

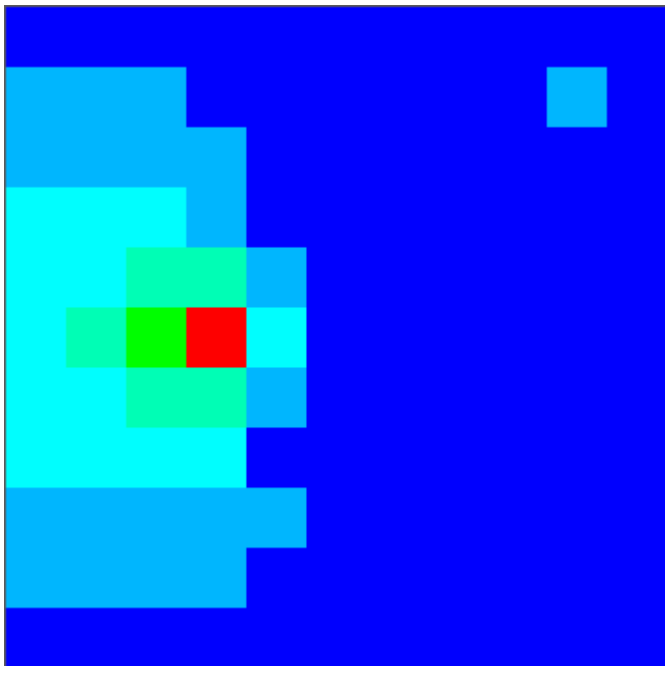

Figure 50: Image produced when the sensor faces to the right of the blackbody.

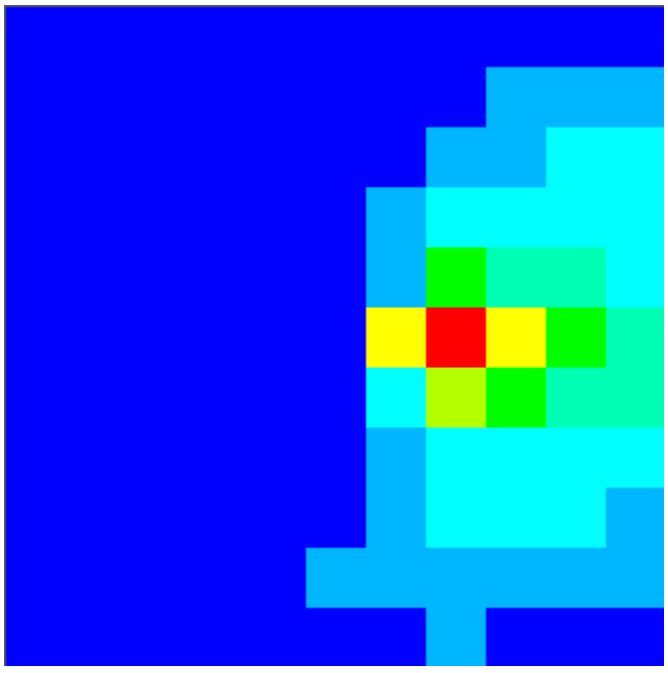

Figure 51: Image produced when the sensor faces to the left of the blackbody.

The image shown in Figure 50 corresponds with the scene change in Figure 48. The blackbody is to the left of the sensor, so the image of the blackbody moved to the left. The same is true with the image in Figure 51 and setup shown in Figure 49. The blackbody is to the right of the sensor, so the image of the blackbody moved to the right. The centre pixels still have a greater response compared to the response of the outer pixels because of the lens, but these images show that thermal imaging is possible. The next task was to have two heat sources in the scene.

8.2.2.2 Introducing a Second Heat Source

Since a second blackbody source was not available, a heat-gun was used as a second heat source. The setup of the sensor and the two heat sources is shown in Figure 52 and Figure 53. The part of the heat-gun that will be hot is the metal tip. The image produced is shown in Figure 54.

Figure 52: Sensor facing the blackbody source and heat gun (front).

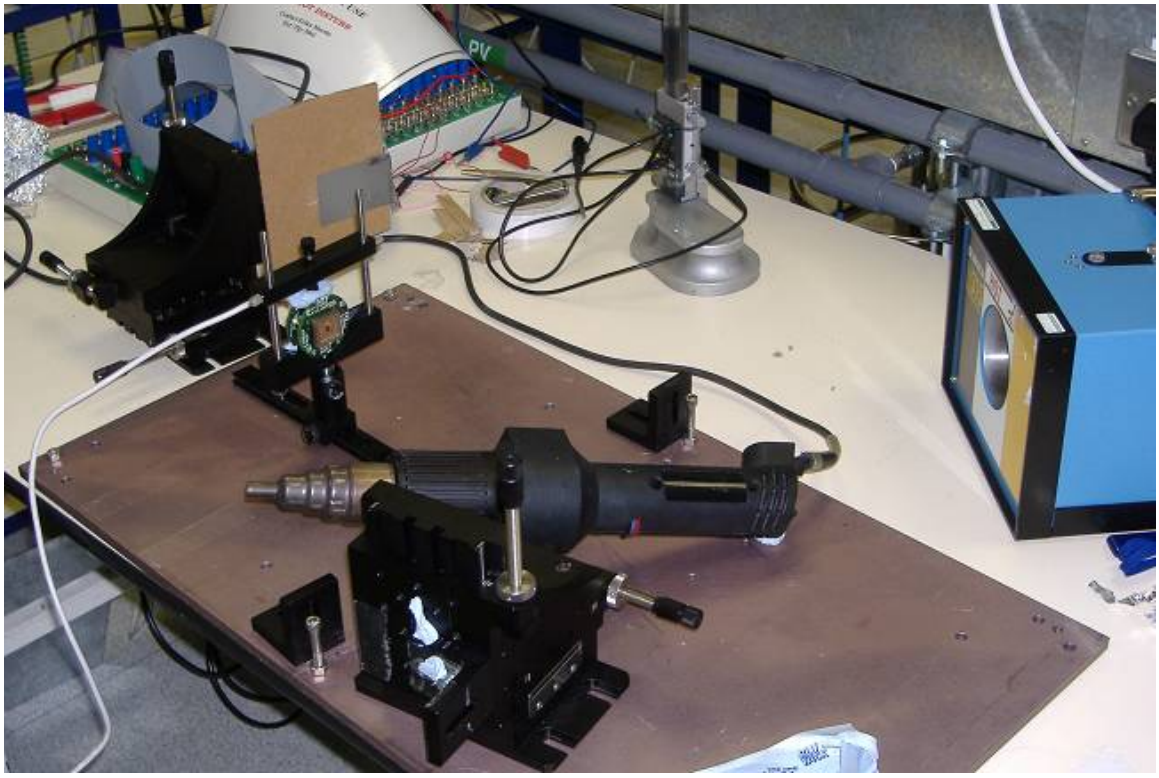

Figure 53: Sensor facing the blackbody source and heat gun (back).

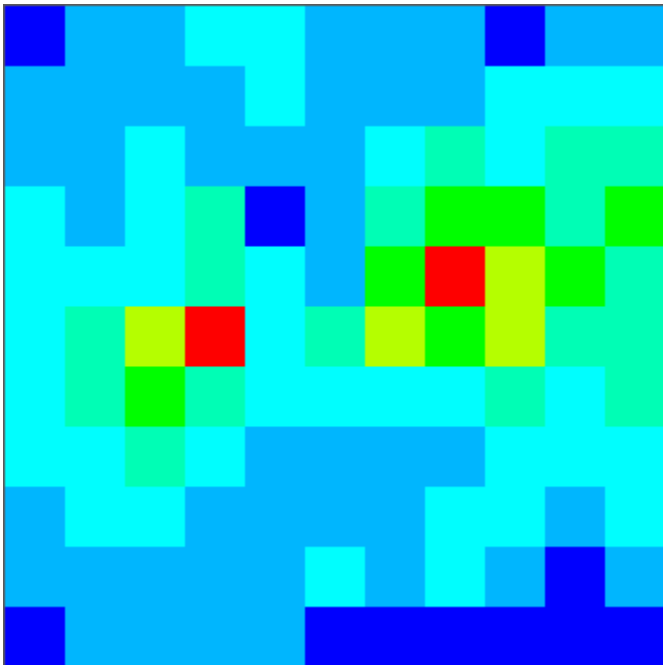

Figure 54: Thermal image produced with two sources.

The image from Figure 54 shows that it is possible to introduce two heat sources and be able to tell them apart in the thermal image we produced. The left side of the

image shows the response from the blackbody source, and the right shows the heat-gun. The setup was modified slightly by moving the heat-gun closer to the sensor and raising it up higher. This is shown in Figure 55, and the imaged produced is shown in Figure 56.

Figure 55: Heat-gun moved closer to the sensor and upwards.

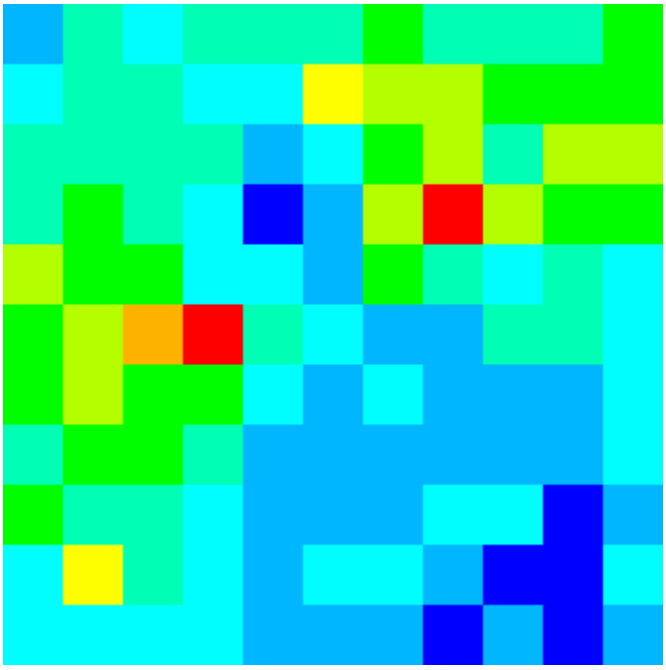

Figure 56: Image produced with the heat-gun moved closer and upwards.

When the heat-gun was moved, the thermal image, shown in Figure 56, updated accordingly. The image of the heat-gun moved upwards and closer to the upper right corner of the thermal image. Figure 54 and Figure 56 still show that the lens is still focusing most of the IR radiation towards the centre pixels.

9 Recommendations

Through constant interaction with the prototype detectors, evaluation boards, AES, and testing equipment and procedures during the course of the project, we have developed recommendations for improving the implementations of and interactions with the detectors. Also included are recommendations for further developing the customer demonstration of the detectors.

9.1 Detector Recommendations

We recommend that ADI research ways to make ADT7301 readings more consistent between sensors. As the product stands right now, there is a great deal of variation in the readings between different sensors. Consistent readings from the ADT7301 are critical for making high precision temperature measurements. Improving the fabrication process or adjusting the internal calibration of the ADT7301 would improve consistency among sensors. With more consistent ADT7301 behaviour, a single point offset correction or general calibration could be applied.

We recommend that ADI use a different type of lens with the sensors. The current lens focuses directly onto the centre pixel of the sensor. Pixels on the outer edge will receive less IR radiation, and have a much lower directivity, making it nearly impossible to make absolute temperature measurements with every pixel. This also makes it hard to create an accurate thermal image of a scene. The new lens should not blur the image on the outer pixels like the current one does.

We recommend that ADI research ways to increase the sensitivity of the pixels. The change in output code over a large range of temperatures is very small compared to the range of code values the AD7794 is able to output. By increasing the sensitivity of the pixels, smaller increases or decreases in temperature will have a much greater effect on the output code. This will eliminate noise as a source of error and also increase the accuracy of making absolute temperature measurements.

We recommend that the AD7794 have a continuous collection mode to stream the data in real-time from the sensor. Currently, the only time the AD7794 performs a conversion is when the AES requests a sample. The filter in the Σ-Δ AD7794 requires two samples to flush out old data, so when multiple pixels are enabled, measurements are not very accurate because old data is never flushed out completely. If the AD7794 is constantly converting the analogue input signal at a high enough update rate, live streaming the output codes will eliminate this source of error.

9.2 Testing Recommendations

We recommend that ADI should repeat our pixel response test for lower temperatures. During our tests, we could not set the blackbody source below room temperature. As a consequence, we could not collect data for temperatures below 25°C. The response of the pixels at lower temperatures needs to be determined.

We recommend that ADI improve the test setups with more reliable materials and more accurate positioning capabilities. The time restriction on our project forced us to use readily available materials and parts when constructing the test setups. The tests we developed also require great attention to the positioning of various elements in the setup. Setups designed specifically for these tests would provide greater control over the testing environment, improve the repeatability and accuracy of results, and eliminate multiple sources of error in collected data.

We recommend that ADI investigate ways to automate the calibration procedures. Manufacturing demands will eventually require the process to be automated, but small-scale automation will be advantageous in the interim. Individually calibrating each of the customer samples will take a considerable amount of time and is prone to error.

9.3 Customer Demonstration Recommendations

We recommend that ADI create a small aperture plate to mount directly over the sensor to limit the field of view of the sensor. With an aperture plate added on to the sensor, the distance to spot ratio of the sensor will greatly increase, which will allow customers to measure the temperature of an object at greater distances. Also, with an aperture mounted on the sensor, the sensor and aperture should be at thermal equilibrium, which will eliminate variation in the aperture temperature as a source of error. Also, having a plate over the detector will protect the delicate wire leads and IC below it while easing insertion and removal.

We recommend using individual calibration equations for each of the detectors distributed to customers. The prototype detectors currently available are not similar enough to apply a single-point or general calibration. If the customer is not planning on testing the raw device operation, the equations will be necessary to see the potential of the detector.

10 Conclusions

ADI succeeded in creating integrated pixel array devices capable of measuring temperature using non-contact thermometry techniques. We implemented and manipulated the devices and their data outputs to draw conclusions and develop a proof of concept that verifies the temperature measurement and thermal imaging potential of the ADiR product line. As preliminary designs, the devices provide repeatable results useful in understanding the different components of the overall system and how they interface. This section reviews the realisations brought about through our research and our specific contributions to the ADiR design project in light of the initial goals of the project.

- **The prototype devices made by ADI are capable of the providing the functionality for which they were initially designed. To establish this functionality, conclusions were drawn about the way the components of the system operated individually and interfaced collectively.**

  The infrared sensing devices provided by ADI are designed for temperature measurement and thermal image display, but until they were actually implemented, no working verifications could be made. The devices are manufactured with raw ADT7301s and AD7794s that need calibration to adjust for offset and gain. The ADT7301s provide an absolute temperature measurement of the physical sensor, while the AD7794 measures the difference in temperature between itself and the object of interest. Once the device is properly calibrated, the next concern is the large field of view. The field of view is affected by both the size of the pixels and the lens. The pixels in the three-by-three array are much larger than those in the eleven-by-eleven array. The eleven-by-eleven array therefore has much greater directivity and is better suited for an imaging application. The lens that is currently on the sensors is not ideal and does not have the effect that ADI desires. A different lens must be used on the final product. The final understanding of the physical device concerns the way it measures temperature. Because it measures the difference between itself and the object it is viewing, any object in the field of view that is at the same temperature as the sensor will not be detected. Any packaging for the final device which will be in the field of view of the sensor therefore must be in thermal equilibrium with it.

- **The final test setup utilised for data collection provided accurate and repeatable results.**

  The test setup utilised for data retrieval was modified multiple times before a reliable and repeatable method was determined and verified. In order to study temperature as a variable, multiple other variables needed to be controlled or

understood. The first variable was the ambient temperature of the sensor. This variable affects the normal operating results of each portion of the device as well as the temperature difference seen by a sensor. The ambient temperature is ultimately necessary to calculate a final temperature. Thermally isolating the sensors behind apertures painted black on the sensing side and reflective metal on the IR source side helped to maintain a fairly constant ambient temperature. Further isolation was necessary from incident IR sources. Placing a cardboard box, which has a low emissivity, over the setup shielded the test setup, eliminated extraneous IR sources, and provided control over the testing environment so that it could be recreated and produce analogous results. Careful notes were taken of the setup dimensions and positioning for future testing.

- **The data collected from the various devices in the ADiR can be used to determine the absolute value of an object at a specified distance.**

One of the key goals of this project was to coordinate the effects and outputs of the multiple devices in the ADiR to obtain an absolute temperature. Once the necessary test methods were developed and the devices properly configured individually, the next step was developing equations, which were applicable to the ADT7301 and AD7794 outputs. The final temperature was the sum of the ambient sensor temperature measured by the ADT7301 and the sensor-to-object temperature difference measured by the thermopile sensor. For the purposes of this project, only the un-packaged detectors were available. The external packaging that will eventually limit the distance-to-spot ratio providing standalone use of the product as a non-contact thermometer had to be simulated using apertures and a controlled environment setup. The proof of concept in this case verifies the ability of the sensor to accurately measure a temperature with a controlled distance to spot ratio utilising our specific setup. The future product will have a much smaller field of view and therefore allow the device to measure temperature over a temperature range.

- **The AES now collects data in a more effective manner and is able to save the data to various formats. It further processes the data to provide general analyses and visualisation.**

The AES originally provided by ADI was only configured to verify communication with one pixel at a time through the evaluation board. The program was then further developed to allow for functional analysis and characterisation. It was configured to take data by cycling through the selected pixels before returning to collect data for a second round of samples. It was reconfigured to allow the user to choose the sensor pixels from which to gather data, the form in which the data is collected, and the amount of data to collect. It was further edited to provide real-time

viewing of the data collection for the user-chosen pixels. Further analysis is provided to view the previously collected samples along with minimum, maximum, and means values.

- **The proof of concept for the three-by-three pixel array included a demonstration utilising the testing apparatus and calibration equations unique to the particular sensor, while the demonstration for the eleven-by-eleven involved the visualisation of object as they were moved across the field of view.**

  ADI has succeeded in designing and manufacturing integrated pixel array detectors capable of absolute temperature measurement and of thermal imaging. The prototype nature of the detectors requires that they be applied under certain conditions to produce the desired results, but that will change with further improved versions of the product. In the meantime, the functionality can be shown by individually calibrating the devices and recreating the testing environments detailed in Chapter 8.

The final manufactured product will be designed for stand-alone use with the capability of producing the absolute temperature of an object at a distance with reasonable accuracy. For the prototype devices and this project, emphasis was placed on developing a demonstration or setup which utilised the currently available prototypes. In a short time after the completion of this particular project, ADI must distribute prototypes or demonstration setups to potential customers that utilise the currently available sensors.

As an innovative technological leader, ADI succeeded in producing non-contact detectors that are can be used in absolute temperature measurement and thermal imaging applications. There is more design work to be done to ease user implementation of the device and to realise the full potential of the next generation technology innovated by Analog Devices, Inc. Now with merited confidence in the abilities of the detectors and knowledge of the implications of its physical implementation, ADI is in a position to reveal their innovative technology, release their new prototypes, and become a leader in non-contact thermometry technology.

References

"AD7794 Datasheet." Analog Devices Inc., 2006.

"ADT7301 Datasheet." Analog Devices Inc., 2006.

"IR to Digital: FAE Training." Analog Devices Inc., 2006.

Burns, Jim. "Resistive Thermometers." Temperature Measurement. EngNetBase, CRC Press LLC., 1999. 10 Aug. 2006. http://www.engnetbase.com.

Gruner, Klaus-Dieter. Principles of Non-Contact Temperature Measurement. Raytek, December 2003.

Porro, Irene and Flanagan, Kathryn. (2001). "The Electromagnetic Spectrum." Retrieved from the World Wide Web on 30th of August:
http://space.mit.edu/CSR/outreach/MULTILING/CHANDRA_ENG_ITA/Slide5.html

Sandberg, Robert J. "Temperature." EngNetBase, CRC Press LLC., 2000. 10 Aug. 2006. <http://www.engnetbase.com>.

Schilz, Jürgen. "Thermoelectric Infrared Sensors (Thermopiles) for Remote Temperature Measurements; Pyrometry." PerkinElmer Optoelectronics 11 July 2000.

Travers, Christine M., Agha Jahanzeb, Donald P. Butler, Zeynep Çelik-Butler (1997). "Fabrication of Semiconducting YBaCuo Surface-Micromachined Bolometer Arrays." Journal of Microelectromechanical Systems. IEEE, 10 Aug. 2006.
http://ieeexplore.ieee.org.

Appendix A – ADT7301 Temperature Forcing Data

The following appendix provides the data utilised to graph the temperature versus blackbody characteristics for the pixel arrays. Also included is a graph for each sensor. A linear trend line was fit to each of the characteristics and used to calibrate the output of the ADT7301. Though an eleven-by-eleven pixel array was temperature forced, the data was obtained for comparison purposes only. The eleven-by-eleven pixel arrays for the purposes of this project are utilised solely for their ability to detect a temperature difference between its physical self and an object.

ADT7301 Calibration		3x3 Detectors					11x11 Detector
		26a	P22	J10	D30	F6	L12
Forced Temperature (°C)	-25	-14.4131	-16.8181	-19.4050	-8.0756	-15.4581	-6.2137
	-20	-9.5412	-11.5225	-13.9000	-4.1600	-11.7593	-1.3494
	-15	-4.5212	-6.2256	-8.6700	-0.0975	-6.2562	4.1331
	-10	0.5950	-0.9031	-3.3319	4.5325	-1.0881	9.4812
	-5	5.6437	4.2537	1.8100	8.5931	4.0756	14.6450
	0	10.6131	9.4219	7.0494	13.1119	9.1612	19.8350
	5	15.6744	14.6987	12.2331	17.7481	14.4300	25.1975
	10	20.8919	20.2375	17.4012	22.7544	19.5625	30.8856
	15	25.9662	25.1225	22.4912	27.5931	24.6662	36.2543
	20	31.9594	30.7537	27.7481	32.1756	29.8643	42.3962
	25	36.1631	35.7600	32.8962	37.5450	34.9950	47.7331
	30	41.3043	41.0593	38.2475	42.1819	40.2100	52.9362
	35	46.5287	46.2637	43.1437	47.1969	45.4094	57.8094
	40	51.6837	51.5062	47.7794	52.1087	50.5762	63.6494
	45	57.0456	56.7344	53.3756	56.9825	55.7844	68.4537
	50	62.9737	61.9706	59.5337	62.6443	61.0106	74.2194
	55	67.5362	67.2287	64.7156	67.8550	66.7587	80.3587
	60	72.4025	72.3912	69.8131	72.8394	71.6944	85.4843
	65	77.5206	77.5369	74.2737	77.7487	76.7481	90.2781
	70	82.3337	82.8587	78.8662	82.0506	81.0869	96.0287
	75	86.9475	88.0750	85.4956	87.7287	86.1581	101.3875
	80	92.5981	93.6718	90.2756	92.4687	91.8762	106.8412
	85	98.4593	99.0137	95.7794	97.7356	97.4662	112.5256
	90	103.4900	104.4675	100.5981	103.0906	101.8837	118.4737
	95	109.2231	109.3362	105.3950	108.2425	106.8419	123.7500
	100	113.6950	114.3181	110.9231	113.9406	112.6144	129.4331

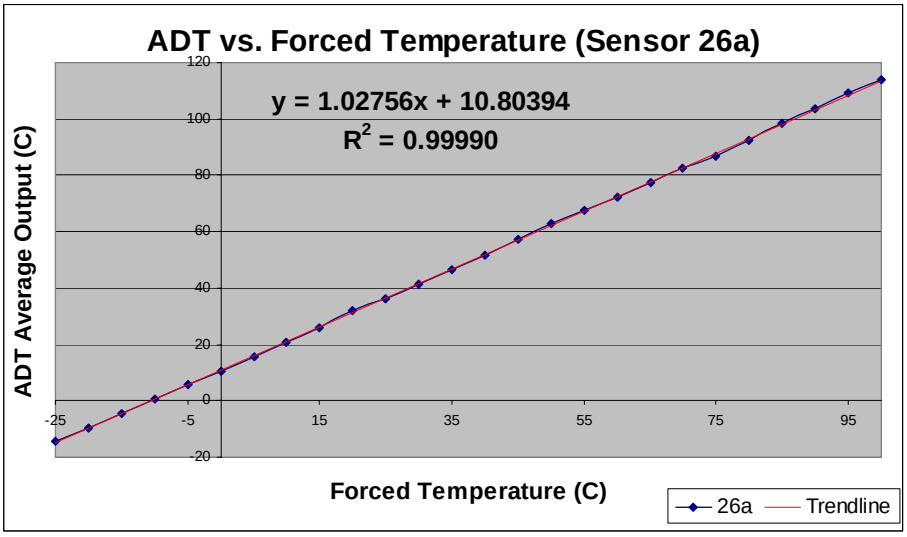
ADT vs. Forced Temperature (Sensor 26a)
y = 1.02756x + 10.80394
R2 = 0.99990
ADT Average Output (C)
Forced Temperature (C)
120
100
80
60
40
20
0
-20
-25
-5
15
35
55
75
95
26a
Trendline

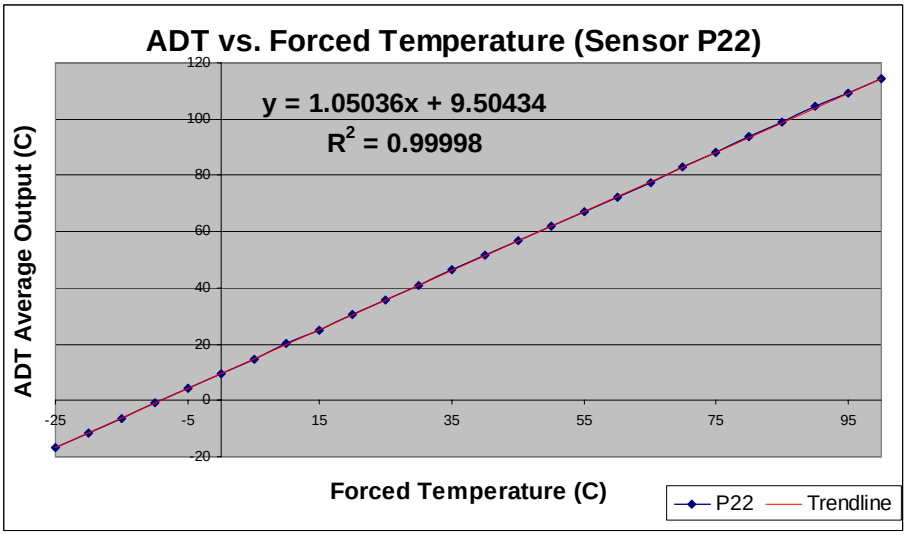
ADT vs. Forced Temperature (Sensor P22)
y = 1.05036x + 9.50434
R2 = 0.99998
ADT Average Output (C)
Forced Temperature (C)
120
100
80
60
40
20
0
-20
-25
-5
15
35
55
75
95
P22
Trendline

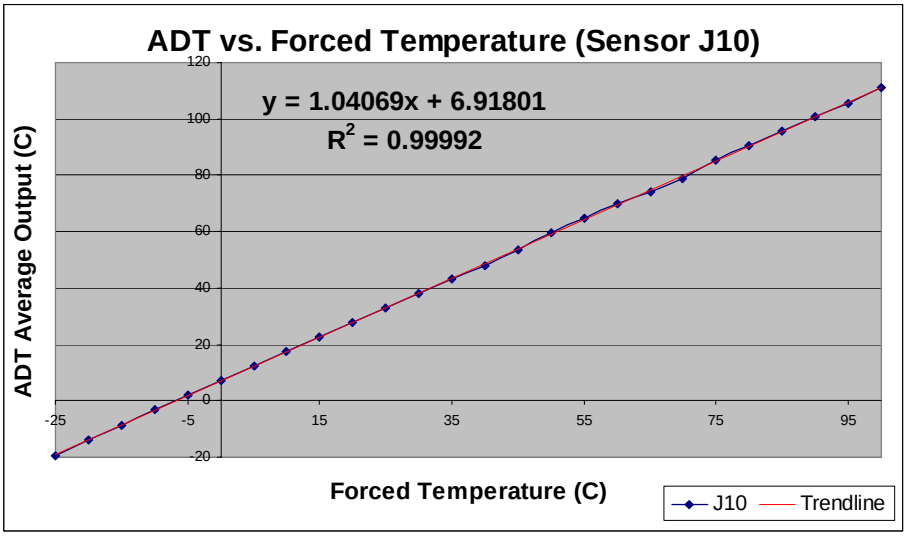
ADT vs. Forced Temperature (Sensor J10)
y = 1.04069x + 6.91801
R2 = 0.99992
ADT Average Output (C)
Forced Temperature (C)
J10
Trendline

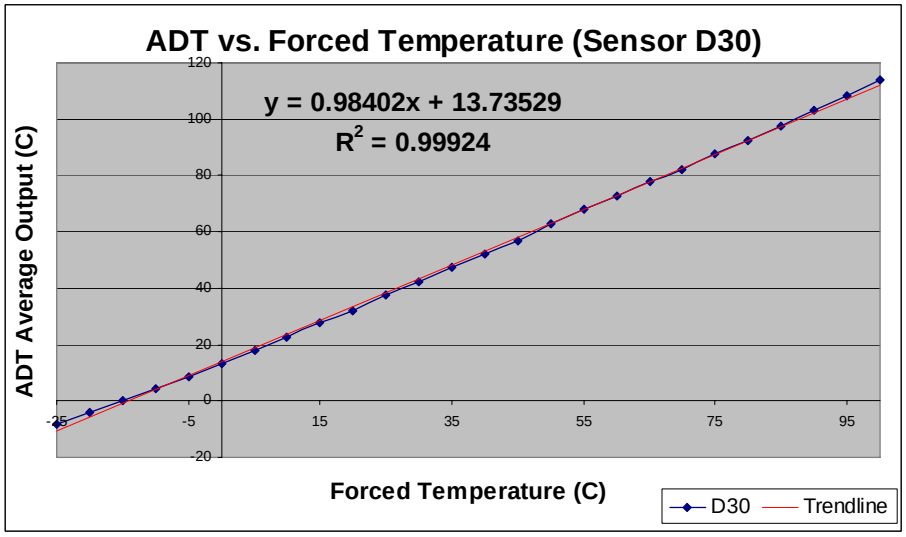
ADT vs. Forced Temperature (Sensor D30)
y = 0.98402x + 13.73529
R2 = 0.99924
ADT Average Output (C)
Forced Temperature (C)
D30
Trendline

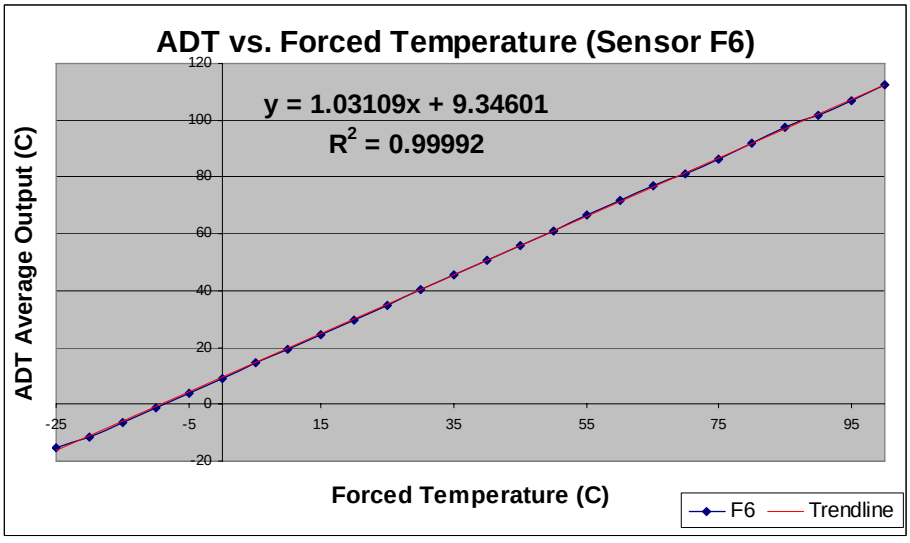
ADT vs. Forced Temperature (Sensor F6)
y = 1.03109x + 9.34601
R2 = 0.99992
ADT Average Output (C)
Forced Temperature (C)
F6
Trendline

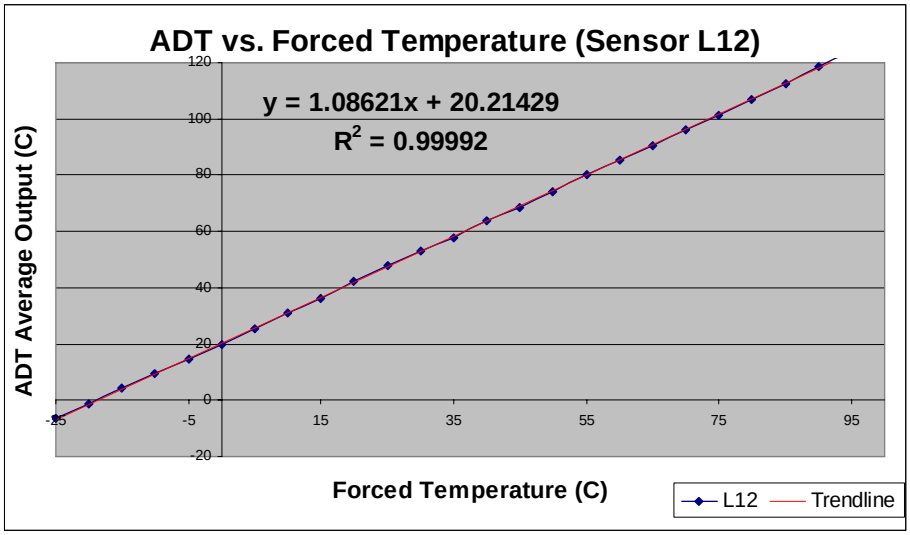
ADT vs. Forced Temperature (Sensor L12)
y = 1.08621x + 20.21429
R2 = 0.99992
ADT Average Output (C)
120
100
80
60
40
20
0
-20
-25
-5
15
35
55
75
95
Forced Temperature (C)
L12
Trendline

Appendix B – ADiR Angular Response Data

The first graph shows the change in response over a full horizontal sweep of 180° rotation. The blue line is pixel 4, the red line is pixel 5, and the green line is pixel 6. The second graph shows the same data, but on a polar plot.

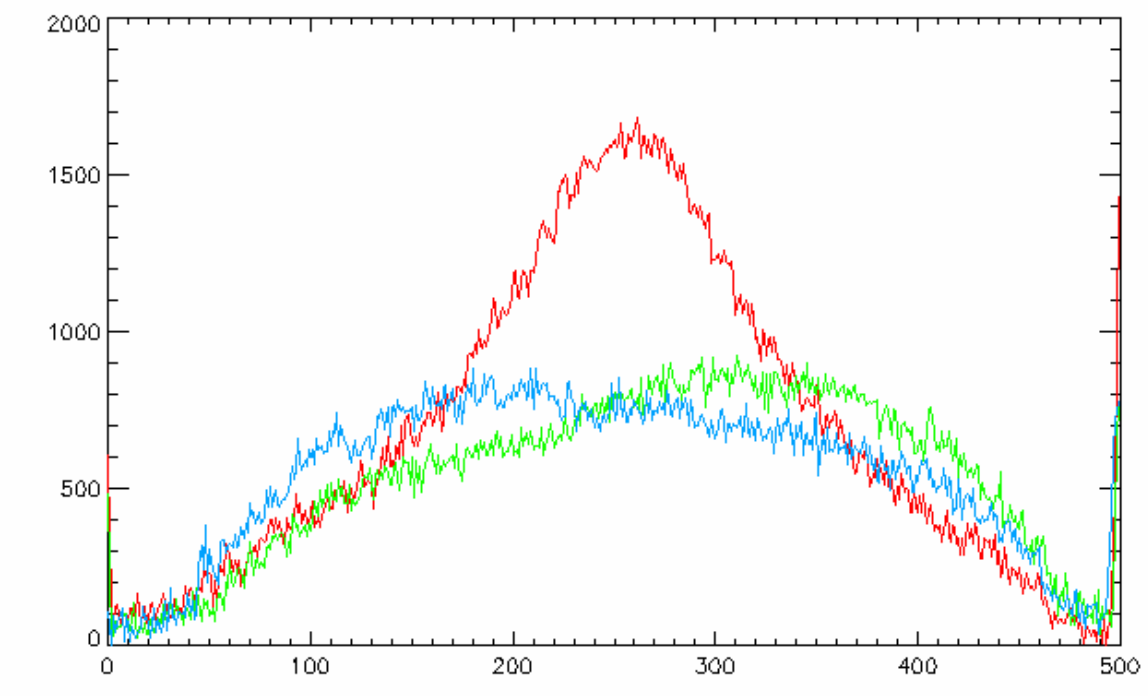

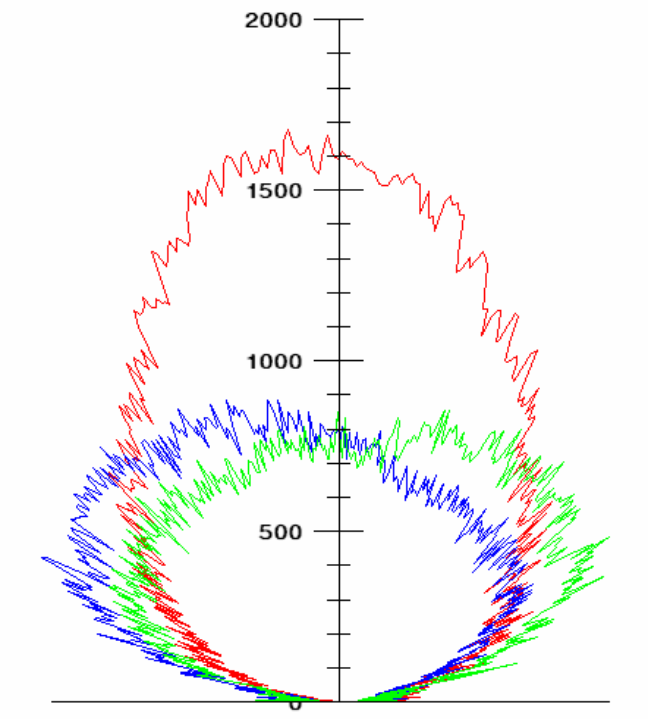

Appendix C – AD7794 Pixel Response Data

The following sections contain the data collected for the pixel response test. The data is broken down into two parts. The first section is the data that was collected when apertures were swapped throughout the test. The second section is the data that was collected when using one aperture per temperature sweep.

C.1 Consecutive Aperture Test

26a A	Large Aperture			Medium Aperture			Small Aperture		
Blackbody	ADC	ADT	Temp Diff	ADC	ADT	Temp Diff	ADC	ADT	Temp Diff
25	8386287	24.94843	0.051568	8386347	24.95177	0.048233	8386365	24.59504	0.404964
30	8386535	25.01411	4.985892	8385897	25.05364	4.946362	8385972	25.03387	4.966128
35	8386907	24.8873	10.1127	8386133	24.86996	10.13004	8385928	24.88608	10.11392
40	8387402	24.82404	15.17596	8386200	24.79425	15.20575	8385753	24.94235	15.05765
45	8387960	24.82799	20.17201	8386294	24.82921	20.17079	8385747	24.85293	20.14707
50	8388633	24.92106	25.07894	8386369	24.85658	25.14342	8385821	24.79972	25.20028
55	8389256	24.87817	30.12183	8386561	24.80974	30.19026	8385848	24.76687	30.23313
65	8390231	24.7611	40.2389	8386930	24.66135	40.33865	8385860	24.77022	40.22978
75	8391467	24.75168	50.24832	8387353	24.64583	50.35417	8385893	24.68933	50.31067
85	8392971	24.83529	60.16471	8387659	24.66743	60.33257	8386007	24.65527	60.34473
105	8396243	24.89399	80.10601	8388710	24.64584	80.35416	8386218	24.65527	80.34473
125	8400064	25.03448	99.96552	8389628	24.731	100.269	8386374	24.70637	100.2936
145	8403765	25.26774	119.7323	8390850	24.78998	120.21	8386586	24.76444	120.2356
165	8408369	25.48154	139.5185	8392048	24.91224	140.0878	8386771	24.9463	140.0537
190	8417484	25.66767	164.3323	8394334	24.6793	165.3207	8387082	24.90524	165.0948
215	8423689	26.20321	188.7968	8396198	24.94052	190.0595	8387833	24.77144	190.2286
240	8431768	26.64206	213.3579	8398805	25.28842	214.7116	8388619	24.91924	215.0808
270	8447610	27.31903	242.681	8401903	25.59102	244.409	8389205	25.43289	244.5671
300	8461043	28.27427	271.7257	8404965	26.74272	273.2573	8388737	26.72478	273.2752

26a B	Large Aperture			Medium Aperture			Small Aperture		
Blackbody	ADC	ADT	Temp Diff	ADC	ADT	Temp Diff	ADC	ADT	Temp Diff
30	8387597	21.98997	8.01003	8386611	22.23387	7.76613	8386141	22.50181	7.498194
35	8387529	22.62252	12.37748	8386386	22.69308	12.30692	8386075	22.70191	12.29809
40	8387866	22.84818	17.15182	8386541	22.79194	17.20806	8386087	22.75909	17.24091
45	8388654	22.81383	22.18617	8386678	22.79953	22.20047	8386106	22.84057	22.15943
50	8389261	22.83997	27.16003	8386878	22.83329	27.16671	8386093	22.84636	27.15364
55	8389939	22.88498	32.11502	8387002	22.82416	32.17584	8386259	22.767	32.233
65	8390946	22.97501	42.02499	8387342	22.99175	42.00825	8386241	22.97744	42.02256
75	8392251	23.09664	51.90336	8387648	23.11854	51.88146	8386265	23.01881	51.98119
85	8393651	23.15108	61.84892	8388053	23.1155	61.8845	8386354	23.07628	61.92372
95	8396052	23.2323	71.7677	8388467	23.24781	71.75219	8386342	23.07628	71.92372
105	8397687	23.38495	81.61505	8389099	23.47407	81.52593	8386265	23.34177	81.65823
125	8401829	23.46829	101.5317	8390067	23.50936	101.4906	8386443	23.48624	101.5138
145	8404108	23.59875	121.4013	8391190	23.58354	121.4165	8386782	23.52061	121.4794
165	8410247	23.81498	141.185	8392197	23.89861	141.1014	8387038	23.64649	141.3535
190	8418913	24.09355	165.9064	8394205	24.09081	165.9092	8387478	23.97496	166.025
215	8429728	24.86084	190.1392	8397054	24.83164	190.1684	8387392	24.7766	190.2234
240	8439072	24.86084	215.1392	8398913	25.85226	214.1477	8387283	25.60654	214.3935
270	8452906	26.33034	243.6697	8401811	26.63659	243.3634	8387666	26.00858	243.9914
300	8468275	26.66821	273.3318	8406019	27.05262	272.9474	8388142	26.70137	273.2986

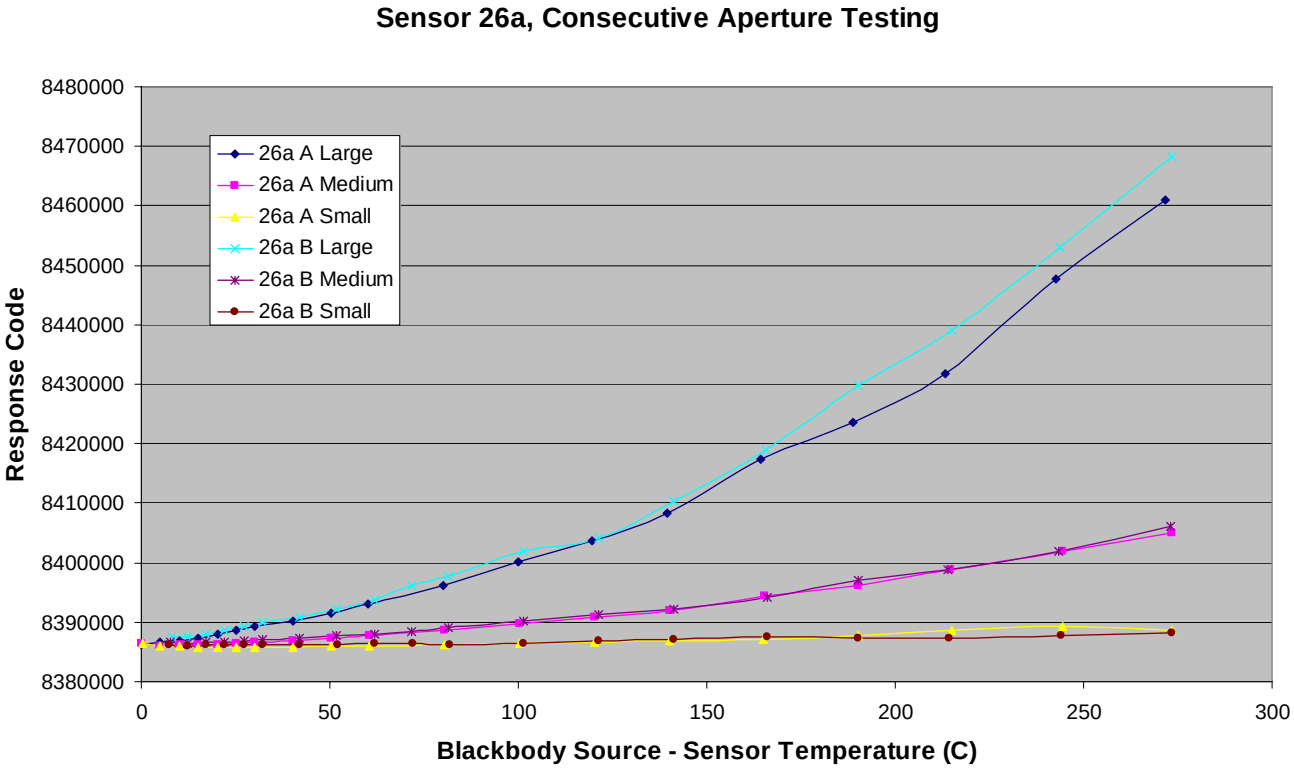

	ADT			Apertures			Box		
Blackbody	ADT L	ADT M	ADT S	Aperture L	Aperture M	Aperture S	Box L	Box M	Box S
25	27.61999	27.62325	27.27385	23.7200	23.9200	23.2800	23.0000	23.3333	
30	27.68431	27.72303	27.70367	23.2000	23.6400	23.5200	22.8000	23.6667	23.0667
35	27.56011	27.54313	27.55892	23.1600	23.2000	23.5600	23.0667	23.1333	23.1333
40	27.49815	27.46897	27.61403	23.0800	22.9600	23.3600	22.9333	23.0000	23.0667
45	27.50202	27.50321	27.52645	23.1200	23.2800	23.1200	23.0000	23.0000	22.9333
50	27.59318	27.53003	27.47433	23.1600	22.8000	23.3200	23.0667	22.8000	23.1333
55	27.55117	27.48415	27.44215	23.4000	22.8800	23.2000	23.0000	22.8000	23.0000
65	27.4365	27.3388	27.44544	22.9600	23.0400	22.6000	23.1333	22.8667	22.5333
75	27.42727	27.3236	27.36621	23.1600	23.5600	22.4400	23.5333	23.8667	22.4000
85	27.50917	27.34476	27.33284	22.5600	22.6000	22.8800	23.0667	22.6667	22.7333
105	27.56666	27.32361	27.33284	23.1200	22.8000	22.0000	23.0000	22.8000	21.9333
125	27.70427	27.40702	27.38289	21.6400	22.5200	22.0400	21.9333	22.8667	21.7333
145	27.93274	27.46479	27.43978	22.6800	22.3200	23.0000	22.9333	21.9333	23.3333
165	28.14215	27.58454	27.6179	21.8000	22.1200	21.6800	21.8667	21.8000	21.8667
190	28.32446	27.35638	27.57769	23.1200	22.6800	22.5200	22.1333	22.1333	21.9333
215	28.84901	27.61224	27.44663	23.4400	23.3600	22.6000	22.3333	22.2000	22.2667
240	29.27885	27.953	27.59139	23.2400	23.1600	23.2400	22.3333	22.4000	22.2667
270	29.94191	28.24938	28.0945	23.7200	23.2800	23.3200	22.2000	22.2000	22.2000
300	30.87754	29.37743	29.35986	23.8400	23.6800	23.6000	22.2000	22.5333	22.2000

ADT, Aperture, and Box Temperatures Recorded During Testing

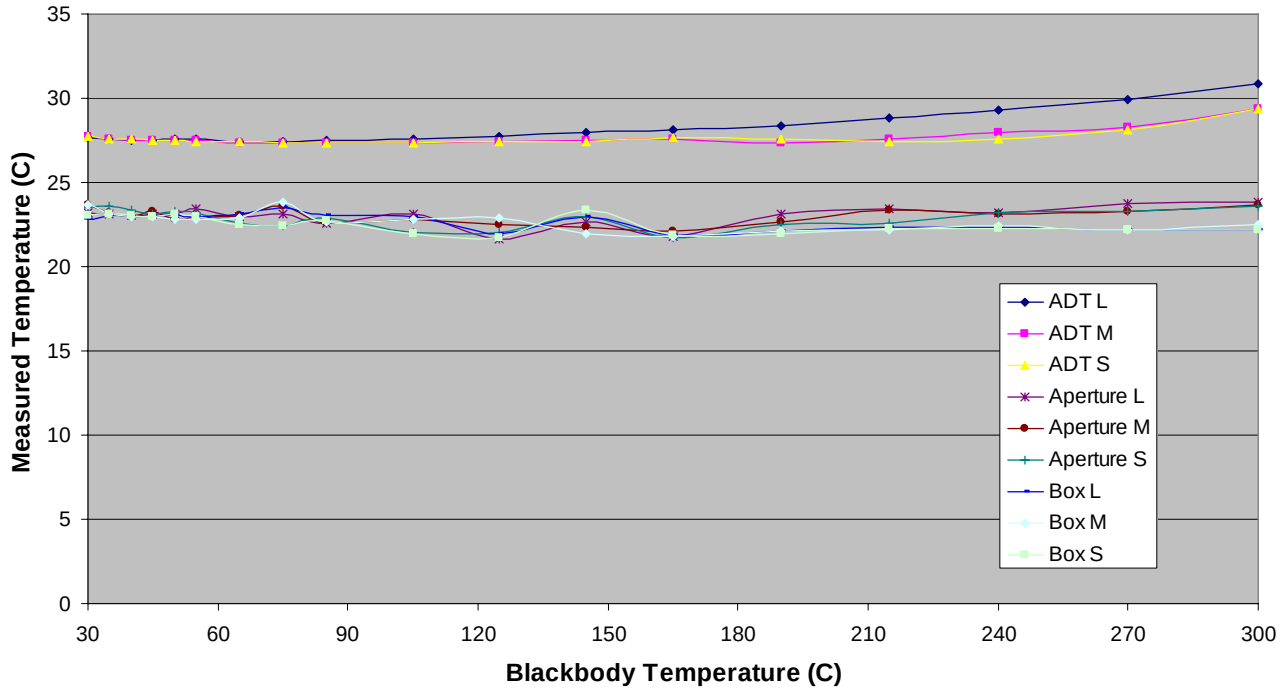

C.2 Individual Aperture Testing

26a A	Large Sep25			Medium Sep26		
Blackbody	ADC	ADT	Temp Diff	ADC	ADT	Temp Diff
30	8386620	24.14555	5.85445	8385840	24.79938	5.200616
35	8387014	24.24289	10.75711	8385928	24.839	10.161
40	8387488	24.34018	15.65982	8386000	24.89678	15.10322
45	8387830	24.41015	20.58985	8386150	24.86932	20.13068
50	8388436	24.51052	25.48948	8386300	24.91189	25.08811
55	8388929	24.49529	30.50471	8386422	24.93017	30.06983
60	8389455	24.63519	35.36481	8386628	24.96366	35.03634
70	8390708	24.63215	45.36785	8387023	25.01838	44.98162
80	8392055	24.70211	55.29789	8387415	25.00317	54.99683
90	8393427	24.80244	65.19756	8387817	25.02747	64.97253
100	8394964	24.96972	75.03028	8388315	25.04881	74.95119
120	8398271	25.10353	94.89647	8389372	25.04574	94.95426
140	8401967	25.28904	114.711	8390558	25.11568	114.8843
160	8406098	26.01892	133.9811	8391974	25.1704	134.8296
180	8411188	26.11626	153.8837	8393356	25.26474	154.7353
200	8416549	26.36865	173.6313	8395010	25.32855	174.6715
220	8422404	26.77008	193.2299	8396760	25.50803	194.492
240	8428654	27.17457	212.8254	8398699	25.58399	214.416
260	8435892	27.62773	232.3723	8400870	25.7452	234.2548
280	8443557	28.22681	251.7732	8403188	25.92469	254.0753
300	8452017	28.68299	271.317	8405766	26.11622	273.8838

26a B	Large Sep26			Medium Sep29		
Blackbody	ADC	ADT	Temp Diff	ADC	ADT	Temp Diff
30	8387018	23.48255	6.517453	8387237	22.03258	7.967423
35	8387050	23.86275	11.13725	8387187	22.25821	12.74179
40	8387371	23.96005	16.03995	8387160	22.45556	17.54444
45	8387713	24.16384	20.83616	8387190	22.63045	22.36955
50	8388067	24.31279	25.68721	8387158	22.84485	27.15515
55	8388589	24.35843	30.64157	8387219	22.9933	32.0067
60	8389070	24.36456	35.63544	8387339	23.08447	36.91553
70	8390207	24.44062	45.55938	8387560	23.25845	46.74155
80	8391438	24.41622	55.58378	8387910	23.31899	56.68101
90	8392709	24.51964	65.48036	8388306	23.39679	66.60321
100	8393993	24.59866	75.40134	8388743	23.45672	76.54328
120	8397039	24.68381	95.31619	8389765	23.52277	96.47723
140	8400294	24.91189	115.0881	8390839	23.61486	116.3851
160	8404243	25.11262	134.8874	8392121	23.75269	136.2473
180	8408548	25.38327	154.6167	8393520	23.8016	156.1984
200	8413358	25.63269	174.3673	8395142	23.90747	176.0925
220	8418626	26.0858	193.9142	8396879	24.10993	195.8901
240	8424387	26.59373	213.4063	8398802	24.27022	215.7298
260				8400889	24.40958	235.5904
280	8437541	27.61561	252.3844	8403175	24.54945	255.4505
300	8445018	28.28464	271.7154	8405692	24.69484	275.3052

26a C	Large Oct3			Medium Oct3		
Blackbody	ADC	ADT	Temp Diff	ADC	ADT	Temp Diff
30	8386844	22.9541	7.0459	8386292	22.8196	7.1804
35	8387430	23.0994	11.9006	8386404	22.9389	12.0611
40	8387948	23.1542	16.8458	8386533	22.9924	17.0076
45	8388607	23.2409	21.7591	8386655	23.0702	21.9298
50	8389222	23.3193	26.6807	8386819	23.1046	26.8954
55	8389894	23.4014	31.5986	8387009	23.1295	31.8705
60	8390592	23.4282	36.5718	8387172	23.1977	36.8023
70	8392067	23.5273	46.4727	8387596	23.2028	46.7972
80	8393626	23.6392	56.3608	8388055	23.2515	56.7485
90	8395430	23.7077	66.2923	8388547	23.2843	66.7157
100	8397251	23.8503	76.1497	8389040	23.3242	76.6758
120	8401396	24.0082	95.9918	8390207	23.3792	96.6208
140	8405863	24.364	115.636	8391484	23.4863	116.5137
160	8411165	24.5802	135.4198	8392943	23.5422	136.4578
180	8416863	24.8664	155.1336	8394597	23.6271	156.3729
200	8423401	25.2413	174.7587	8396388	23.736	176.264
220	8430519	25.6945	194.3055	8398406	23.8792	196.1208
240	8438156	26.2434	213.7566	8400571	24.0459	215.9541
260	8446647	26.7784	233.2216	8402907	24.2259	235.7741
280	8455894	27.4416	252.5584	8405521	24.4309	255.5691
300	8466026	28.132	271.868	8408377	24.6407	275.3593

26a D	Large Oct3			Medium Oct3		
Blackbody	ADC	ADT	Temp Diff	ADC	ADT	Temp Diff
30	8386880	23.2518	6.7482	8385966	23.3059	6.6941
35	8387337	23.4005	11.5995	8386099	23.288	11.712
40	8387971	23.4431	16.5569	8386266	23.2685	16.7315
45	8388654	23.2746	21.7254	8386422	23.2664	21.7336
50	8389361	23.3263	26.6737	8386583	23.2625	26.7375
55	8389903	23.4376	31.5624	8386832	23.2612	31.7388
60	8390554	23.5325	36.4675	8386975	23.2594	36.7406
70	8392062	23.5632	46.4368	8387412	23.2533	46.7467
80	8393630	23.6645	56.3355	8387870	23.2637	56.7363
90	8395430	23.7712	66.2288	8388372	23.2971	66.7029
100	8397138	23.965	76.035	8388922	23.2883	76.7117
120	8401348	24.0656	95.9344	8390044	23.3248	96.6752
140	8406006	24.2247	115.7753	8391339	23.3649	116.6351
160	8411090	24.5379	135.4621	8392789	23.4337	136.5663
180	8416916	24.7834	155.2166	8394456	23.4857	156.5143
200	8423536	25.1024	174.8976	8396293	23.5723	176.4277
220	8430564	25.5254	194.4746	8398276	23.6846	196.3154
240	8438192	26.1525	213.8475	8400446	23.8372	216.1628
260	8446621	26.6369	233.3631	8402809	23.989	236.011
280	8455856	27.2485	252.7515	8405367	24.2785	255.7215
300	8466035	27.879	272.121	8408251	24.4342	275.5658

P22 A	Large Oct2			Medium Oct2		
Blackbody	ADC	ADT	Temp Diff	ADC	ADT	Temp Diff
30	8388196	22.6673	7.3327	8388713	20.784	9.216
35	8388698	22.8648	12.1352	8388449	21.3317	13.6683
40	8389229	23.0246	16.9754	8388441	21.5974	18.4026
45	8389827	23.143	21.857	8388467	21.8217	23.1783
50	8390459	23.2028	26.7972	8388547	22.0086	27.9914
55	8391130	23.3013	31.6987	8388377	22.3962	32.6038
60	8391821	23.3748	36.6252	8388551	22.5325	37.4675
70	8393476	23.4063	46.5937	8388973	22.6655	47.3345
80	8395242	23.4777	56.5223	8389327	22.7419	57.2581
90	8397085	23.5664	66.4336	8389841	22.8142	67.1858
100	8398952	23.6636	76.3364	8390411	22.8978	77.1022
120	8403575	23.6907	96.3093	8391675	22.9484	97.0516
140	8408454	23.8906	116.1094	8393024	23.1245	116.8755
160	8413931	24.0537	135.9463	8394581	23.2483	136.7517
180	8420065	24.5119	155.4881	8396354	23.3691	156.6309
200	8426896	24.8356	175.1644	8398287	23.4843	176.5157
220	8434380	25.3598	194.6402	8400507	23.5973	196.4027
240	8442422	25.887	214.113	8402902	23.7633	216.2367
260	8451540	26.3044	233.6956	8405466	23.841	236.159
280	8461466	26.9066	253.0934	8408265	24.0215	255.9785
300	8472092	27.6322	272.3678	8411390	24.234	275.766

P22 B	Large Oct3			Medium Oct3		
Blackbody	ADC	ADT	Temp Diff	ADC	ADT	Temp Diff
30	8387720	23.3977	6.6023	8387003	23.3894	6.6106
35	8388287	23.5464	11.4536	8387128	23.4741	11.5259
40	8388900	23.5943	16.4057	8387270	23.5458	16.4542
45	8389492	23.6711	21.3289	8387420	23.5833	21.4167
50	8390223	23.7223	26.2777	8387609	23.6187	26.3813
55	8390849	23.8023	31.1977	8387807	23.6517	31.3483
60	8391666	23.8862	36.1138	8387971	23.7026	36.2974
70	8393162	23.9433	46.0567	8388422	23.7344	46.2656
80	8394785	24.0504	55.9496	8388873	23.769	56.231
90	8396596	24.1459	65.8541	8389396	23.8056	66.1944
100	8398410	24.2676	75.7324	8389919	23.8359	76.1641
120	8402813	24.4176	95.5824	8391161	23.8835	96.1165
140	8407417	24.6297	115.3703	8392536	23.9382	116.0618
160	8412706	24.9049	135.0951	8394014	23.998	136.002
180	8418635	25.131	154.869	8395731	24.1418	155.8582
200	8425436	25.4648	174.5352	8397632	24.2227	175.7773
220	8432722	25.9096	194.0904	8399730	24.3902	195.6098
240	8440548	26.377	213.623	8401980	24.5083	215.4917
260	8449341	26.8908	233.1092	8404489	24.6579	235.3421
280	8458786	27.6173	252.3827	8407186	24.8284	255.1716
300	8469249	28.1428	271.8572	8410165	25.0227	274.9773

P22 C	Large Oct4			Medium Oct4		
Blackbody	ADC	ADT	Temp Diff	ADC	ADT	Temp Diff
30	8388371	21.972	8.028	8388288	21.3165	8.6835
35	8389026	21.9675	13.0325	8388181	21.6652	13.3348
40	8389605	22.0868	17.9132	8388205	21.8301	18.1699
45	8390212	22.1722	22.8278	8388166	22.0886	22.9114
50	8390804	22.2861	27.7139	8388222	22.2382	27.7618
55	8391576	22.4016	32.5984	8388374	22.3135	32.6865
60	8392143	22.4858	37.5142	8388486	22.3938	37.6062
70	8393582	22.5798	47.4202	8388865	22.4653	47.5347
80	8395298	22.7654	57.2346	8389298	22.5483	57.4517
90	8397288	22.8511	67.1489	8389765	22.6292	67.3708
100	8399286	22.9392	77.0608	8390328	22.675	77.325
120	8403539	23.0942	96.9058	8391480	22.7565	97.2435
140	8408496	23.3051	116.6949	8392810	22.8517	117.1483
160	8414026	23.6538	136.3462	8394308	22.9237	137.0763
180	8420202	24.0498	155.9502	8396036	23.0335	156.9665
200	8427172	24.4455	175.5545	8397932	23.1349	176.8651
220	8434686	24.8936	195.1064	8400034	23.2763	196.7237
240	8442798	25.4841	214.5159	8402286	23.3995	216.6005
260	8451907	25.9165	234.0835	8404743	23.5589	236.4411
280	8461827	26.4594	253.5406	8407462	23.7261	256.2739
300	8472767	27.0589	272.9411	8410437	23.929	276.071

P22 D	Large Oct5			Medium Oct5		
Blackbody	ADC	ADT	Temp Diff	ADC	ADT	Temp Diff
30	8388116	23.2557	6.7443	8388272	22.4974	7.5026
35	8388576	23.4646	11.5354	8388329	22.6063	12.3937
40	8389140	23.5729	16.4271	8388359	22.7643	17.2357
45	8389714	23.6574	21.3426	8388257	23.0284	21.9716
50	8390488	23.7422	26.2578	8388264	23.2105	26.7895
55	8391062	23.8784	31.1216	8388392	23.3507	31.6493
60	8391798	23.9394	36.0606	8388487	23.4191	36.5809
70	8393418	24.0212	45.9788	8388917	23.4947	46.5053
80	8394969	24.1069	55.8931	8389122	23.7895	56.2105
90	8396937	24.1828	65.8172	8389485	23.8329	66.1671
100	8398881	24.2861	75.7139	8389969	23.8761	76.1239
120	8403128	24.3988	95.6012	8391267	23.9246	96.0754
140	8408038	24.5904	115.4096	8392452	23.998	116.002
160	8413467	24.8299	135.1701	8393980	24.101	135.899
180	8419691	25.0974	154.9026	8395710	24.1593	155.8407
200	8426557	25.4125	174.5875	8397487	24.2453	175.7547
220	8433856	25.7882	194.2118	8399524	24.3256	195.6744
240	8442161	26.25	213.75	8401873	24.4631	215.5369
260	8451005	26.7638	233.2362	8404194	24.624	235.376
280	8460694	27.2609	252.7391	8406906	24.788	255.212
300	8471337	27.9241	272.0759	8409842	25.0034	274.9966

J10 A	Large Oct2			Medium Oct2		
Blackbody	ADC	ADT	Temp Diff	ADC	ADT	Temp Diff
30	8387775	23.3737	6.6263	8387017	23.0891	6.9109
35	8388429	23.2857	11.7143	8386965	23.2059	11.7941
40	8388983	23.3146	16.6854	8387121	23.2512	16.7488
45	8389574	23.362	21.638	8387301	23.2785	21.7215
50	8390163	23.4158	26.5842	8387472	23.2866	26.7134
55	8390743	23.4641	31.5359	8387639	23.3014	31.6986
60	8391365	23.532	36.468	8387839	23.3362	36.6638
70	8392589	23.6905	46.3095	8388241	23.3623	46.6377
80	8394360	23.7242	56.2758	8388690	23.3716	56.6284
90	8396035	23.8019	66.1981	8389170	23.4065	66.5935
100	8397817	23.8839	76.1161	8389684	23.4007	76.5993
120	8401849	24.0121	95.9879	8390823	23.4377	96.5623
140	8406246	24.1863	115.8137	8392108	23.4734	116.5266
160	8410984	24.449	135.551	8393534	23.5575	136.4425
180	8416614	24.8742	155.1258	8395138	23.6116	156.3884
200	8422795	25.1427	174.8573	8396920	23.7221	176.2779
220	8429664	25.4502	194.5498	8398877	23.8058	196.1942
240	8437085	25.9378	214.0622	8401046	23.9374	216.0626
260	8445094	26.6759	233.3241	8403378	24.0953	235.9047
280	8454019	27.0849	252.9151	8405892	24.2445	255.7555
300	8463837	27.8611	272.1389	8408726	24.4241	275.5759

J10 B	Large Oct3			Medium Oct3		
Blackbody	ADC	ADT	Temp Diff	ADC	ADT	Temp Diff
30	8388238	21.5084	8.4916	8387273	22.3645	7.6355
35	8388887	21.4979	13.5021			
40	8389385	21.5982	18.4018	8387434	22.5963	17.4037
45	8389887	21.6723	23.3277	8387526	22.6705	22.3295
50	8390448	21.8135	28.1865	8387687	22.7371	27.2629
55	8390940	21.9414	33.0586	8387803	22.7888	32.2112
60	8391682	22.0083	37.9917	8388005	22.8143	37.1857
70	8392916	22.1492	47.8508	8388379	22.8362	47.1638
80	8394591	22.2492	57.7508	8388812	22.8861	57.1139
90	8396158	22.3519	67.6481	8389287	22.8942	67.1058
100	8398023	22.4615	77.5385	8389773	22.9476	77.0524
120	8401930	22.599	97.401	8390861	22.9915	97.0085
140	8406308	22.8506	117.1494	8392100	23.0419	116.9581
160	8411172	23.1002	136.8998	8393428	23.1056	136.8944
180	8416706	23.5434	156.4566	8395032	23.2599	156.7401
200	8422948	23.8214	176.1786	8396767	23.3734	176.6266
220	8429741	24.268	195.732	8398586	23.5013	196.4987
240	8437099	24.7361	215.2639	8400677	23.6587	216.3413
260	8445208	25.2535	234.7465	8402936	23.8614	236.1386
280	8454100	25.7934	254.2066	8405362	24.0617	255.9383
300	8463886	26.4306	273.5694	8408042	24.2562	275.7438

J10 C	Large Oct4			Medium Oct4		
Blackbody	ADC	ADT	Temp Diff	ADC	ADT	Temp Diff
30	8388879	21.7696	8.2304	8387059	22.7299	7.2701
35	8389325	22.0225	12.9775	8387168	22.8224	12.1776
40	8389771	22.275	17.725	8387284	22.9032	17.0968
45	8390277	22.4705	22.5295	8387438	22.9404	22.0596
50	8390761	22.6861	27.3139	8387608	22.9942	27.0058
55	8391375	22.8401	32.1599	8387778	23.0428	31.9572
60	8391991	22.9674	37.0326	8387955	23.0623	36.9377
70	8393406	23.1266	46.8734	8388347	23.1167	46.8833
80	8394948	23.2887	56.7113	8388774	23.1695	56.8305
90	8396650	23.4497	66.5503	8389283	23.1948	66.8052
100	8398478	23.5998	76.4002	8389778	23.256	76.744
120	8402514	23.8109	96.1891	8390911	23.2944	96.7056
140	8407105	24.0467	115.9533	8392141	23.371	116.629
160	8412054	24.3698	135.6302	8393586	23.4461	136.5539
180	8417965	24.6797	155.3203	8395179	23.5281	156.4719
200	8424517	25.0061	174.9939	8396980	23.6425	176.3575
220	8431567	25.5378	194.4622	8398891	23.7527	196.2473
240	8439197	26.0862	213.9138	8401032	23.9866	216.0134
260	8447618	26.5753	233.4247	8403361	24.1397	235.8603
280	8456927	27.1819	252.8181	8405901	24.3112	255.6888
300	8467059	27.7939	272.2061	8408679	24.4932	275.5068

J10 D	Large Oct5			Medium Oct5		
Blackbody	ADC	ADT	Temp Diff	ADC	ADT	Temp Diff
30	8389206	21.1949	8.8051	8386832	23.0918	6.9082
35	8389259	21.8786	13.1214	8386958	23.2125	11.7875
40	8389597	22.2645	17.7355	8387126	23.2776	16.7224
45	8390131	22.4603	22.5397	8387267	23.3293	21.6707
50	8390565	22.6966	27.3034	8387431	23.3983	26.6017
55	8391216	22.8362	32.1638	8387583	23.4527	31.5473
60	8391787	22.9843	37.0157	8387776	23.5046	36.4954
70	8393256	23.1101	46.8899	8388195	23.5431	46.4569
80	8394592	23.3401	56.6599	8388632	23.5917	56.4083
90	8396470	23.4539	66.5461	8389138	23.6218	66.3782
100	8398261	23.589	76.411	8389648	23.6449	76.3551
120	8402427	23.7632	96.2368	8390773	23.7142	96.2858
140	8406852	24.0368	115.9632	8392038	23.7479	116.2521
160	8412184	24.2647	135.7353	8393455	23.8332	136.1668
180	8417945	24.5493	155.4507	8395054	23.9217	156.0783
200	8424404	25.1952	174.8048	8396838	24.0374	175.9626
220	8431387	25.6396	194.3604	8398776	24.1265	195.8735
240	8439109	26.0606	213.9394	8400879	24.2713	215.7287
260	8447597	26.618	233.382	8403207	24.4283	235.5717
280	8456858	27.2065	252.7935	8405756	24.673	255.327
300	8467051	27.8299	272.1701	8408545	24.8463	275.1537

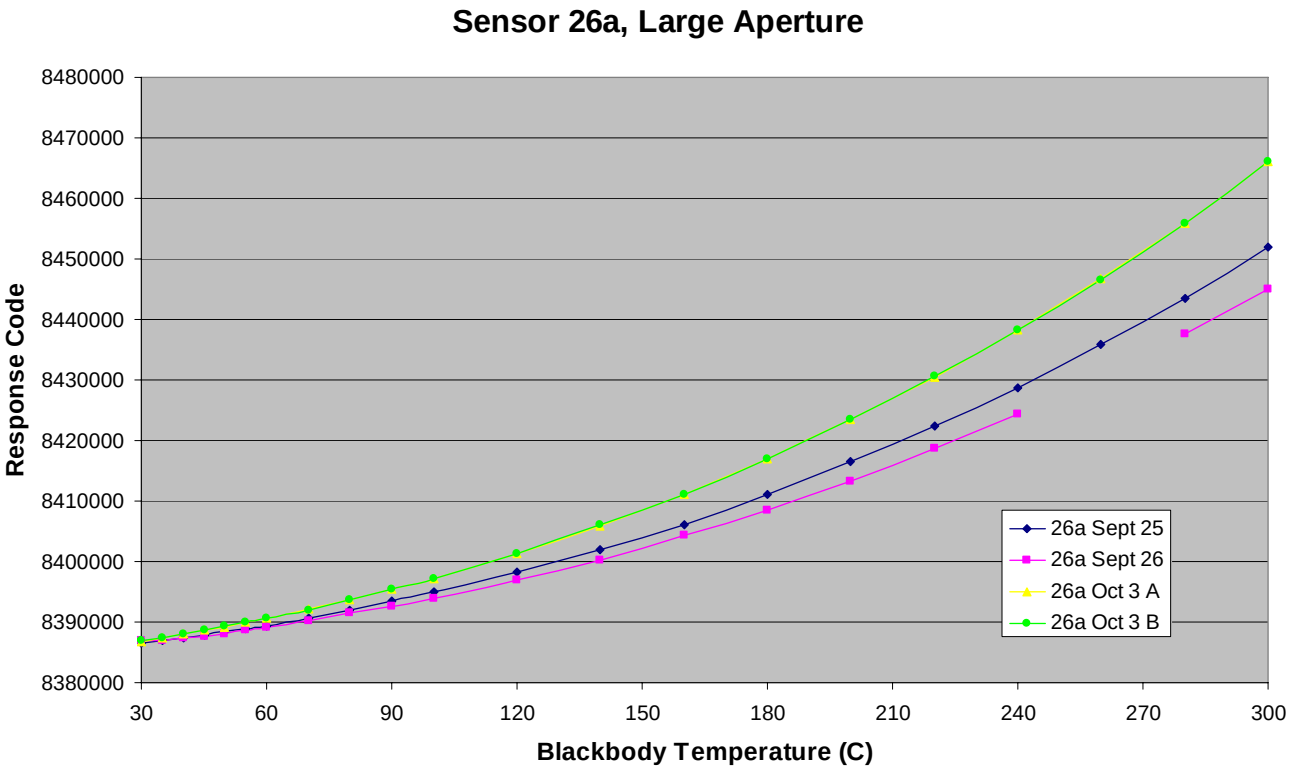
Sensor 26a, Large Aperture
Response Code
8480000
8470000
8460000
8450000
8440000
8430000
8420000
8410000
8400000
8390000
8380000
30
60
90
120
150
180
210
240
270
300
Blackbody Temperature (C)
26a Sept 25
26a Sept 26
26a Oct 3 A
26a Oct 3 B

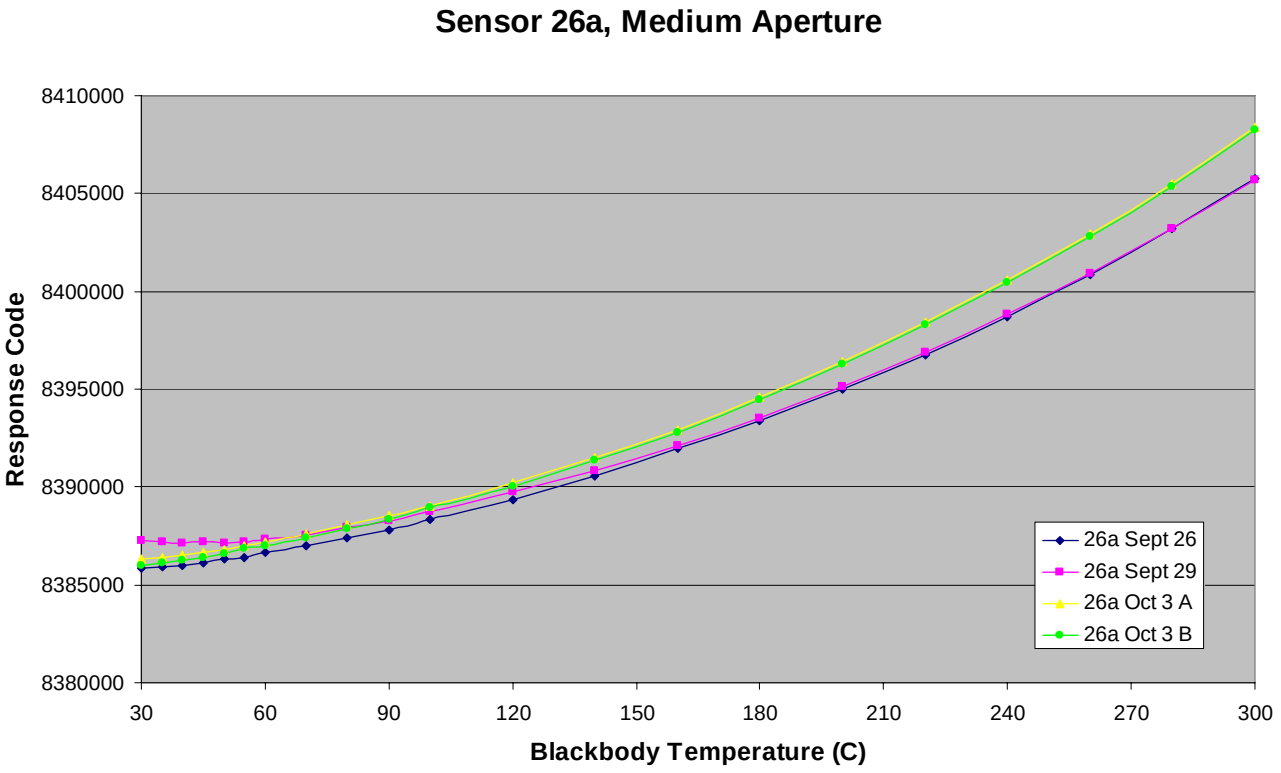
Sensor 26a, Medium Aperture
Response Code
8410000
8405000
8400000
8395000
8390000
8385000
8380000
30
60
90
120
150
180
210
240
270
300
Blackbody Temperature (C)
26a Sept 26
26a Sept 29
26a Oct 3 A
26a Oct 3 B

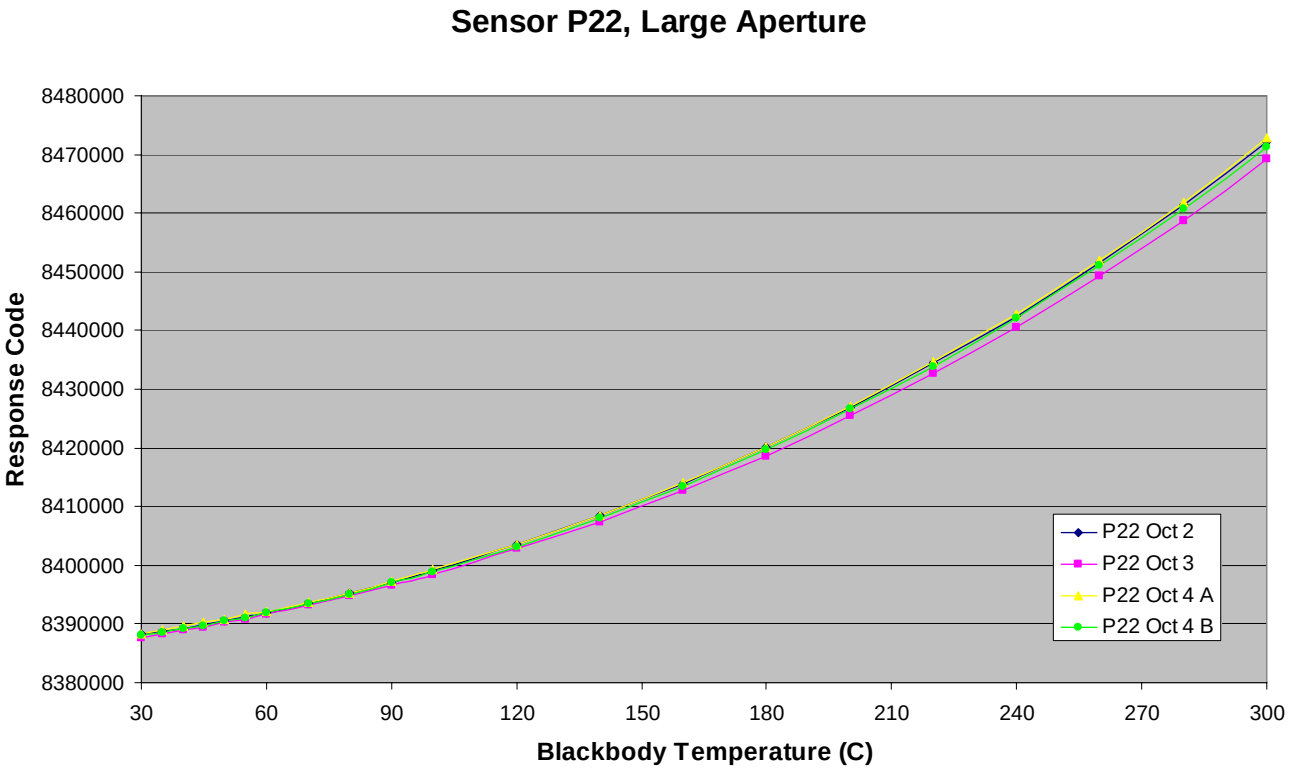
Sensor P22, Large Aperture
Response Code
8480000
8470000
8460000
8450000
8440000
8430000
8420000
8410000
8400000
8390000
8380000
30
60
90
120
150
180
210
240
270
300
Blackbody Temperature (C)
P22 Oct 2
P22 Oct 3
P22 Oct 4 A
P22 Oct 4 B

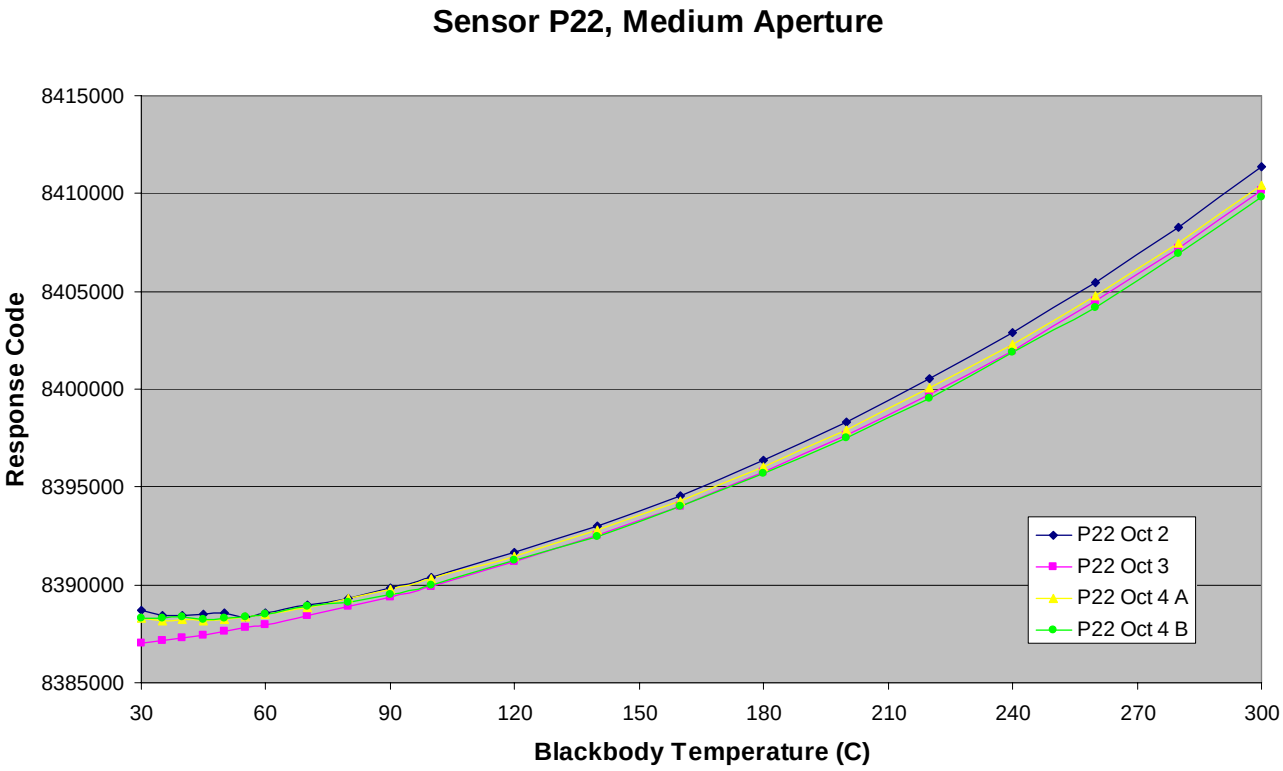
Sensor P22, Medium Aperture
Response Code
8415000
8410000
8405000
8400000
8395000
8390000
8385000
30
60
90
120
150
180
210
240
270
300
Blackbody Temperature (C)
P22 Oct 2
P22 Oct 3
P22 Oct 4 A
P22 Oct 4 B

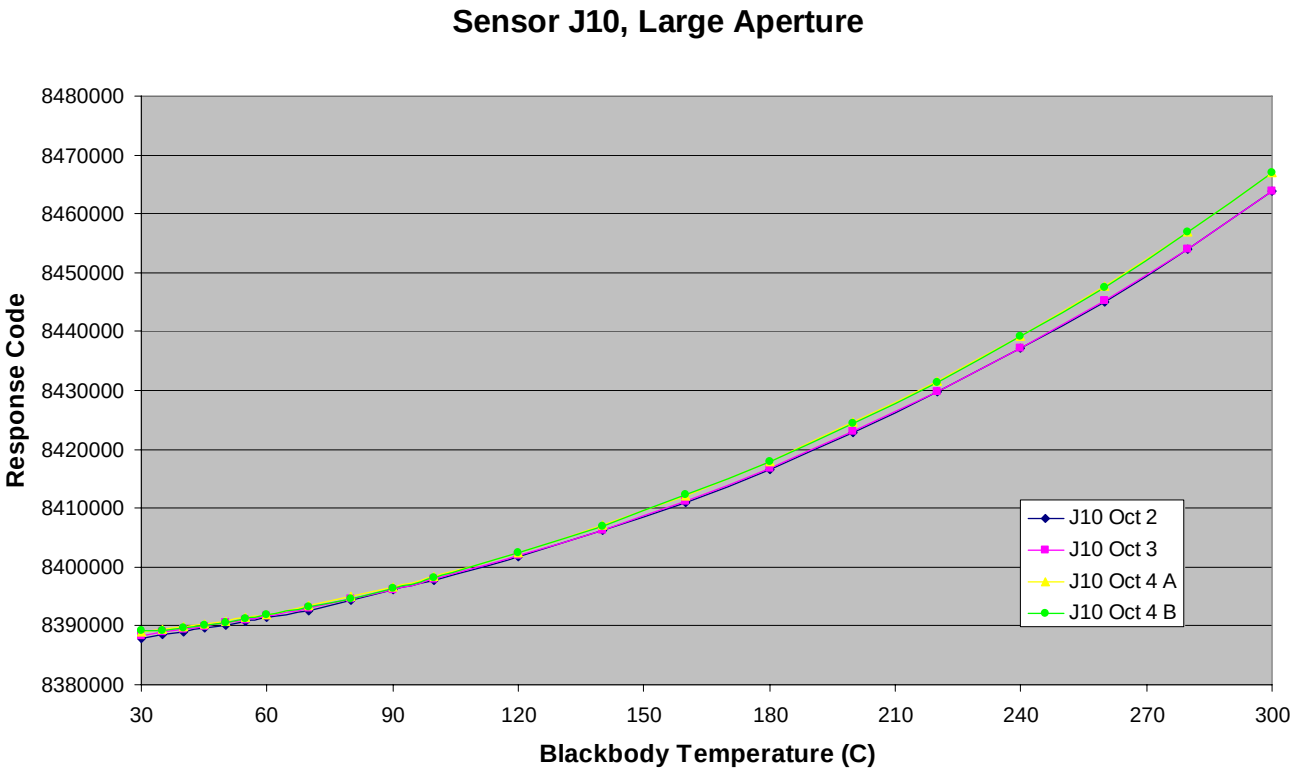
Sensor J10, Large Aperture
Response Code
8480000
8470000
8460000
8450000
8440000
8430000
8420000
8410000
8400000
8390000
8380000
30
60
90
120
150
180
210
240
270
300
Blackbody Temperature (C)
J10 Oct 2
J10 Oct 3
J10 Oct 4 A
J10 Oct 4 B

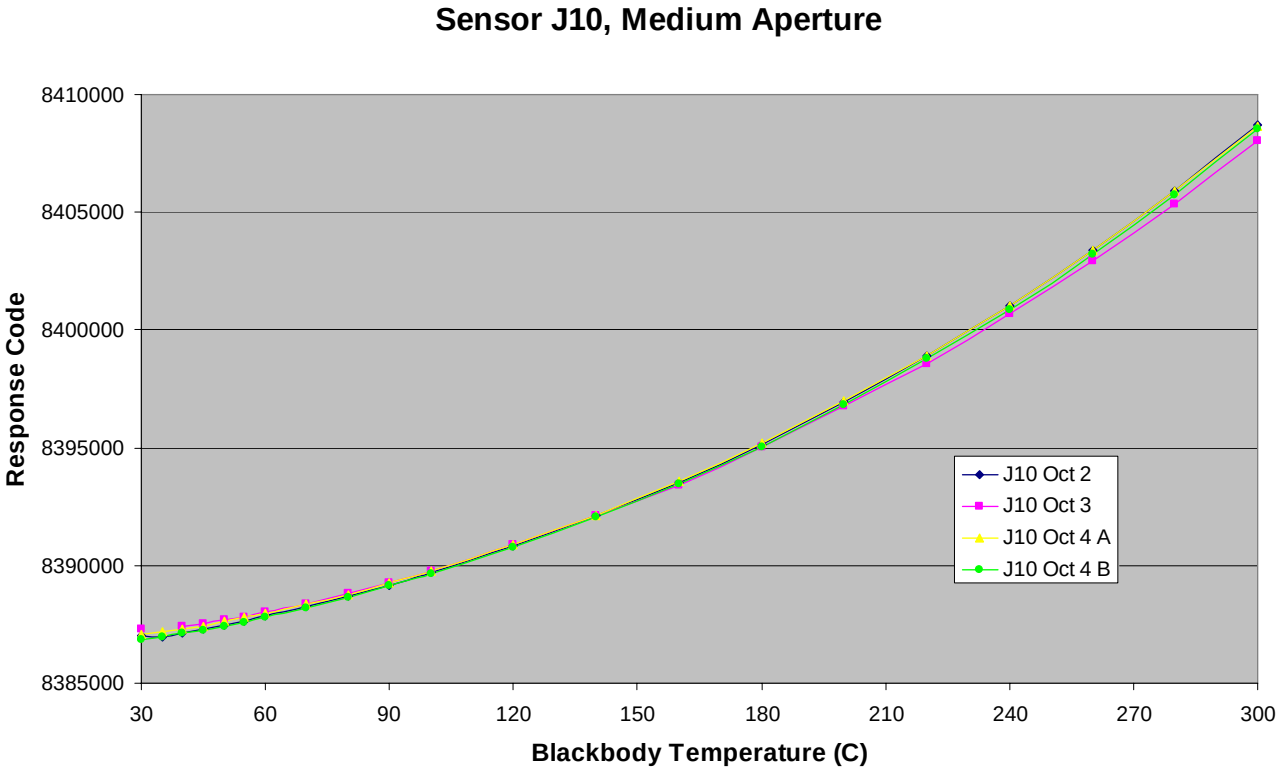
Sensor J10, Medium Aperture
Response Code
8410000
8405000
8400000
8395000
8390000
8385000
30
60
90
120
150
180
210
240
270
300
Blackbody Temperature (C)
J10 Oct 2
J10 Oct 3
J10 Oct 4 A
J10 Oct 4 B

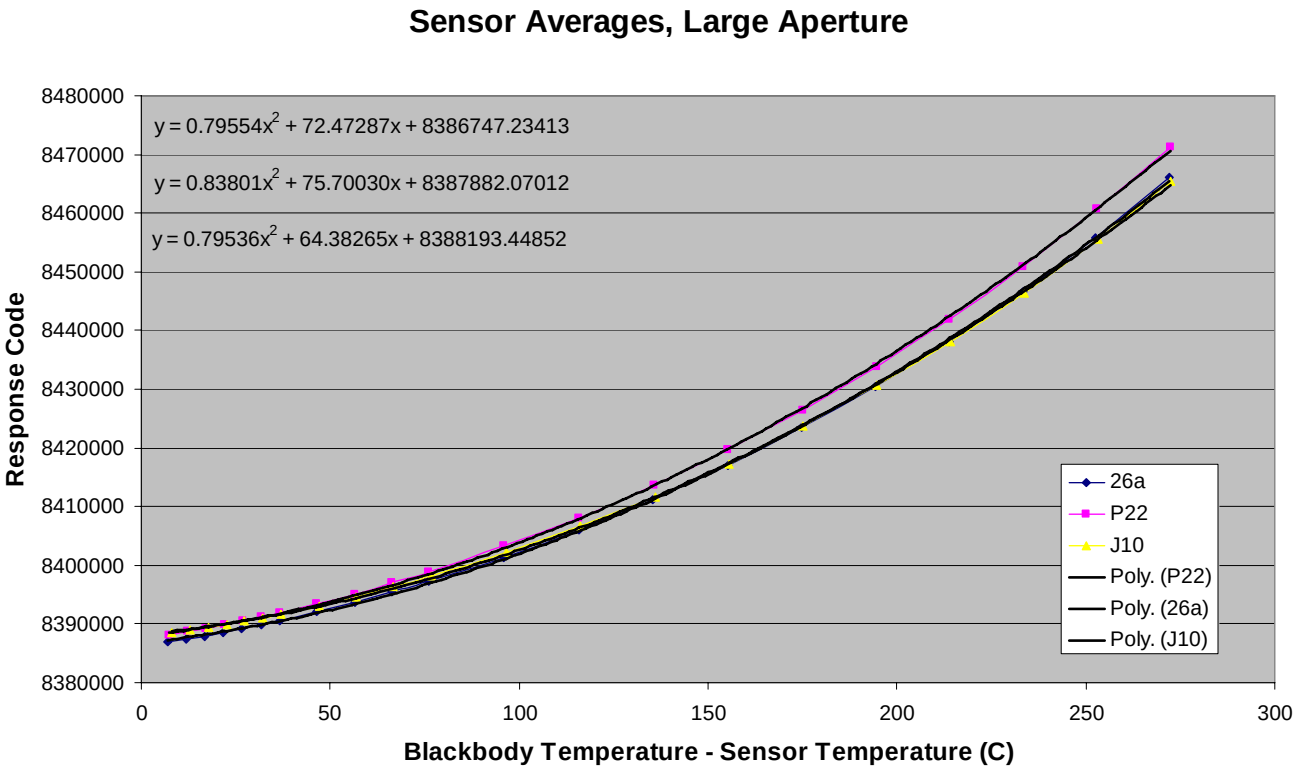
Sensor Averages, Large Aperture
y = 0.79554x2 + 72.47287x + 8386747.23413
y = 0.83801x2 + 75.70030x + 8387882.07012
y = 0.79536x2 + 64.38265x + 8388193.44852
Response Code
8480000
8470000
8460000
8450000
8440000
8430000
8420000
8410000
8400000
8390000
8380000
0
50
100
150
200
250
300
Blackbody Temperature - Sensor Temperature (C)
26a
P22
J10
Poly. (P22)
Poly. (26a)
Poly. (J10)

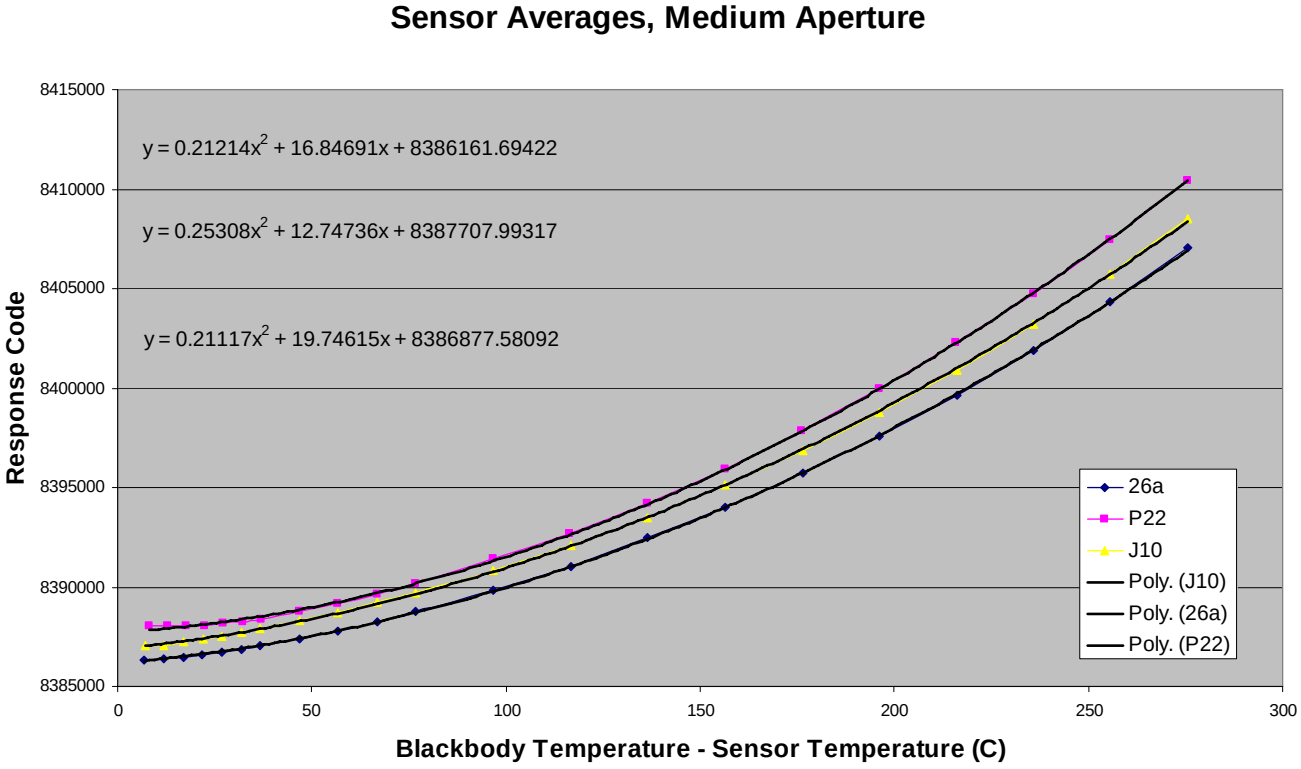
Sensor Averages, Medium Aperture
y = 0.21214x2 + 16.84691x + 8386161.69422
y = 0.25308x2 + 12.74736x + 8387707.99317
y = 0.21117x2 + 19.74615x + 8386877.58092
Response Code
8415000
8410000
8405000
8400000
8395000
8390000
8385000
0
50
100
150
200
250
300
Blackbody Temperature - Sensor Temperature (C)
26a
P22
J10
Poly. (J10)
Poly. (26a)
Poly. (P22)

Sensor	Aperture	Conversion Equation
26a	Large	$Temp = 1.12015\left(\sqrt{Code - 8385101} - 40.49586\right)$
	Medium	$Temp = 2.13760\left(\sqrt{Code - 8385714} - 21.19027\right)$
P22	Large	$Temp = 1.09238\left(\sqrt{Code - 8386172} - 41.34690\right)$
	Medium	$Temp = 1.98779\left(\sqrt{Code - 8387546} - 12.66955\right)$
J10	Large	$Temp = 1.12129\left(\sqrt{Code - 8386890} - 36.09583\right)$
	Medium	$Temp = 2.17613\left(\sqrt{Code - 8386416} - 21.48505\right)$

Appendix D – Heated Aperture Plate Data

The medium aperture plate was heated to around 30°C, and setup the same way as in the pixel response test. However, the blackbody was kept constant at 150°C. Every 30 seconds, the temperature of the plate was recorded, along with the output code from the sensor. The plate temperature was plotted against the output code, and the ADC conversion equation was used to convert the collected codes into a temperature difference.

Plate Temperature	ADC	Calculated Temp Diff - 160
28.7	8399338	64.54025208
27.95	8398536	56.68408256
27.15	8397865	49.91283773
26.6	8397335	44.42376394
26.2	8396896	39.7745904
25.5	8396540	35.93844384
25.1	8396294	33.23859093
24.55	8396058	30.6241433
24.45	8395844	28.22912899
23.85	8395556	24.95063601
23.65	8395494	24.23760765
23.1	8395322	22.25827438
23	8395114	19.82201338
22.9	8395015	18.66317848
22.6	8394952	17.90969299

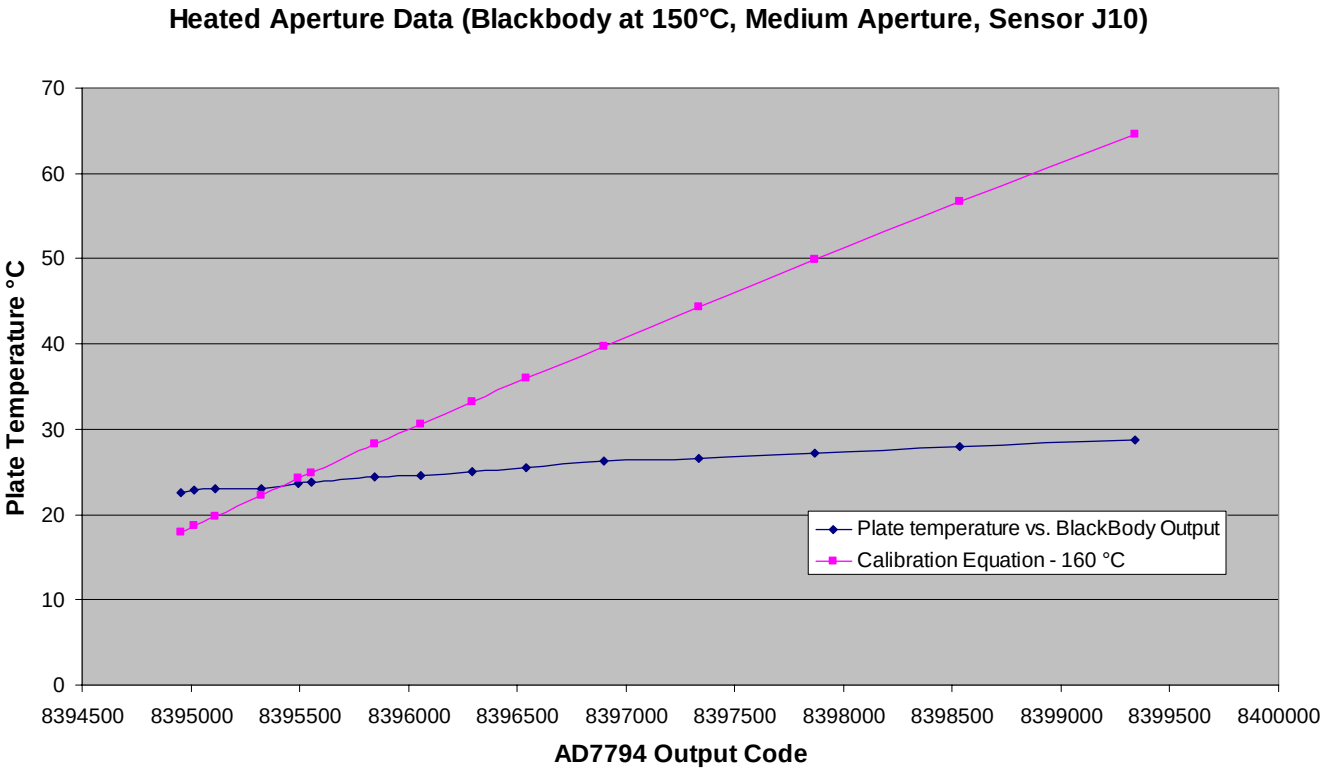
Heated Aperture Data (Blackbody at 150°C, Medium Aperture, Sensor J10)
Plate Temperature °C
70
60
50
40
30
20
10
0
8394500
8395000
8395500
8396000
8396500
8397000
8397500
8398000
8398500
8399000
8399500
8400000
AD7794 Output Code
Plate temperature vs. BlackBody Output
Calibration Equation - 160 °C

Appendix E –AES Block Diagrams

The sections of Appendix E describe the major processes involved with the AES. They are broken down into three sections: processes specific to the three-by-three detector, processes specific to the eleven-by-eleven sensor detector, and processes shared by the two.

E.1 Three-by-three Sensor Software Processes

The three-by-three detector processes include two data collection modes that differ only slightly for the eleven-by-eleven detector and one data collection mode that is not used by the eleven-by-eleven AES. These modes are the Real Time, Analysis, and Temperature modes.

E.1.1 Real Time Process

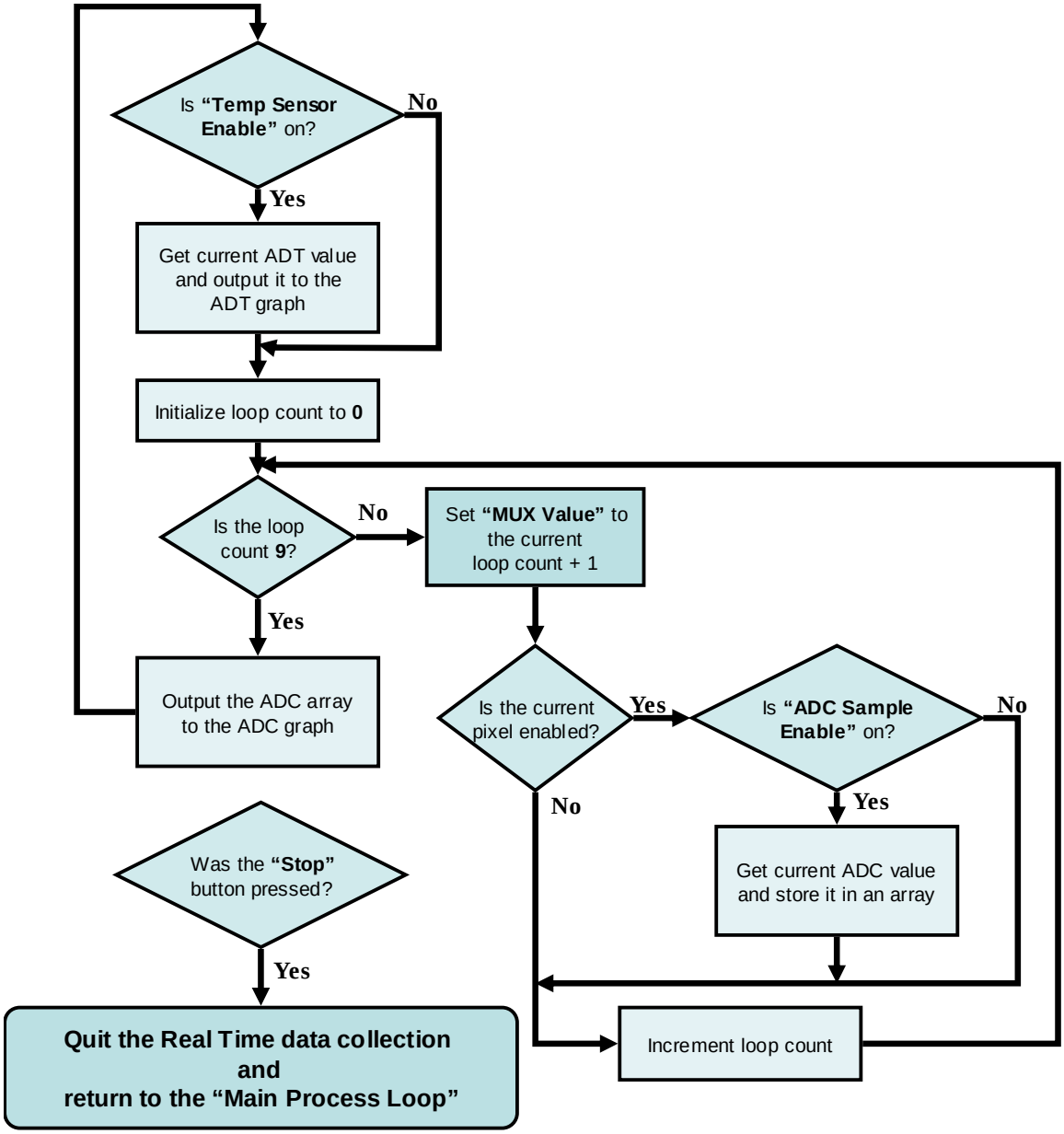

E.1.2 Analysis Process

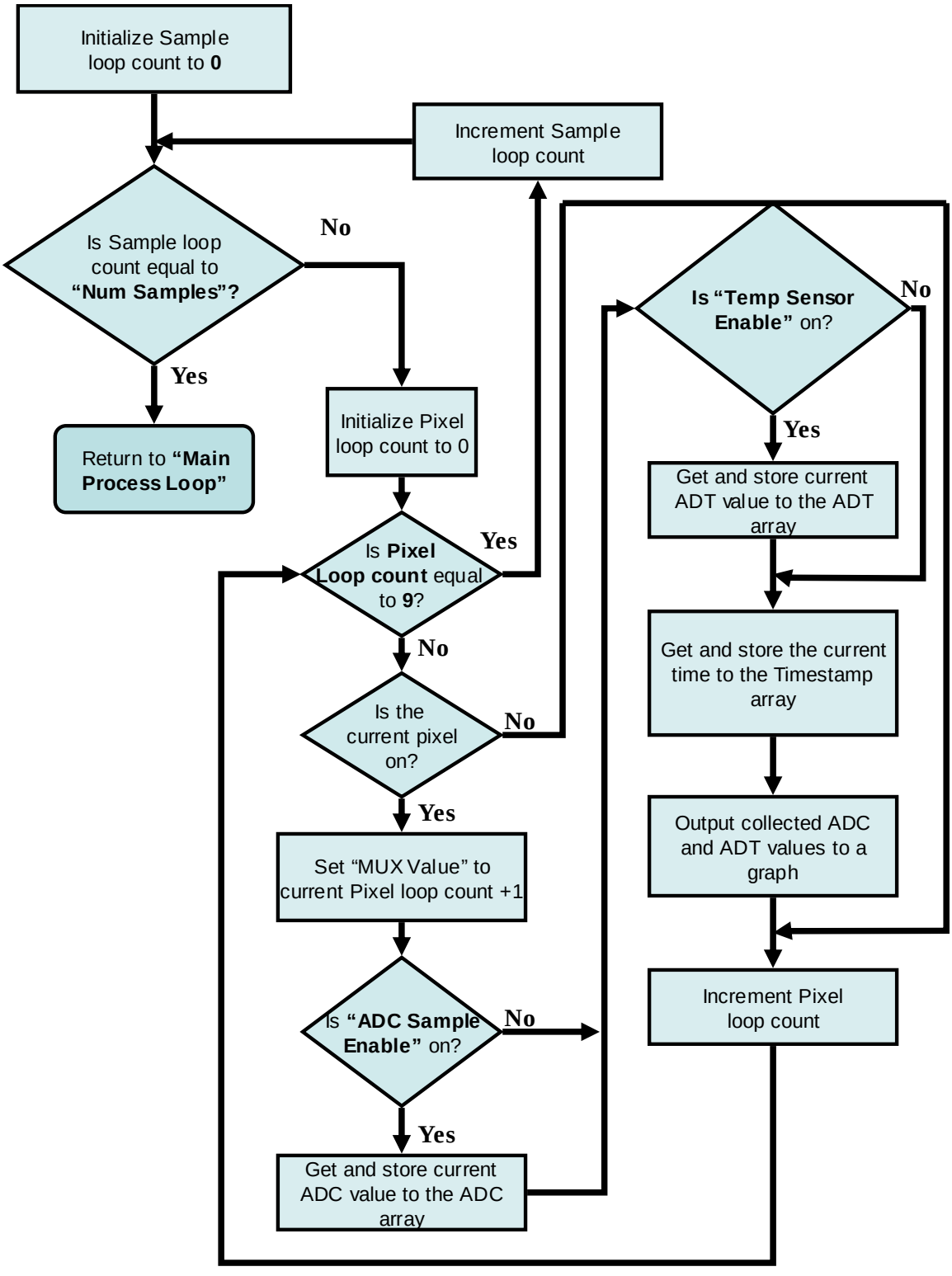

E.1.3 Temperature Process

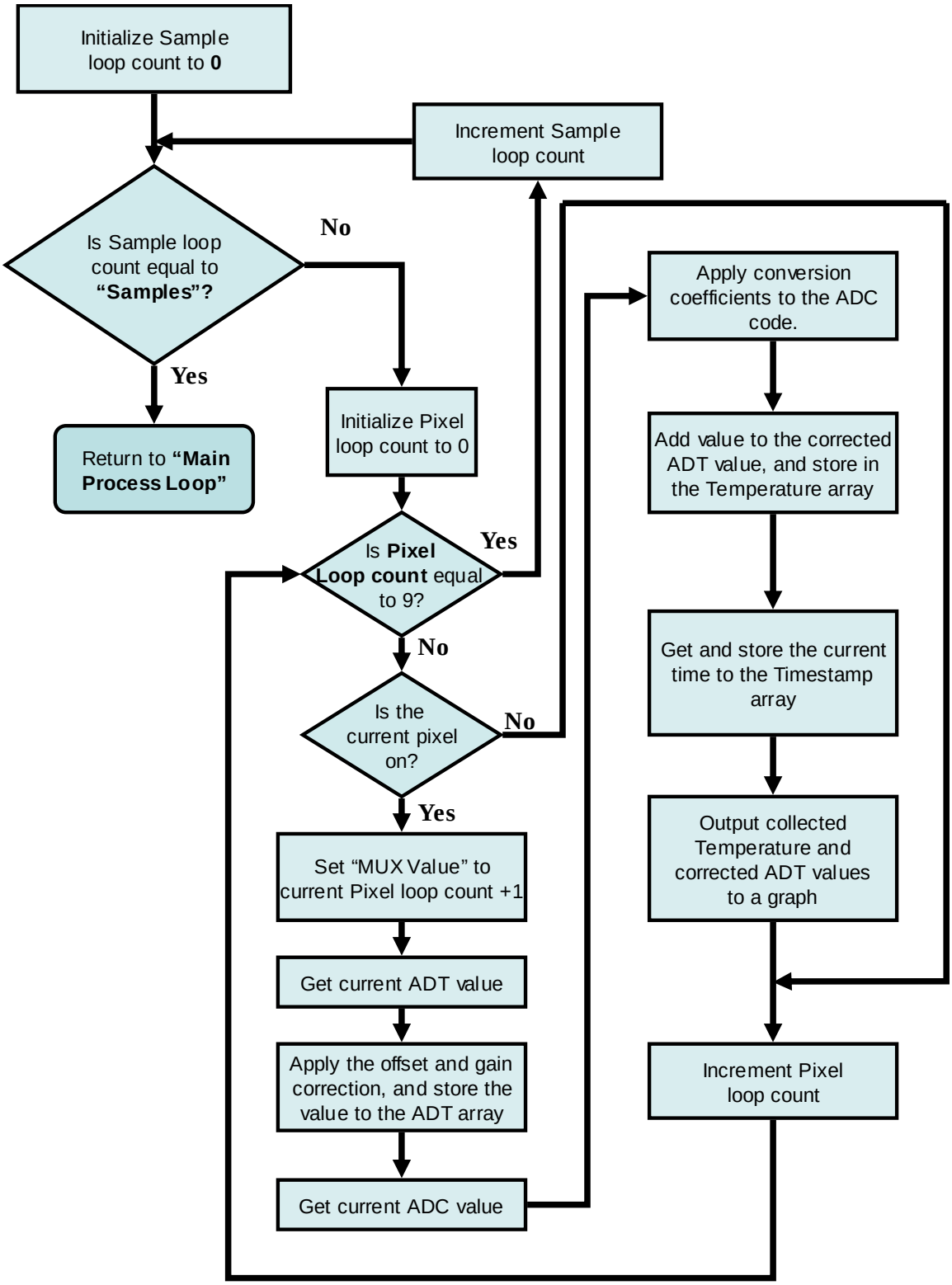

E.2 Eleven-by-eleven Sensor Software Processes

The eleven-by-eleven sensor evaluation has one data collection mode not used by the three-by-three software, and two data collection modes slightly different. These modes are the Real Time, Analysis, and Imager modes. The eleven-by-eleven software also has a thermal imaging process to create an image for the Imager mode.

E.2.1 Real Time Process

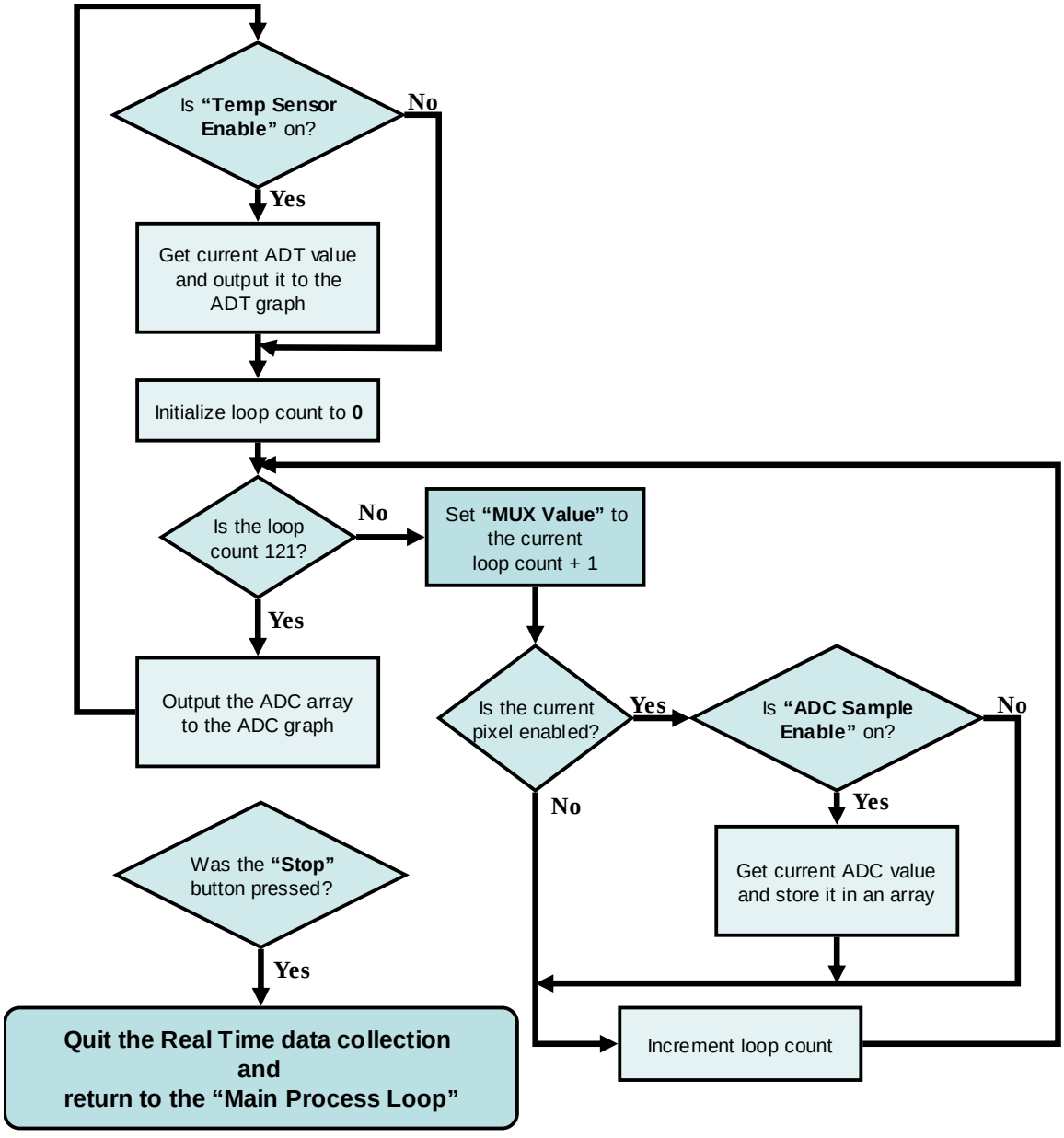

E.2.2 Analysis Process

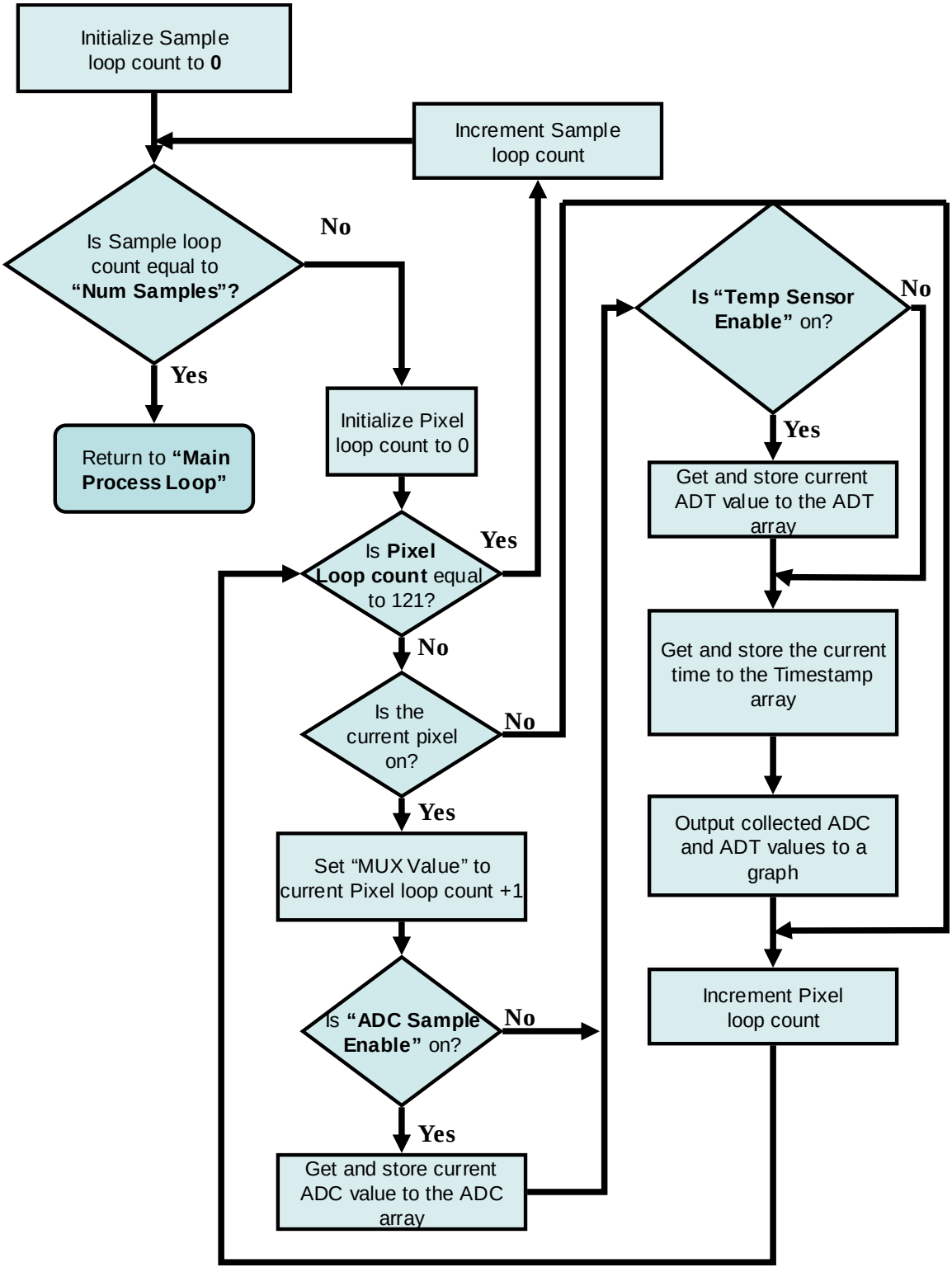

E.2.3 Imaging Process

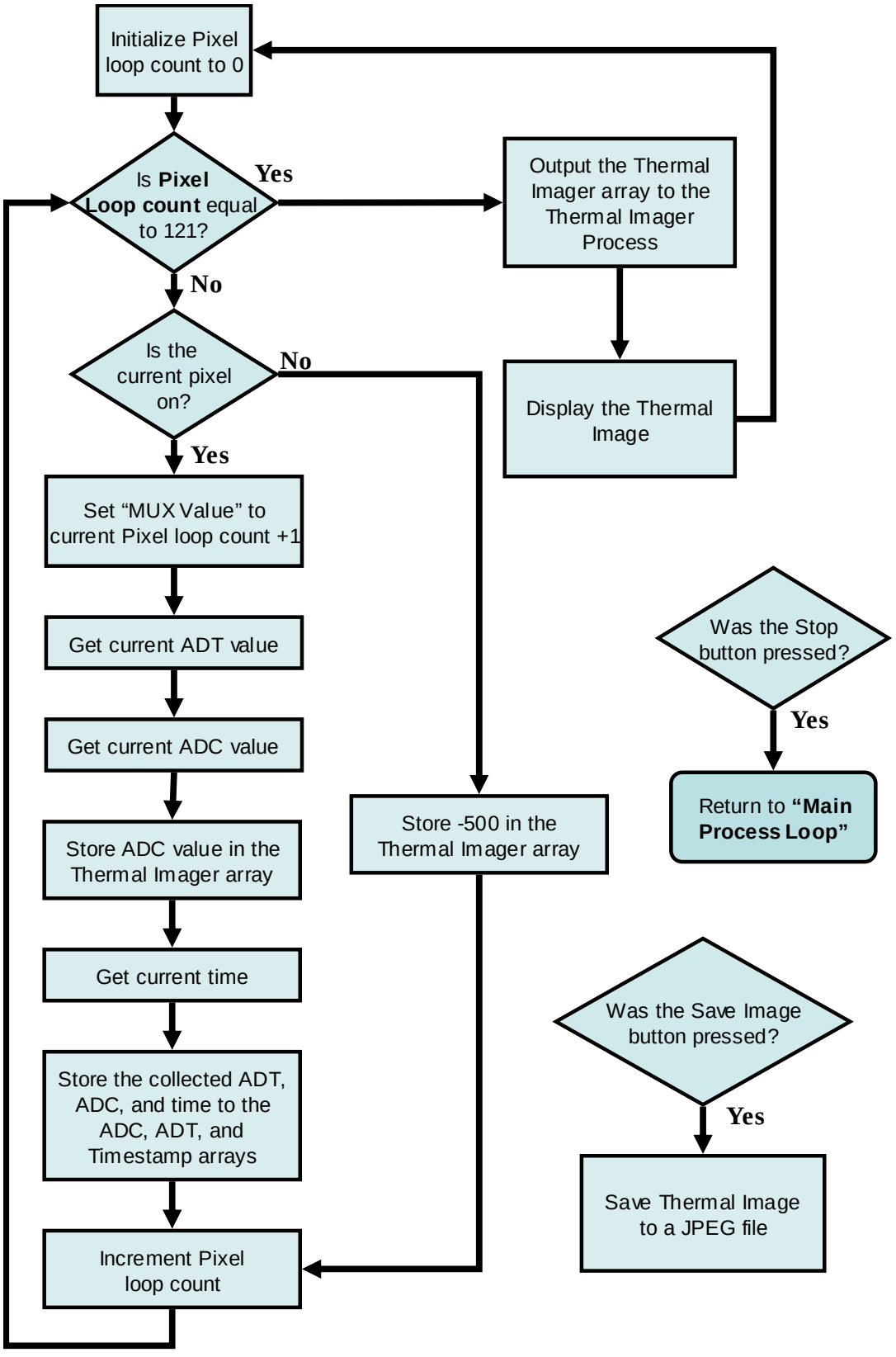

E.2.4 Thermal Image Display Process

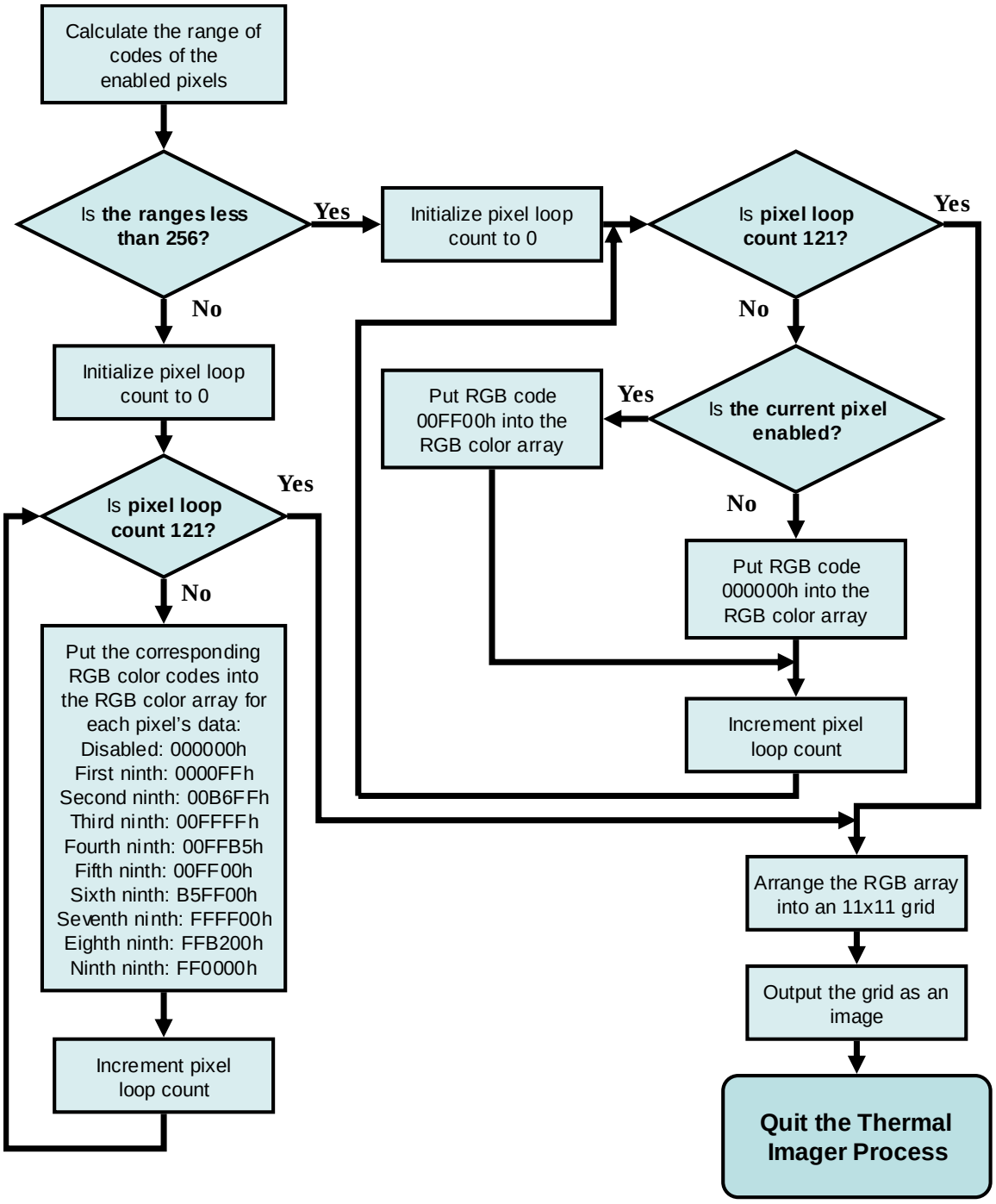

E.3 Shared Processes

Both the three-by-three and eleven-by-eleven sensor software have some common processes. These processes are the Main Process Loop and the three saving processes.

E.3.1 Main Loop

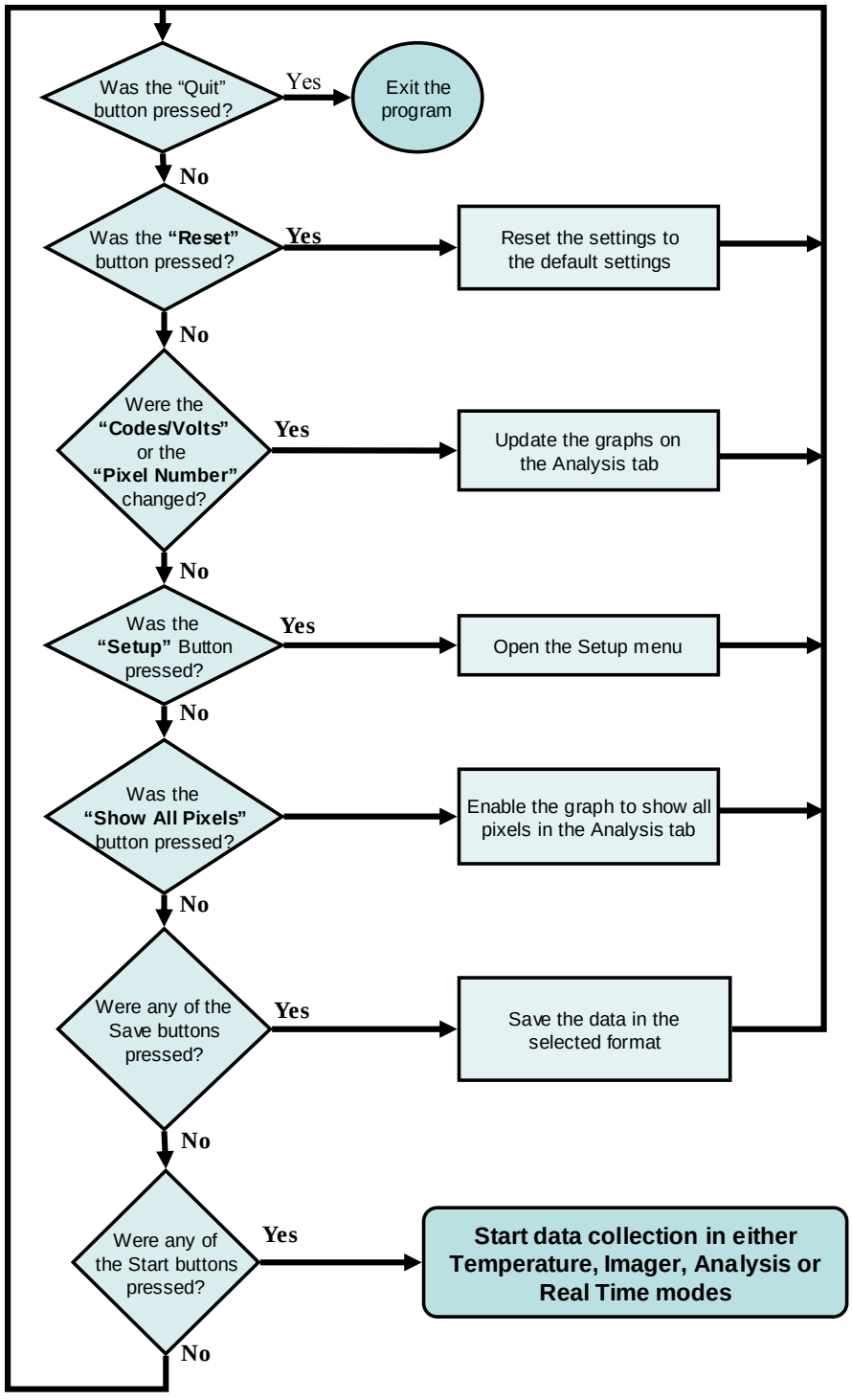

E.3.2 Saving Processes

There are three saving processes used based on the format the user would like to save the data. One process saves to an Excel file, another to a MatLab M file, and the third to a comma separated value format.

E.3.2.1 Save to Excel

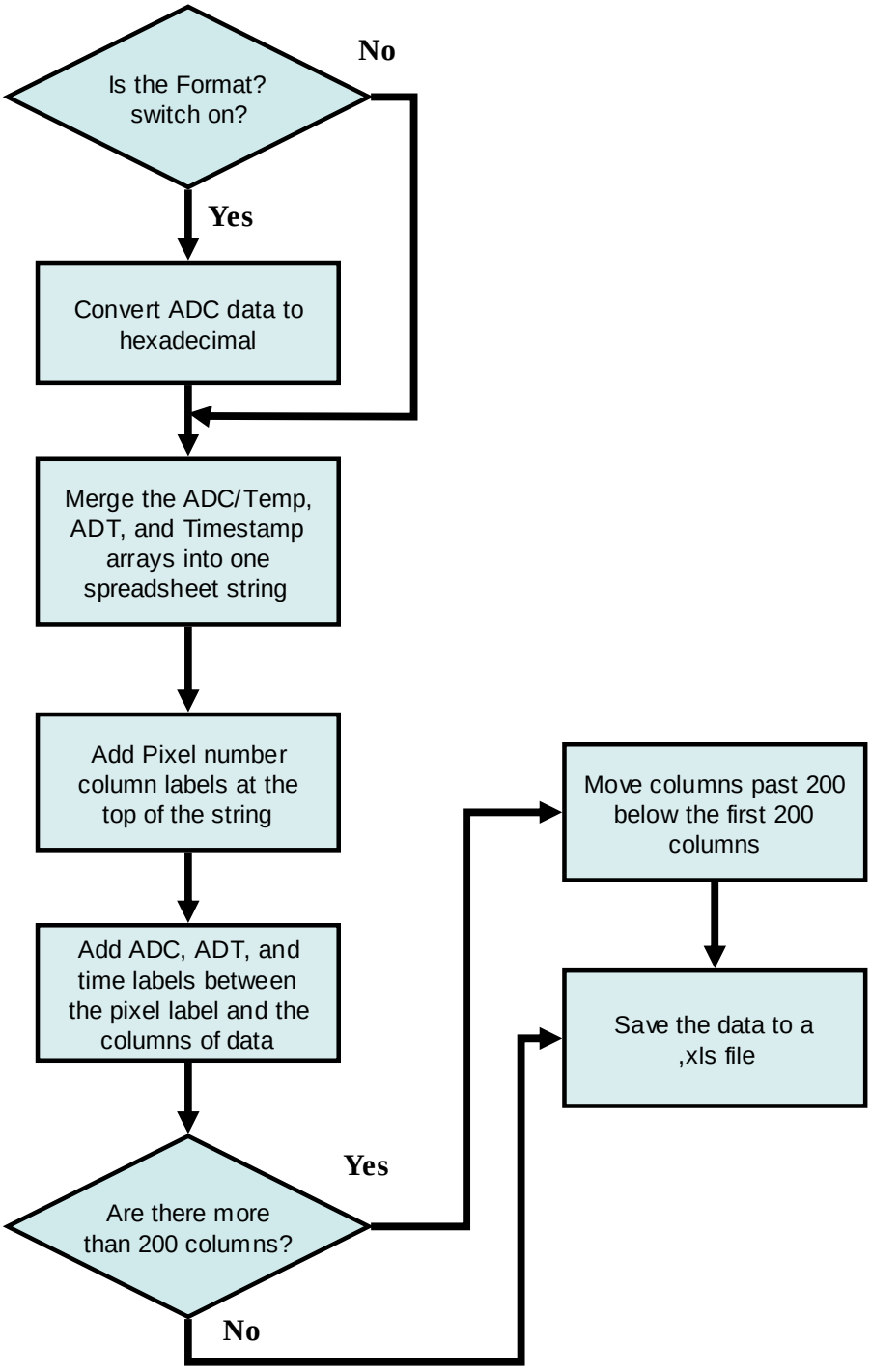

E.3.2.2 Save to MatLab

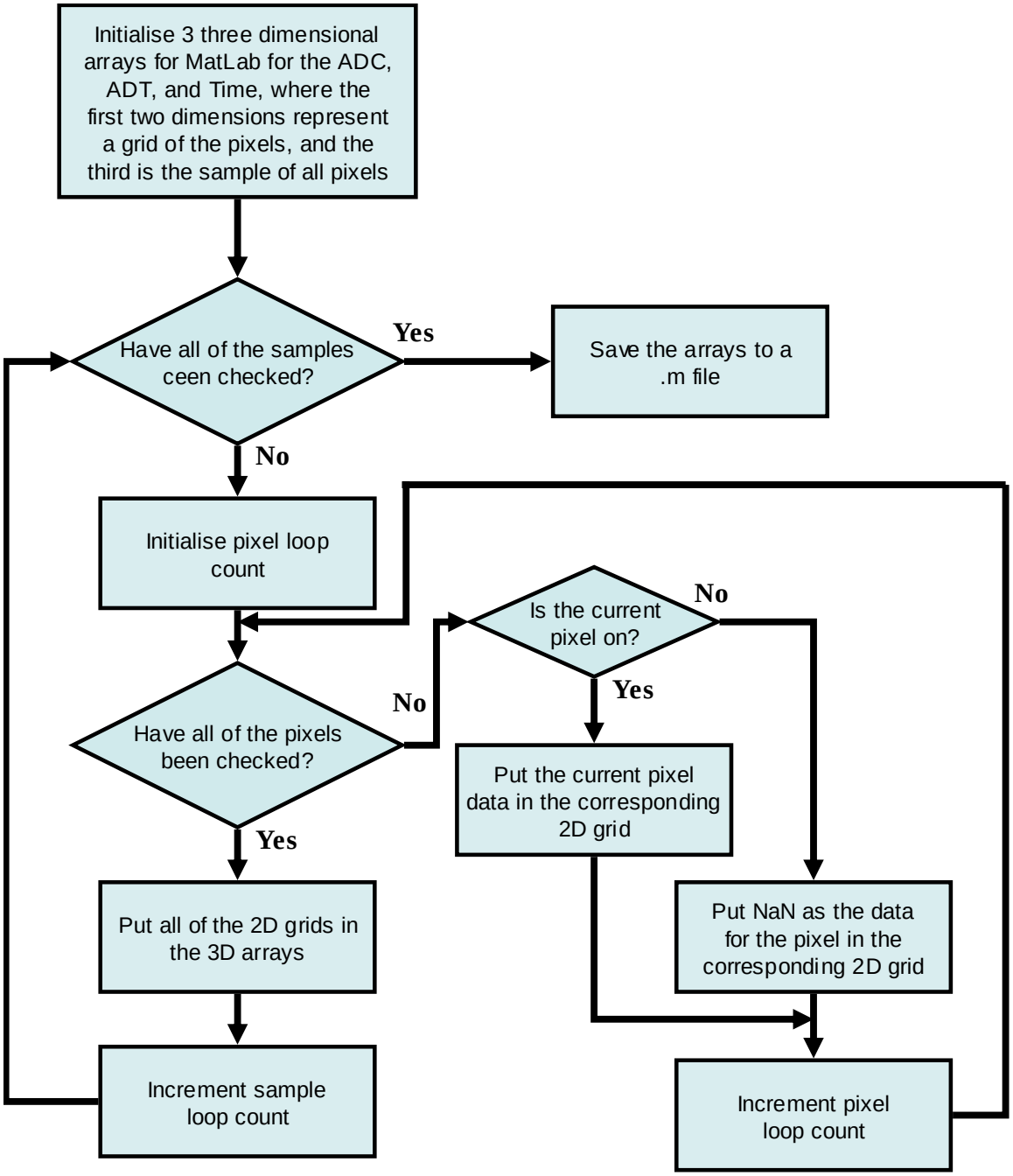

E.3.2.3 Save to Comma Separated Values

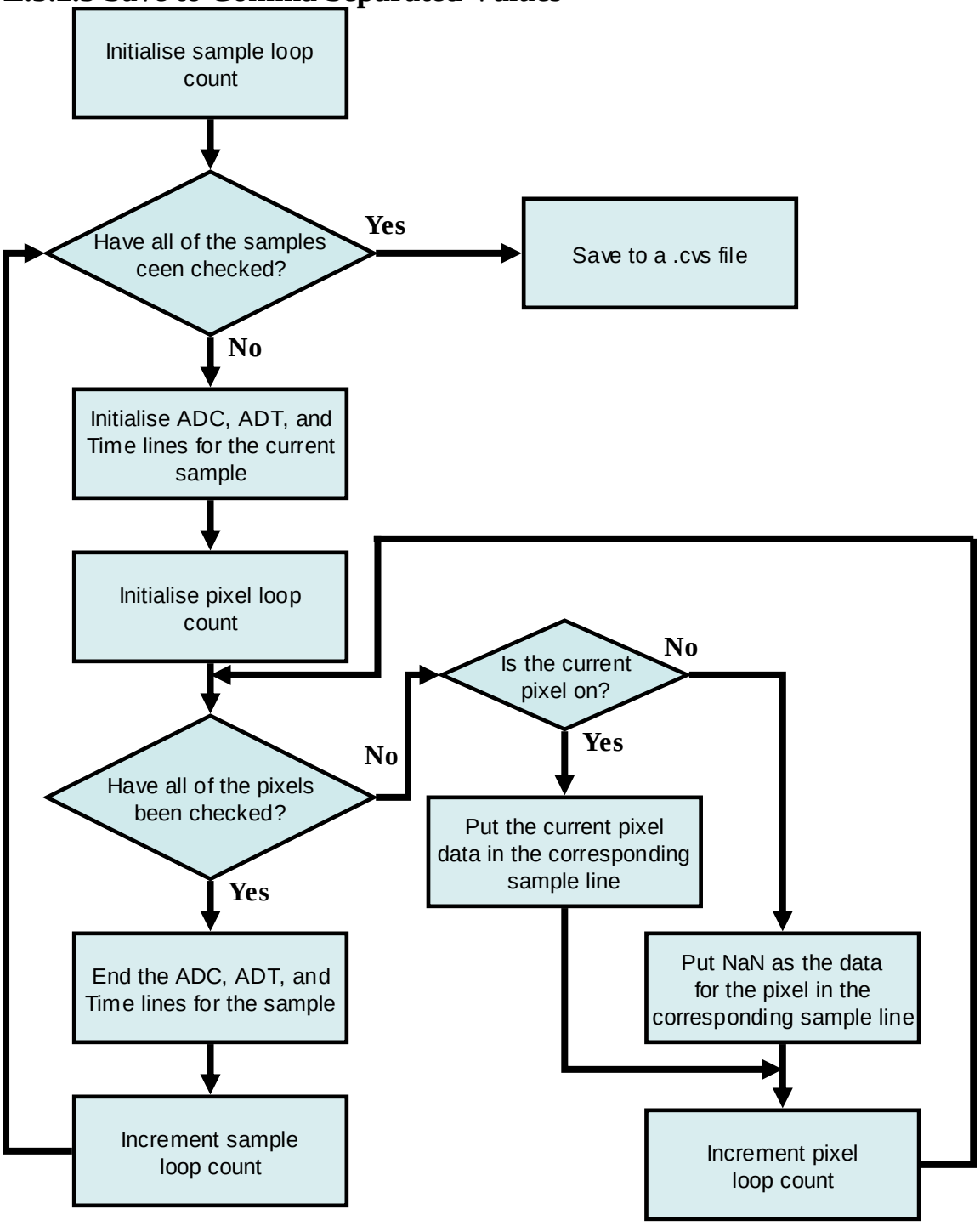

E.3.3 Example Save Formats

The following sections provide examples of each of the three formats data can be saved in. The first format is an Excel format, followed by a MatLab format, then a comma separated value format.

E.3.3.1 Excel Format

Pixel 1				Pixel 5				Pixel 9		
ADC	ADT	Time		ADC	ADT	Time		ADC	ADT	Time
8389245	29.7812	`13:54:00.687		8388819	29.875	`13:54:01.375		8385840	29.6875	`13:54:02.062
8389100	29.8437	`13:54:02.750		8388705	29.8125	`13:54:03.437		8385846	29.8125	`13:54:04.125
8389167	29.7812	`13:54:04.812		8388762	29.8437	`13:54:05.500		8385795	29.75	`13:54:06.187
8389148	29.8437	`13:54:06.875		8388721	29.8437	`13:54:07.562		8385766	29.9062	`13:54:08.250
8389012	29.875	`13:54:08.937		8388643	29.9687	`13:54:09.625		8385622	29.8437	`13:54:10.312
8389040	29.875	`13:54:11.000		8388661	30.0625	`13:54:11.687		8385711	29.8125	`13:54:12.375
8388980	29.9062	`13:54:13.062		8388668	29.8437	`13:54:13.750		8385665	29.9062	`13:54:14.437
8389010	29.9062	`13:54:15.125		8388653	30.0625	`13:54:15.812		8385758	29.875	`13:54:16.500
8388996	29.9062	`13:54:17.171		8388641	30	`13:54:17.859		8385780	29.875	`13:54:18.546
8389019	29.9062	`13:54:19.234		8388642	29.875	`13:54:19.921		8385639	29.9062	`13:54:20.609

E.3.3.2 MatLab Format

ADC = cat(3, [8389245 NaN NaN; NaN 8388819 NaN; NaN NaN 8385840], [8389100 NaN NaN; NaN 8388705 NaN; NaN NaN 8385846], [8389167 NaN NaN; NaN 8388762 NaN; NaN NaN 8385795], [8389148 NaN NaN; NaN 8388721 NaN; NaN NaN 8385766], [8389012 NaN NaN; NaN 8388643 NaN; NaN NaN 8385622], [8389040 NaN NaN; NaN 8388661 NaN; NaN NaN 8385711], [8388980 NaN NaN; NaN 8388668 NaN; NaN NaN 8385665], [8389010 NaN NaN; NaN 8388653 NaN; NaN NaN 8385758], [8388996 NaN NaN; NaN 8388641 NaN; NaN NaN 8385780], [8389019 NaN NaN; NaN 8388642 NaN; NaN NaN 8385639])

ADT = cat(3, [29.7812 NaN NaN; NaN 29.8750 NaN; NaN NaN 29.6875], [29.8437 NaN NaN; NaN 29.8125 NaN; NaN NaN 29.8125], [29.7812 NaN NaN; NaN 29.8437 NaN; NaN NaN 29.7500], [29.8437 NaN NaN; NaN 29.8437 NaN; NaN NaN 29.9062], [29.8750 NaN NaN; NaN 29.9687 NaN; NaN NaN 29.8437], [29.8750 NaN NaN; NaN 30.0625 NaN; NaN NaN 29.8125], [29.9062 NaN NaN; NaN 29.8437 NaN; NaN NaN 29.9062], [29.9062 NaN NaN; NaN 30.0625 NaN; NaN NaN 29.8750], [29.9062 NaN NaN; NaN 30.0000 NaN; NaN NaN 29.8750], [29.9062 NaN NaN; NaN 29.8750 NaN; NaN NaN 29.9062])

Timestamps = cat(3, ['13:54:00.687' 'NaN' 'NaN'; 'NaN' '13:54:01.375' 'NaN'; 'NaN' 'NaN' '13:54:02.062'], ['13:54:02.750' 'NaN' 'NaN'; 'NaN' '13:54:03.437' 'NaN'; 'NaN' 'NaN' '13:54:04.125'], ['13:54:04.812' 'NaN' 'NaN'; 'NaN' '13:54:05.500' 'NaN'; 'NaN' 'NaN' '13:54:06.187'], ['13:54:06.875' 'NaN' 'NaN'; 'NaN' '13:54:07.562' 'NaN'; 'NaN' 'NaN' '13:54:08.250'], ['13:54:08.937' 'NaN' 'NaN'; 'NaN' '13:54:09.625' 'NaN'; 'NaN' 'NaN' '13:54:10.312'], ['13:54:11.000' 'NaN' 'NaN'; 'NaN' '13:54:11.687' 'NaN'; 'NaN' 'NaN' '13:54:12.375'], ['13:54:13.062' 'NaN' 'NaN'; 'NaN' '13:54:13.750' 'NaN'; 'NaN' 'NaN' '13:54:14.437'], ['13:54:15.125' 'NaN' 'NaN'; 'NaN' '13:54:15.812' 'NaN'; 'NaN' 'NaN' '13:54:16.500'], ['13:54:17.171' 'NaN' 'NaN'; 'NaN' '13:54:17.859' 'NaN'; 'NaN' 'NaN' '13:54:18.546'], ['13:54:19.234' 'NaN' 'NaN'; 'NaN' '13:54:19.921' 'NaN'; 'NaN' 'NaN' '13:54:20.609'])

E.3.3.3 Comma Separated Values

"Sample 1 ADC",8389245,NaN,NaN,NaN,8388819,NaN,NaN,NaN,8385840
"Sample 1 ADT",29.7812,NaN,NaN,NaN,29.8750,NaN,NaN,NaN,29.6875
"Sample 1 Time",13:54:00.687,NaN,NaN,NaN,13:54:01.375,NaN,NaN,NaN,13:54:02.062

"Sample 2 ADC",8389100,NaN,NaN,NaN,8388705,NaN,NaN,NaN,8385846
"Sample 2 ADT",29.8437,NaN,NaN,NaN,29.8125,NaN,NaN,NaN,29.8125
"Sample 2 Time",13:54:02.750,NaN,NaN,NaN,13:54:03.437,NaN,NaN,NaN,13:54:04.125

"Sample 3 ADC",8389167,NaN,NaN,NaN,8388762,NaN,NaN,NaN,8385795
"Sample 3 ADT",29.7812,NaN,NaN,NaN,29.8437,NaN,NaN,NaN,29.7500
"Sample 3 Time",13:54:04.812,NaN,NaN,NaN,13:54:05.500,NaN,NaN,NaN,13:54:06.187

"Sample 4 ADC",8389148,NaN,NaN,NaN,8388721,NaN,NaN,NaN,8385766
"Sample 4 ADT",29.8437,NaN,NaN,NaN,29.8437,NaN,NaN,NaN,29.9062
"Sample 4 Time",13:54:06.875,NaN,NaN,NaN,13:54:07.562,NaN,NaN,NaN,13:54:08.250

"Sample 5 ADC",8389012,NaN,NaN,NaN,8388643,NaN,NaN,NaN,8385622
"Sample 5 ADT",29.8750,NaN,NaN,NaN,29.9687,NaN,NaN,NaN,29.8437
"Sample 5 Time",13:54:08.937,NaN,NaN,NaN,13:54:09.625,NaN,NaN,NaN,13:54:10.312

"Sample 6 ADC",8389040,NaN,NaN,NaN,8388661,NaN,NaN,NaN,8385711
"Sample 6 ADT",29.8750,NaN,NaN,NaN,30.0625,NaN,NaN,NaN,29.8125
"Sample 6 Time",13:54:11.000,NaN,NaN,NaN,13:54:11.687,NaN,NaN,NaN,13:54:12.375

"Sample 7 ADC",8388980,NaN,NaN,NaN,8388668,NaN,NaN,NaN,8385665
"Sample 7 ADT",29.9062,NaN,NaN,NaN,29.8437,NaN,NaN,NaN,29.9062
"Sample 7 Time",13:54:13.062,NaN,NaN,NaN,13:54:13.750,NaN,NaN,NaN,13:54:14.437

"Sample 8 ADC",8389010,NaN,NaN,NaN,8388653,NaN,NaN,NaN,8385758
"Sample 8 ADT",29.9062,NaN,NaN,NaN,30.0625,NaN,NaN,NaN,29.8750
"Sample 8 Time",13:54:15.125,NaN,NaN,NaN,13:54:15.812,NaN,NaN,NaN,13:54:16.500

"Sample 9 ADC",8388996,NaN,NaN,NaN,8388641,NaN,NaN,NaN,8385780
"Sample 9 ADT",29.9062,NaN,NaN,NaN,30.0000,NaN,NaN,NaN,29.8750
"Sample 9 Time",13:54:17.171,NaN,NaN,NaN,13:54:17.859,NaN,NaN,NaN,13:54:18.546

"Sample 10 ADC",8389019,NaN,NaN,NaN,8388642,NaN,NaN,NaN,8385639
"Sample 10 ADT",29.9062,NaN,NaN,NaN,29.8750,NaN,NaN,NaN,29.9062
"Sample 10 Time",13:54:19.234,NaN,NaN,NaN,13:54:19.921,NaN,NaN,NaN,13:54:20.609

Appendix F – Demonstration of the 3x3 array

The following table contains the temperatures measured by the sensor 26a applying our calibration equations using the large aperture.

Blackbody temperature(°C)	Measured temperature(°C)	Error Percentage
50	52.34791	4.69
75	74.50186	0.66
100	101.5572	1.56
125	124.0585	0.75
150	146.2111	2.52
175	170.5803	2.52
200	193.9599	3.02
225	217.6627	3.26
250	242.1597	3.13
275	266.8161	2.97
300	292.3142	2.56

The following table contains the temperatures measured by the sensor 26a applying our calibration equations using the medium aperture.

Blackbody temperature(°C)	Measured temperature(°C)	Error Percentage
50	68.23701	36.47402
75	90.17699	20.23599
100	106.3409	6.3409
125	123.3669	1.30648
150	148.0184	1.321067
175	171.1846	2.180229
200	194.2469	2.87655
225	213.9445	4.913556
250	230.586	7.7656
275	259.5751	5.609055
300	274.173	8.609